

Structural Requirements for Catalysis:  
Studies on RTEM-1  $\beta$ -lactamase

Thesis by Todd Alan Richmond

In Partial Fulfillment of the Requirements  
for the Degree of  
Doctor of Philosophy

California Institute of Technology  
Pasadena, California

1994

(Submitted January 3, 1994)

*To My Parents*

## Acknowledgments

I would like to thank my advisor, Jack Richards, for giving me a chance to pursue a variety of interesting research projects under his direction. Having the freedom to try new things, and attempt experiments outside the normal scope of the lab, along with lively Thursday lunch discussions all contributed to a very well rounded education. Also, Jack's enthusiastic support and extraordinary patience during times both good and bad were vital to my finishing here. I would also like to thank my committee chairman, Harry Gray, for similar encouragement and examples of how not to peak too soon.

Science is not done in a vacuum (although sometimes it does suck...). There are so many people who contribute to one's Ph.D., it is difficult to cite everyone. I would like to thank all of the members of the Richards' group, past and present, for assistance and diversions scientific and otherwise. Specifically, I would like to thank Marc Labgold for teaching me my first molecular biology techniques, and Dave Long and Mikee Emerling for getting me addicted to bicycles. Also, Claire Slutter must be mentioned, for her special blend of lab help and expertise, sprinkled with liberal bits of verbal abuse and comedy.

I could not have attempted the variety of experiments without copious amounts of collaborative assistance. I would like to thank Neil Farrow for running the  $^{15}\text{N}$  spectra, and Marc Hillmyer for considerable synthetic input. The "fancy" NMR experiments were all run by Scott Ross, and his expertise and effort, along with his advisor Steve Mayo, were essential to getting any signal at all from the labeled protein.

I was lucky enough to have a rather large array of extracurricular activities involving a rather eclectic cast of characters. The far ranging adventures with the members of the Pasadena Mountain Bike Club; the "Snow Ride" will not be forgotten. The afternoons spent on the fresh cut grass at Brookside Golf Course with *"the foursome"* were critical to my education in things other than science. Hopefully Steve Burrato, Gary

Guthart, Marc Hillmyer and myself can meet again to tear up the grass. However it was softball that occupied most of my non-science athletic activities, and the number of teams I played on, and people I played with on both City and Caltech leagues teams precludes a complete roster. Sunday mornings with the B.B.'s were epic, as were the pitchers at B.C. afterward (@ 10:30 A.M.?). 3 'n' Beer delivered similar festive times. The greatest moments of softball were on the Caltech diamonds, and Hum Baby Scum will live forever in the annals of Caltech softball....champions in 1990, but still not engraved on the trophy!

There were also a variety of other distractions, and I would like to acknowledge Dan Jones, Wayne Larson, Mike Rock, Marc Hillmyer, and many others too numerous to mention, for taking part in a series of parties and other events involving a variety of phases. Also thanks to musical groups The Sirens (I can now say I played at the club where River Phoenix died), Caltech Jazz bands, and the CMD Jazz Quartet .

Penultimately, I would like to thank my wife Melissa for vast amounts of support and encouragement, along with her own obtuse and sarcastic take on things both scientific and absurd. Although some may say that getting married while in grad school is a mistake, and not for those serious, I wouldn't have had it any other way. Actually I don't think I would have finished without her, so the naysayers were wrong. Thanks Zippy, I love you. Also, thanks to the cats; Mingus, Miles, and Sauza. No matter what happens in lab, your cats are always there...wanting food...knocking over things...meowing at 4 A.M.

Finally I must thank my parents. My journey to this point has not exactly been smooth, and I must admit I have been a bit of a handful. However, no matter what idiotic situation I got myself into, I could always come home. Luckily, I got my act together in time to take advantage of what was probably my last chance. I guess the third time (college) was a charm. I surely would not be where I am now without my parents, and I must tell them that I love them both. Thanks.

**ABSTRACT:**  $\beta$ -lactamases are a group of enzymes that confer resistance to penam and cephem antibiotics by hydrolysis of the  $\beta$ -lactam ring, thereby inactivating the antibiotic. Crystallographic and computer modeling studies of RTEM-1  $\beta$ -lactamase have indicated that Asp 132, a strictly conserved residue among the class A  $\beta$ -lactamases, appears to be involved in substrate binding, catalysis, or both. To study the contribution of residue 132 to  $\beta$ -lactamase function, site saturation mutagenesis was used to generate mutants coding for all 20 amino acids at position 132. Phenotypic screening of all mutants indicated that position 132 is very sensitive to amino acid changes, with only N132C, N132D, N132E, and N132Q showing any appreciable activity. Kinetic analysis of three of these mutants showed increases in  $K_M$ , along with substantial decreases in  $k_{cat}$ . Efforts to trap a stable acyl-enzyme intermediate were unsuccessful. These results indicate that residue 132 is involved in substrate binding, as well as catalysis, and supports the involvement of this residue in acylation as suggested by Strynadka *et al.*

Crystallographic and computer modeling studies of RTEM-1  $\beta$ -lactamase have indicated that Lys 73 and Glu 166, two strictly conserved residues among the class A  $\beta$ -lactamases, appear to be involved in substrate binding, catalysis, or both. To study the contribution of these residues to  $\beta$ -lactamase function, site saturation mutagenesis was used to generate mutants coding for all 20 amino acids at positions 73 and 166. Then all 400 possible combinations of mutants were created by combinatorial mutagenesis. The colonies harboring the mutants were screened for growth in the presence of ampicillin. The competent colonies' DNA were sequenced, and kinetic parameters investigated. It was found that lysine is essential at position 73, and that position 166 only tolerated fairly conservative changes (Aspartic acid, Histidine, and Tyrosine). These functional mutants exhibited decreased  $k_{cat}$ 's, but  $K_M$  was close to wild-type levels. The results of the combinatorial mutagenesis experiments indicate that Lys is absolutely required for activity at position 73; no mutation at residue 166 can compensate for loss of the long side chain

amine. The active mutants found--K73K/E166D, K73K/E166H, and K73K/E166Y were studied by kinetic analysis. These results reaffirmed the function of residue 166 as important in catalysis, specifically deacylation.

The identity of the residue responsible for enhancing the active site serine (Ser 70) in RTEM-1  $\beta$ -lactamase has been disputed for some time. Recently, analysis of a crystal structure of RTEM-1  $\beta$ -lactamase with covalently bound intermediate was published, and it was suggested that Lys 73, a strictly conserved residue among the class A  $\beta$ -lactamases, was acting as a general base, activating Ser 70. For this to be possible, the  $pK_a$  of Lys 73 would have to be depressed significantly. In an attempt to assay the  $pK_a$  of Lys 73, the mutation K73C was made. This mutant protein can be reacted with 2-bromoethylamine, and activity is restored to near wild type levels.  $^{15}\text{N}$ -2-bromoethylamine hydrobromide and  $^{13}\text{C}$ -2-bromoethylamine hydrobromide were synthesized. Reacting these compounds with the K73C mutant gives stable isotopic enrichment at residue 73 in the form of aminoethylcysteine, a lysine homologue. The  $pK_a$  of an amine can be determined by NMR titration, following the change in chemical shift of either the  $^{15}\text{N}$ -amine nuclei or adjacent  $^{13}\text{C}$  nuclei as pH is changed. Unfortunately, low protein solubility, along with probable label scrambling in the  $^{13}\text{C}$  experiment, did not permit direct observation of either the  $^{15}\text{N}$  or  $^{13}\text{C}$  signals. Indirect detection experiments were used to observe the protons bonded directly to the  $^{13}\text{C}$  atoms. Two NMR signals were seen, and their chemical shift change with pH variation was noted. The peak which was determined to correspond to the aminoethylcysteine residue shifted from 3.2 ppm down to 2.8 ppm over a pH range of 6.6 to 12.5. The  $pK_a$  of the amine at position 73 was determined to be  $\sim 10$ . This indicates that residue 73 does not function as a general base in the acylation step of the reaction. However the experimental measurement takes place in the absence of substrate. Since the enzyme undergoes conformational changes upon substrate binding, the measured  $pK_a$  of the free enzyme may not correspond to the  $pK_a$  of the enzyme substrate complex.

**Table of Contents**

Acknowledgment.....	iii
Abstract.....	v
List of Figures and Tables.....	ix
Nomenclature and Abbreviations.....	xv
Chapter 1. Introduction to Aspects of Protein Chemistry and RTEM-1 $\beta$ -lactamase.....	1
Introduction.....	2
References.....	29
Chapter 2. Site-Saturation of Residue 132 in RTEM-1 $\beta$ -lactamase.....	32
Introduction.....	33
Materials and Methods.....	40
Results.....	49
Discussion.....	62
References.....	67
Chapter 3. Combinatorial Mutagenesis of Residues 73 and 166 in RTEM-1 $\beta$ -lactamase.....	70
Introduction.....	71
Materials and Methods.....	79
Results.....	86
Discussion.....	89
References.....	101

Chapter 4.	Attempts to Determine the pKa of an Active Site Residue in RTEM-1 $\beta$ -lactamase via Site-Directed Mutagenesis, Chemical Modification, and NMR Spectroscopy.....	104
	Introduction.....	105
	Materials and Methods.....	118
	Results.....	125
	Discussion.....	146
	References.....	166



## List of Figures and Tables

### Chapter 1. Introduction to Aspects of Protein Chemistry and $\beta$ -lactamase.

Figure 1.	Ionizable amino acid side chains and their $pK_a$ 's.....	3
Figure 2.	Structure of a tetrapeptide showing poly amide linkages.....	4
Figure 3.	Charge separation and conjugation in a peptide bond.....	5
Figure 4.	Hydrogen bonding interactions in protein secondary structural elements.....	7
Figure 5.	Reaction coordinate diagram for an enzymatic reaction.....	10
Figure 6.	Second-order reaction of acetate with aryl acetate.....	12
Figure 7.	Effect of approximation on reaction rates.....	12
Figure 8.	Examples of catalysis in an enzyme active site.....	14
Figure 9.	Charge relay system in the active site of serine proteases.....	15
Figure 10.	Representative $\beta$ -lactam antibiotics.....	18
Figure 11.	The process of bacterial cell wall biosynthesis.....	19
Figure 12.	Carboxypeptidase interactions with $\beta$ -lactam antibiotics.....	20
Figure 13.	Structural analogy between $\beta$ -lactam and D-Ala-D-Ala peptide.....	22
Figure 14.	Interaction of $\beta$ -lactamase with $\beta$ -lactam antibiotic.....	23
Figure 15.	Sequence alignment for Class A $\beta$ -lactamases.....	25
Figure 16.	Structure of RTEM-1 $\beta$ -lactamase with hydrogen bonding interaction at the active site.....	26
Figure 17.	Proposed detailed mechanism of action of $\beta$ -lactamase.....	27

### Chapter 2. Site Saturation of residue 132 in RTEM-1 $\beta$ -lactamase

Figure 1.	Representative $\beta$ -lactam antibiotics.....	34
Figure 2.	Overall mechanism of action of $\beta$ -lactamase.....	35

Figure 3.	Structure of RTEM-1 $\beta$ -lactamase.....	36
Figure 4.	Sequence alignment showing conservation of residue 132.....	38
Figure 5.	Active site structure highlighting residue 132.....	39
Figure 6.	Scheme for introduction of unique restriction sites by site-directed mutagenesis.....	42
Figure 7.	Map of pJN-Sax vector.....	43
Figure 8.	Cassette mutagenesis scheme for site-saturation of residue 132.....	44
Figure 9.	Complementary oligonucleotides for site saturation of residue 132.....	46
Figure 10.	Agarose gel of restriction digest indicating presence of <i>Sac</i> I and <i>Sac</i> II sites in pJN.....	50
Figure 11.	Sequencing gel showing creation of <i>Sac</i> I site in pJN.....	51
Figure 12.	Sequencing gel showing creation of <i>Sac</i> II site in pJN.....	52
Figure 13.	Agarose gel showing restriction digest of pJN-Sax for cassette mutagenesis.....	53
Figure 14.	Typical sequencing gel for position 132 from cassette mutagenesis.....	54
Figure 15.	Plot of phenotypic resistance for N132X mutants.....	55
Figure 16.	FPLC trace for purification of N132X mutants.....	57
Figure 17.	PAGE analysis of FPLC fractions for N132X mutants.....	58
Figure 18.	Kinetic scheme for $\beta$ -lactamase catalyzed hydrolysis of lactams.....	59
Figure 19.	Plot of absorbance vs. time for $\beta$ -lactamase catalyzed hydrolysis of benzyl penicillin.....	60
Table 1.	Kinetic parameters for selected N132X mutants.....	61

Figure 20.	Autoradiograph of PAGE using N132X mutants and $^{14}\text{C}$ -benzyl penicillin.....	63
Figure 21.	Detailed mechanism of action of RTEM-1 $\beta$ -lactamase.....	66

### Chapter 3. Combinatorial Mutagenesis of Residues 73 and 166 in RTEM-1 $\beta$ -lactamase.

Figure 1.	Representative $\beta$ -lactam antibiotics.....	72
Figure 2.	Overall mechanism of action of $\beta$ -lactamase.....	73
Figure 3.	Sequence alignment of $\beta$ -lactamases showing conservation of Lys 73 and Glu 166.....	74
Figure 4.	Active site structure highlighting residues 73 and 166.....	76
Figure 5.	Phenotypic resistance plots for K73X and E166X mutants.....	77
Figure 6.	Scheme for combinatorial mutagenesis of residues 73 and 166.....	78
Figure 7.	Cassette mutagenesis scheme for site-saturation of sites 73 and 166.....	82
Figure 8.	Map of pJN vector.....	83
Figure 9.	Scheme for subcloning mutants into pJN expression vector.....	85
Figure 10.	Agarose gel showing restriction digest and fragments used in combinatorial mutagenesis.....	88
Figure 11.	FPLC trace for purification of active mutants.....	90
Figure 12.	Kinetic scheme of $\beta$ -lactamase catalyzed hydrolysis of $\beta$ -lactams.....	91
Table 1.	Kinetic parameters for active combinatorial mutants.....	92
Figure 13.	Kinetic pH profiles for K73K/E166D and K73K/E166H mutants.....	93
Figure 14.	Postulated involvement of Glu 166 in deacylation.....	95

Figure 15.	Possible involvement of Tyr 166 in deacylation.....	96
Figure 16.	Postulated involvement of Lys 73 in acylation.....	98
Figure 17.	Experiments involving unnatural amino acid incorporation and chemical modification at residue 73.....	99

**Chapter 4. Direct  $pK_a$  determination by site-directed mutagenesis, chemical modification and NMR spectroscopy.**

Figure 1.	Representative $\beta$ -lactam antibiotics.....	106
Figure 2.	Overall mechanism of action of $\beta$ -lactamase.....	107
Figure 3.	Arrangement of residues in the active site.....	109
Figure 4.	Acylation step in $\beta$ -lactam hydrolysis reaction catalyzed by $\beta$ -lactamase showing Lys 73 as general base.....	110
Figure 5.	Restoration of activity by reaction with ethyleneimine.....	112
Figure 6.	Chemical modification of K73C mutant by bromoethylamine.....	113
Figure 7.	$^{13}\text{N}$ -(2)-bromoethylamine hydrobromide synthesis scheme.....	114
Figure 8.	$^{13}\text{C}$ -(2)-bromoethylamine hydrobromide synthesis scheme.....	115
Figure 9.	Plot of chemical shift vs. pH for $^{15}\text{N}$ in lysine.....	116
Figure 10.	Table of $^{13}\text{C}$ chemical shifts at different pH's for lysine.....	117
Figure 11.	Outline of HMQC NMR experiment.....	126
Figure 12.	$^1\text{H}$ NMR spectra of $^{15}\text{N}$ -(2)-bromoethylphthalimide.....	128
Figure 13.	$^1\text{H}$ NMR spectra of $^{15}\text{N}$ -(2) bromoethylamine hydrobromide.....	130
Figure 14.	$^1\text{H}$ NMR spectra of $^{13}\text{C}$ -BOC-glycine.....	131
Figure 15.	$^{13}\text{C}$ NMR spectra of $^{13}\text{C}$ -BOC-glycine.....	132
Figure 16.	$^1\text{H}$ NMR spectra of $^{13}\text{C}$ -BOC-ethanolamine.....	134
Figure 17.	$^{13}\text{C}$ NMR spectra of $^{13}\text{C}$ -BOC-ethanolamine.....	135

Figure 18.	$^1\text{H}$ NMR spectra of $^{13}\text{C}$ -(2)-bromoethylamine hydrobromide.....	136
Figure 19.	$^{13}\text{C}$ NMR spectra of $^{13}\text{C}$ -(2)-bromoethylamine hydrobromide.....	137
Figure 20.	FPLC purification trace of K73C mutant.....	138
Figure 21.	PAGE of FPLC fractions for K73C mutant.....	139
Figure 22.	Plot of absorbance vs. time for hydrolysis of benzyl penicillin catalyzed by K73C before and after labeling.....	141
Figure 23.	$^{15}\text{N}$ NMR spectra of K73AEC $\beta$ -lactamase.....	142
Figure 24.	$^{13}\text{C}$ NMR spectra of aminoethylcysteine.....	143
Figure 25.	$^{13}\text{C}$ NMR spectra of K73AEC $\beta$ -lactamase.....	144
Figure 26.	HMQC experiment on $^{13}\text{C}$ -(2)-bromoethylamine.....	145
Figure 27.	$^1\text{H}$ spectra of $^{13}\text{C}$ -K73AEC $\beta$ -lactamase.....	147
Figure 28.	HMQC experiment on $^{13}\text{C}$ -K73AEC $\beta$ -lactamase.....	148
Figure 29.	HMQC experiment on wild type control.....	149
Figure 30.	HMQC experiment on repurified $^{13}\text{C}$ -K73AEC $\beta$ -lactamase.....	150
Figure 31.	HMQC experiment on repurified $^{13}\text{C}$ -K73AEC $\beta$ -lactamase showing control experiments.....	151
Figure 32.	Label scrambling for $^{13}\text{C}$ aminoethylation.....	154
Figure 33.	Calculated chemical shift values for aminoethylcysteine.....	156
Figure 34.	HMQC experiment on new $^{13}\text{C}$ -K73AEC $\beta$ -lactamase sample.....	157
Figure 35.	HMQC NMR titration spectra for pH 6.6 and 7.7.....	159
Figure 36.	HMQC NMR titration spectra for pH 8.5 and 9.8.....	160
Figure 37.	HMQC NMR titration spectra for pH 12.5.....	161
Figure 38.	Plot of chemical shift vs. pH for first peak in HMQC NMR titration experiment.....	162

Figure 39. Plot of chemical shift vs. pH for second peak in HMQC  
NMR titration experiment.....164

## Nomenclature and Abbreviations

Mutants are specified as Asn132Gly or N132G; asparagine at position 132 has been changed to glycine. The one-letter codes are: alanine, A; arginine, R; asparagine, N; aspartate, D; cysteine, C; glutamate, E; glutamine, Q; glycine, G; histidine, H; isoleucine, I; leucine, L; lysine, K; methionine, M; phenylalanine, F; proline, P; serine, S; threonine, T; tryptophan, W; tyrosine, Y; valine, V. Bromoethylamine is abbreviated BEA, and aminoethylcysteine is AEC. Polyacrylamide gel electrophoresis is PAGE. All remaining abbreviations are described where applicable.

## **Chapter 1**

Introduction to Aspects of Protein Chemistry and  $\beta$ -lactamase



## INTRODUCTION

Of the three main classes of biological molecules, nucleic acids, fatty acids and proteins, proteins exhibit the widest range of structures and functions (1). Proteins and peptides are polyamides composed of  $\alpha$ -amino acids, and most proteins are only made up from a pool of the twenty so called "natural" amino acids. Amino acids are molecules containing an amino group, a carboxylic acid group, and another group (R) which determines the identity of the amino acid. All of the naturally occurring amino acids are chiral (except glycine, in which R=hydrogen), and of the two possible enantiomers, only the L-enantiomer is found in most peptides and proteins. The R groups can be classified into two main arrays--polar and non-polar. Most of the nonpolar amino acids have R groups that are hydrocarbon in nature, and can be important in hydrophobic interactions. Many of the polar R groups have ionizable R groups (or side chains), are involved in a variety of interactions, and can function in catalysis (Figure 1).

Linking  $\alpha$ -amino acids together, the amino group of one condensing with the carboxylate of another, gives an amide called a peptide (Figure 2), with larger peptides considered proteins. The lone pair of the nitrogen is in conjugation with the carbonyl double bond as shown in Figure 3, which gives the C-N bond partial double bond character. It is energetically favorable for each of the atoms attached to the C-N bond to be in the same plane and thus the barrier to rotation is rather high ( $\sim 80 \text{ kJ mol}^{-1}$ )(2). It follows that there is not free rotation in the peptide chain about NH-CO bonds.

The typical charge separation in a peptide bond is shown in Figure 3. Contrary to predictions from resonance structures, the nitrogen has a negative rather than a positive charge. The charge separation gives each amino acid an associated dipole which interacts with neighboring dipoles (3). The peptide backbone is therefore quite polar and particularly available for hydrogen bonding (Figure 3), since the amide protons will readily interact with electron rich carbonyl oxygens. Amides are much less nucleophilic than

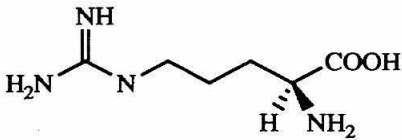
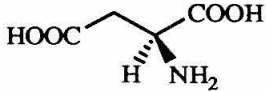
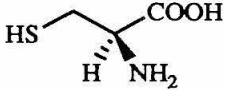
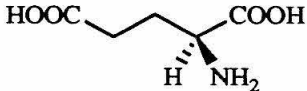
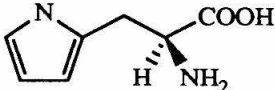
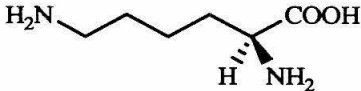
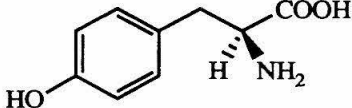
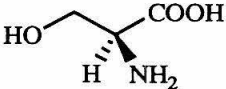
<u>Name</u>	<u>Structure</u>	<u>pK<sub>a</sub></u>
arginine		12.5
aspartic acid		3.9
cysteine		9.3
glutamic acid		4.3
histidine		6.1
lysine		10.5
tyrosine		9.1
serine		>13

Figure 1. Name, structure, and pK<sub>a</sub> of amino acids with ionizable side chains.

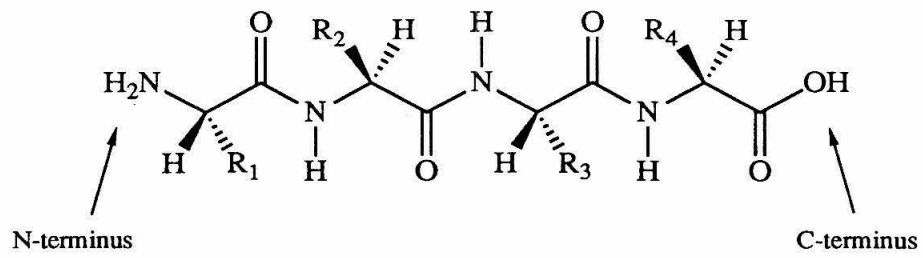
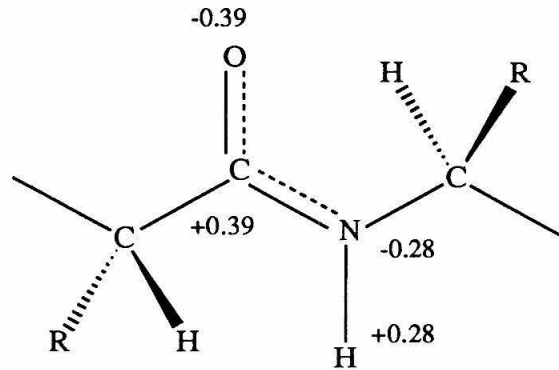
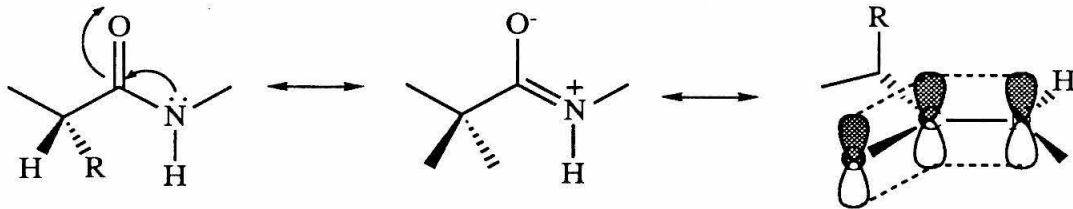


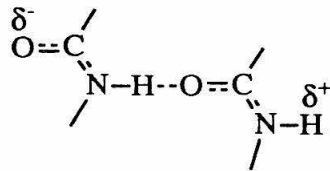
Figure 2. Tetra peptide illustrating linear arrangement of amino acids



Typical charges on atoms of the peptide bond



Conjugation in peptide bonds. Effective overlap between the nitrogen lone pair and the carbonyl group requires coplanarity of the p-orbitals of N, C, and O.



Hydrogen bonding between peptide bonds

Figure 3. Some features of the peptide bond.

amines because the lone pair on nitrogen is conjugated (Figure 3) with the carbonyl and hence not readily available for donation to electrophiles. Peptides are therefore difficult to alkylate or acylate and are only weakly basic (4).

The linear sequence of amino acids is known as the primary structure of a protein. Protein chains are coiled or folded in an ordered way dependent upon a number of interactions including maximization of hydrogen bonding between amino acid residues, hydrophobic effects and other forces (5). The primary sequence often folds into discrete organized elements of structure called secondary structure. These include  $\alpha$ -helices,  $\beta$ -sheets, and  $\beta$ -turns (Figure 4). Secondary structural elements often comprise important domains of proteins. The overall structure, often a combination of secondary structural elements along with sections of random coil, is known as the tertiary structure or overall fold. Many proteins also exist as multimers of identical or mixed protein subunits, and this multimeric arrangement is called quaternary structure.

The most abundant conformation in proteins is an ordered coil known as the  $\alpha$ -helix. The  $\alpha$ -helix (Figure 4) is right-handed, and the bulky side-chains project outwards from the helix, thus experiencing little steric hindrance. The helix has 3.6 residues per turn and the backbone NH of each amino acid residue hydrogen bonds to the carbonyl of the fourth residue towards the N-terminal end. The  $\beta$ -pleated sheet is a conformation in which protein chains align themselves side-by-side (Figure 4). The alignment may be either parallel, with all N-terminal groups at the same end, or anti-parallel, with N-terminal ends close to the C-terminal ends of neighboring chains. In either case, the chains are organized by hydrogen bonding and the flat peptide regions alternate between two directions to give a pleated shape. In small peptides a parallel sheet is only feasible intermolecularly, but an intramolecular antiparallel  $\beta$ -sheet structure becomes likely if a peptide chain undergoes a hairpin bend. The most common type of hairpin bend is called the  $\beta$ -turn (Figure 4). There is

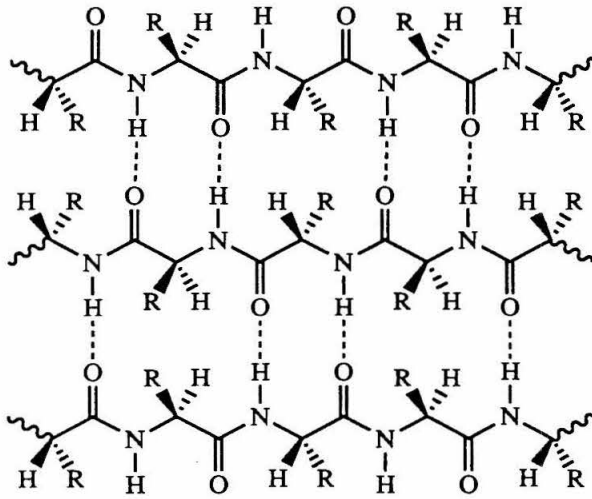
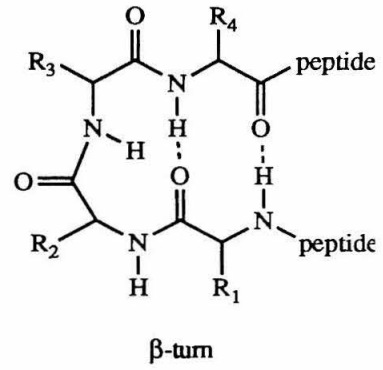
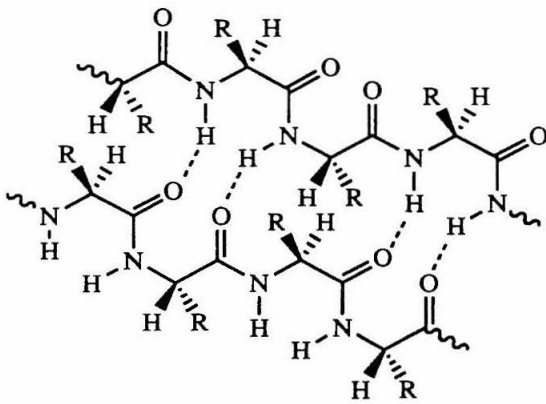
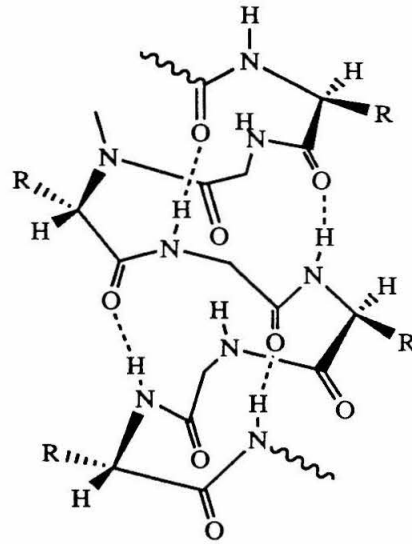
anti-parallel  $\beta$ -pleated sheet $\beta$ -turnparallel  $\beta$ -pleated sheet $\alpha$ -helix

Figure 4. Hydrogen bonding interactions in protein secondary structures.

steric crowding in the region of the turn which restricts the type of amino acid which may be present. Glycine, proline, and D-amino acids are favored in these positions.

The structures of many globular proteins have been determined by X-ray crystallography or by NMR spectroscopy in solution (6). The forces which maintain a protein's conformation are non-covalent interactions (except for disulfide linkages). Polar groups often occur near other polar groups or on the surface of the protein while nonpolar groups cluster together, usually near the center of the molecule. Other non-amino acid components are regularly seen in proteins, especially carbohydrates, metals, and small organic molecules called co-factors. The latter two cofactors are frequently seen in enzymes.

Enzymes are proteins that catalyze reactions in biological systems. The first enzyme to be recognized as a protein was jack bean urease (7), which catalyzes the hydrolysis of urea to  $\text{CO}_2$  and  $\text{NH}_3$ . Enzymes can have molecular weights of several thousand to several million, yet can catalyze reactions on molecules as small as  $\text{N}_2$  and  $\text{CO}_2$ . There are a wide variety of rationalizations for enzyme catalysis. According to Kraut (8), modern theories of enzyme catalysis can be traced to Haldane (9), who introduced the concept that an enzyme-substrate complex requires additional activation energy prior to reaction. Transition-state theory was then developed by Eyring (10); this is the basis for the hypothesis of Pauling (11) whose vision of an enzyme was a flexible template designed by evolution to be complementary to the structure of a substrate at the transition state of the reaction rather than at the ground state. As the reaction proceeds toward the transition state, the enzyme interacts more effectively with the transition state geometry and electronic environment (increased binding energy), which consequently accelerates the reaction. This phenomenon is referred to as transition-state stabilization.

The substrate in an enzyme catalyzed reaction only binds to a small area of the enzyme referred to as the active site of the enzyme. The interactions between enzyme and

substrate must be quite specific in order to attain a rate increase. It has been suggested (12) that the large binding energies between substrate and enzyme result from close packing of atoms within the protein, and that the large size may be required to achieve this. Therefore, the entire protein outside of the active site may be functioning as a scaffold to hold the active site in the proper geometry for catalysis.

The two key features of enzyme catalysis are specificity and rate acceleration. The active site contains elements responsible for both of these properties, and these features are not necessarily distinguishable. Specificity refers to both specificity of binding and specificity of reaction. Enzyme catalysis begins with an interaction between the substrate and the enzyme known as the ES, or Michaelis complex. The binding specificity is conferred by certain active site constituents which are involved in binding interactions with the substrate. These interactions include covalent, electrostatic, ion-dipole, dipole-dipole, hydrogen-bonding, charge-transfer, hydrophobic, hydrophilic, and van der Waals interactions. Binding specificity can be absolute, where only one substrate forms an ES complex with a particular enzyme that leads to product formation. Or binding specificity can be very broad, in which case many molecules of related structure can be bound and processed by the enzyme.

Reaction specificity arises from other constituents of the active site, namely, specific acid base, and nucleophilic functional group of amino acids and specific coenzymes or cofactors. In general, catalysts stabilize the transition-state energy relative to the ground state, and this decrease in  $\Delta G^\ddagger$  is responsible for the resulting rate acceleration (Figure 5). An enzyme has various ways of inducing catalysis; by destabilization of the ES complex, by stabilization of the transition states, by destabilization of intermediates, and during product release. Consequently, multiple steps, each having small  $\Delta G^\ddagger$  values, may be involved. As a result of these multiple catalytic steps, rate accelerations of  $10^{10}$  over the



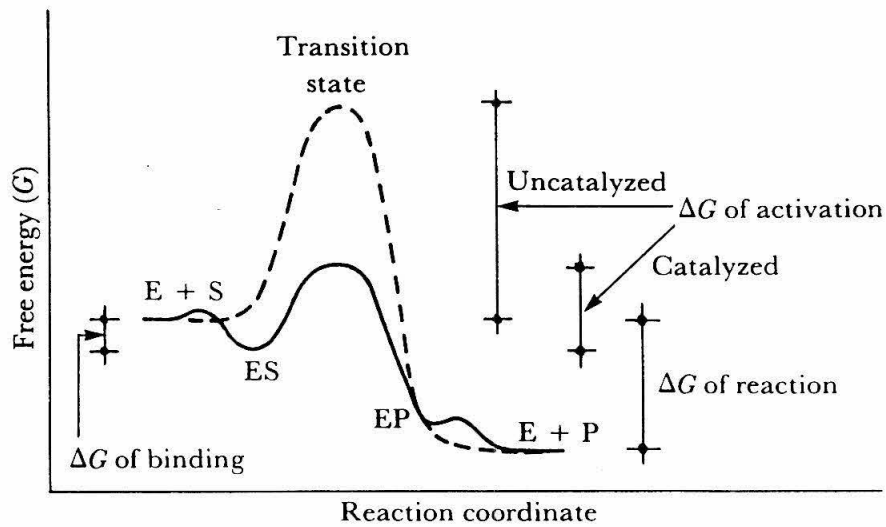


Figure 5. Reaction coordinate diagram for an enzyme catalyzed reaction. From "Biochemistry, A Problems Approach," Wood, W.B. *et al.*, Benjamin/Cummings, Menlo Park, 1981.

corresponding non-enzymatic reactions are possible. Catalysis in general, however, does not alter the equilibrium of a reversible reaction.

The number of molecules of substrate converted to product per unit time per molecule of enzyme active site is the turnover number. Triose phosphate isomerase is one of the most efficient enzymes (13), having a turnover number of  $3500 \text{ sec}^{-1}$ . As there are two other important steps to enzyme catalysis, namely substrate binding and product release, high turnover numbers are only useful if these two steps occur at faster rates. This is not always the case.

Once substrate binds to the active site of the enzyme, there are various tools that enzymes utilize to catalyze the conversion of substrate to product (14-16). Some of the most common mechanisms are approximation, general acid-base catalysis, covalent catalysis, and electrostatic catalysis. In approximation, the enzyme binds the substrate close to the reaction center, resulting in a loss of rotational and translational entropies of the substrate. Because the catalytic groups and substrate are now part of the same molecule, the reaction becomes first order rather than second order, and the concentration of the reacting groups is essentially increased. This phenomenon can be illustrated with non enzymatic model studies such as the second-order reaction of acetate with an aryl acetate (Figure 6). If the rate constant  $k$  for this reaction is set equal to  $1.0 \text{ M}^{-1}\text{sec}^{-1}$ , then the effect of decreasing the rotational and translational entropy is determined by measuring the corresponding first-order rate constants for related intramolecular reactions. Figure 7 illustrates that holding reacting groups in close proximity increases the reaction rate (17,18).

While first and second-order rate constants cannot be directly compared, the efficiency of an intramolecular reaction can be defined by effective molarity (EM), which is the concentration of the moiety required to cause the intermolecular reaction to proceed at the observed rate of the intramolecular reaction. The EM is calculated by dividing the first-

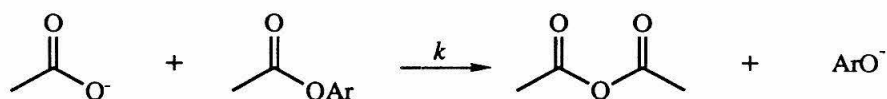


Figure 6. Second-order reaction of acetate with aryl acetate

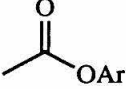
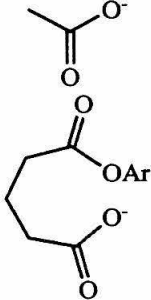
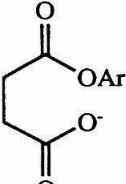
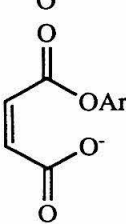
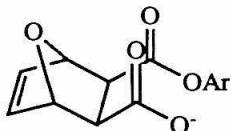
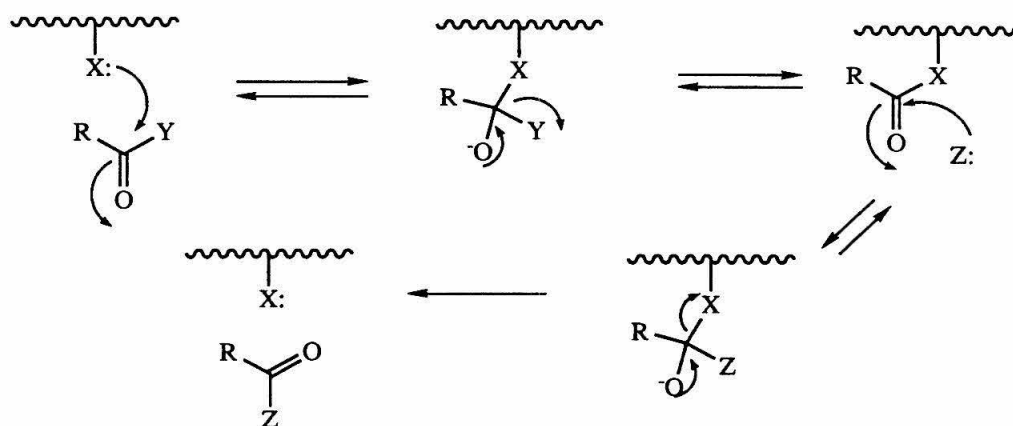
<u>Reactants</u>	<u><math>k_{\text{obs}}</math> (30°)</u>	<u>Relative rate. <math>k</math></u>	<u>Effective Molarity</u>
	$3.36 \times 10^{-7} \text{ M}^{-1} \text{ s}^{-1}$	$1.0 \text{ M}^{-1} \text{ s}^{-1}$	
	$7.39 \times 10^{-5} \text{ s}^{-1}$	$220 \text{ s}^{-1}$	220 M
	$1.71 \times 10^{-2} \text{ s}^{-1}$	$5.1 \times 10^4 \text{ s}^{-1}$	$5.1 \times 10^4 \text{ M}$
	$7.61 \times 10^{-1} \text{ s}^{-1}$	$2.3 \times 10^6 \text{ s}^{-1}$	$2.3 \times 10^6 \text{ M}$
	$3.93 \text{ s}^{-1}$	$1.2 \times 10^7 \text{ s}^{-1}$	$1.2 \times 10^7 \text{ M}$

Figure 7. Effect of Approximation on Reaction Rates (13,14)

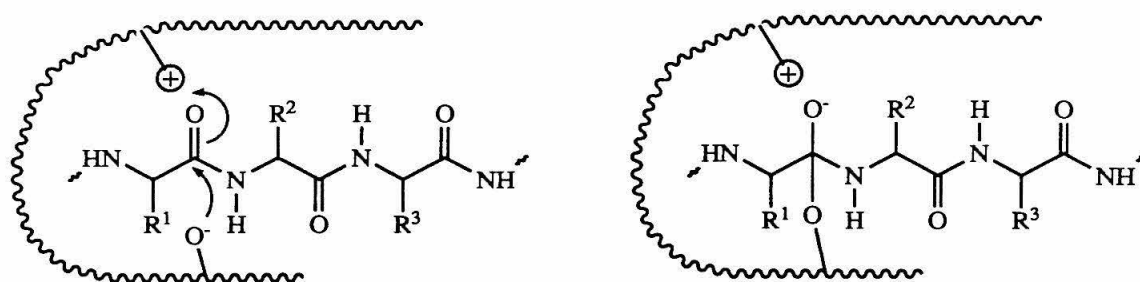
order rate constant for the intramolecular reaction by the second-order rate constant for the corresponding intermolecular reaction (Figure 7). This indicates that acetate ion would have to be a concentration of 220 M in order for the intermolecular reaction to proceed at a rate comparable to that of the glutarate monoester reaction. Thus the effect of decreasing the entropy is significant. Effective molarities for a wide range of intramolecular reactions have been measured (18), and the efficiency of intramolecular catalysis can be as high as  $10^{16}$  M for relative systems. Thus, holding groups near to one another in an enzyme-substrate complex can be an important contributor to catalysis.

In any reaction where proton transfer occurs, general acid catalysis and or general base catalysis is effective. Unlike reactions in solution, an enzyme can utilize acid and base catalysis simultaneously (Figure 8). It is important to appreciate the fact that the  $pK_a$  values of amino acid side-chain groups within the active site of enzymes are not necessarily the same as those measured in solution (19). The simultaneous donation of a proton to a carbonyl and removal of an  $\alpha$ -proton could account for the ability of an enzyme to deprotonate relatively high  $pK_a$  carbon acids and make the corresponding enols (20). Therefore, removal of seeming higher  $pK_a$  protons from substrate by active site bases may not be as unreasonable as would appear if only solution chemistry were taken into consideration.

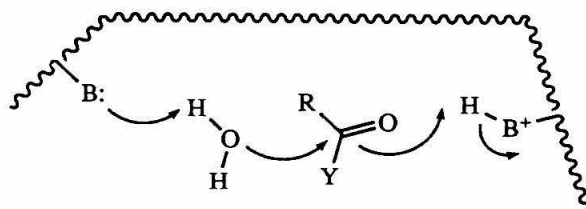
The enzyme  $\alpha$ -chymotrypsin, a serine protease, can illustrate general acid-base catalysis (21). It utilizes as active site serine residue in the catalytic cleavage of peptide bonds. A serine hydroxyl would normally be a poor nucleophile. However, aspartic acid and histidine residues nearby have been implicated in the microscopic conversion of the serine to an alkoxide by a mechanism call the charge relay system (Figure 9). This catalytic triad involves the aspartate carboxyl interacting with the histidine imidazole which, in turn, removes a proton from the serine hydroxyl group. On the basis of the solution  $pK_a$  values,



Nucleophilic catalysis in an enzyme.



Electrostatic stabilization of the transition state in an active site.



Simultaneous acid and base catalysis in an enzyme active site.

Figure 8. Examples of catalysis in an enzyme active site.



this would be expected to be a high-energy process; presumably the  $pK_a$  values at the active site are different from those in solution.

Some enzymes can use nucleophilic amino acid side chains in the active site to form covalent bonds with the substrate. A second substrate can then react with this enzyme-substrate intermediate to generate product (Figure 8). The most common active site nucleophiles are the thiol group of cysteine, the hydroxyl group of serine, the imidazole of histidine, the amino group of lysine, and the carboxyl groups of aspartate and glutamate. These nucleophilic groups are activated by deprotonation, often by a neighboring base, or by a water molecule which is deprotonated in a general base reaction. If the substrate in an enzyme catalyzed reaction were a peptide, nucleophilic catalysis using a serine hydroxyl would yield an ester intermediate which is much more subject to hydrolysis than the starting amide. This is the mechanism followed by the serine proteases (22). The greatest catalytic advantage in using an active site residue instead of water directly is that the former is a unimolecular reaction (since the substrate is bound to the enzyme, attack by the serine residue is equivalent to an intramolecular reaction), which is entropically favored over the bimolecular reaction with water. Also, alkoxides and thiolates are better nucleophiles than hydroxide (23).

Electrostatic interactions may not be as obvious as shown in Figure 8. Instead of a full positive charge in the enzyme there may be one or more local dipoles having partial positive charges directed at the forming transition state anion. In the case of the serine protease subtilisin it has been suggested that the lowering of the free energy of the activated complex is due largely to hydrogen bonding of the developing oxyanion with protein residues. When the suspected active site proton donor was replaced by a leucine residue using site-directed mutagenesis techniques, the  $k_{cat}$  greatly diminished, but the  $K_m$  remained the same, indicating the importance of the hydrogen bonding to catalysis (24). Furthermore, a mutant of subtilisin in which all three of the catalytic triad residues (Ser

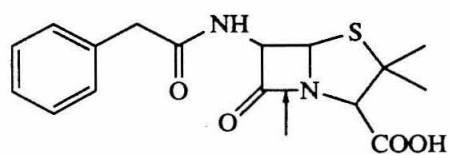
221, His 64, Asp 32) were replaced by alanine residues was still able to hydrolyze amides  $10^3$  times faster than the uncatalyzed hydrolysis rate (albeit  $2 \times 10^6$  time slower than the wild-type enzyme)(25). This suggest that factors other than nucleophilic and general base catalysis must be important. Sophisticated free energy calculation of serine protease active sites indicated that the primary mechanism for rate acceleration is derived from electrostatic stabilization in the transition state (26).

### **$\beta$ -LACTAMASE**

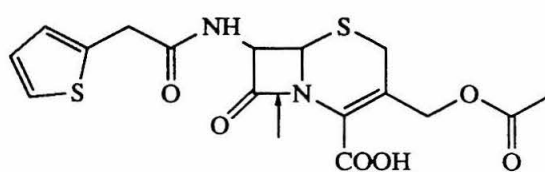
In 1929, Alexander Fleming discovered the existence of a compound produced by certain fungi that inhibited the growth of bacteria in media on which the fungi were growing (27). Penicillin and the other related penam and cephem antibiotics (Figure 10) have since been shown to block bacterial cell wall biosynthesis by inhibiting the crosslinking of cell wall peptidoglycans by the D-Ala-D-Ala carboxypeptidases and transferases (28). The DD-carboxypeptidase/transpeptidases (29) comprise a class of low-molecular weight penicillin binding proteins characterized by their ability to catalyze acyl transfer reactions from D-alanyl-D-alanine-terminated peptides and depsipeptide analogs (Figure 11). These enzymes are responsible for crosslinking the peptidoglycan bacterial cell wall, and involve a covalent acyl-enzyme intermediate with the C-1 D-alanine residue and an active site serine (30). This intermediate can be attacked by the  $\epsilon$ -amino group of a lysine residue from an adjacent peptide strand of the peptidoglycan, which results in the stabilized crosslinked structure, or hydrolyzed by a water molecule, which results in overall removal of one D-alanine residue. Additionally, the n-terminus of another peptide can attack, giving another crosslinked structure.

In addition to the usual D-alanyl peptide substrates,  $\beta$ -lactam antibiotics also interact with the carboxypeptidases. The  $\beta$ -lactam antibiotics, however, are inhibitors. Since the carboxyl and amino portions of the  $\beta$ -lactam antibiotic are still attached following the initial





benzyl penicillin



cephalothin

Figure 10. Representative  $\beta$ -lactam antibiotics. Benzyl penicillin is a member of the penam family, cephalothin is a cephem. Arrow points to bond broken during hydrolysis.

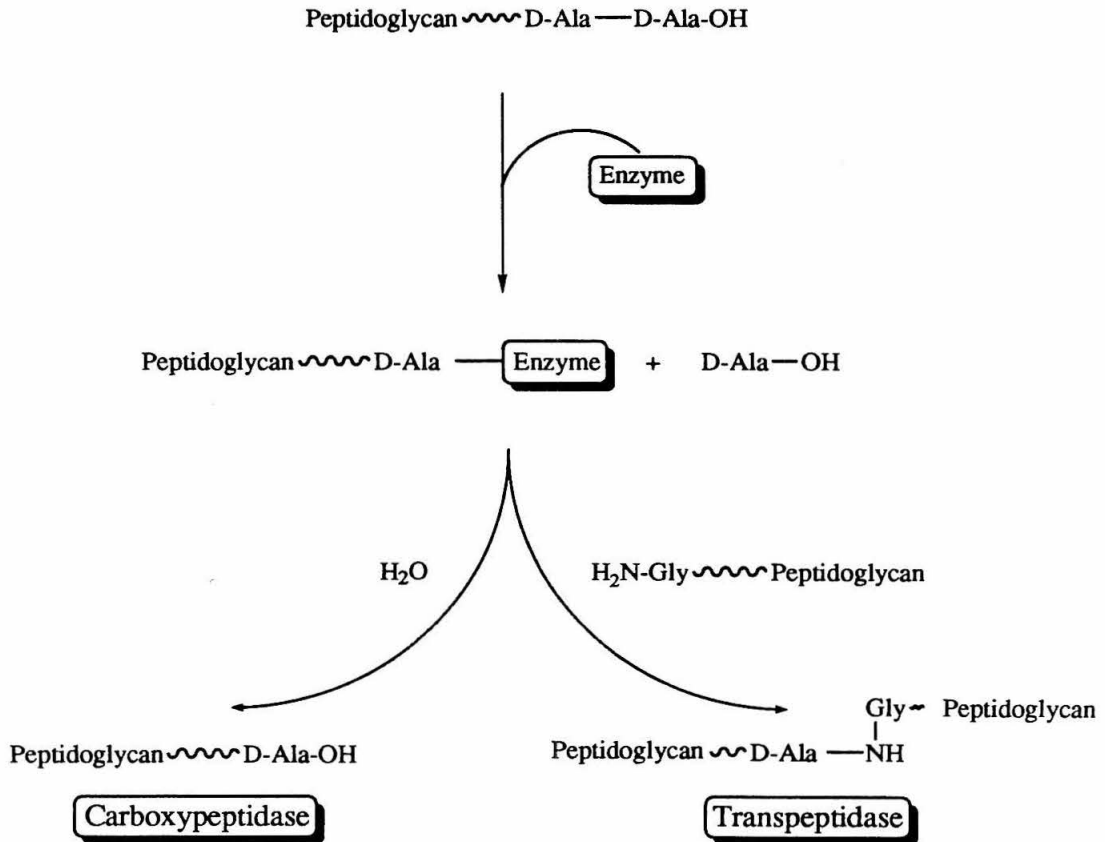


Figure 11. The process of bacterial cell wall biosynthesis. The strands of peptidoglycan are targeted by the D,D-carboxypeptidase, resulting in the hydrolysis of the terminal D-alanine residue. The acyl-enzyme intermediate can then be deacylated by water or an amino acceptor, the latter resulting in a stabilized crosslinked structure.

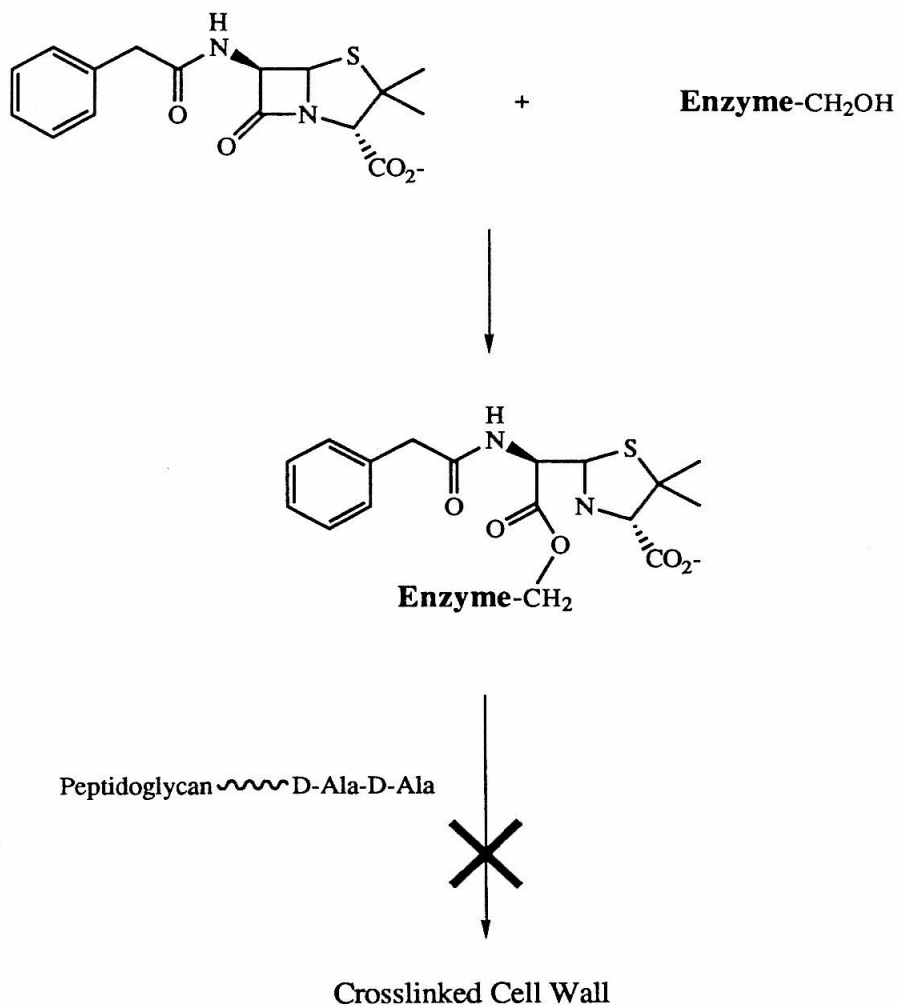


Figure 12. The D-Ala-D-Ala carboxypeptidases interact with the  $\beta$ -lactam antibiotics via nucleophilic attack on the lactam carbonyl by the active site serine residue. The resulting acyl-enzyme intermediate is a stable covalent species and prevents the enzyme from crosslinking the bacterial cell wall peptidoglycan.

hydrolysis reaction, water or another peptide is prevented from entering the active site, and hydrolysis of the acyl-enzyme intermediate is blocked, thus inhibiting the enzyme (Figure 12). This prevents the crosslinking of the cell wall peptidoglycans and results in the eventual lysis of the cell. Tipper and Strominger initially proposed that the  $\beta$ -lactam antibiotics function as structural analogs to the D-ala-D-ala dipeptide (31), and thereby "fool" the enzyme into binding the antibiotic (Figure 13). They were successful in proving this hypothesis by pulse-chase experiments (32).

In 1940, Abraham and Chain discovered that extracts from certain bacteria would neutralize the antibiotic effect of penicillin (33). These extracts were shown to contain a variety of enzymes capable of hydrolyzing the  $\beta$ -lactam ring of penicillin, yet were not inactivated in the process, as were the PBP's (Penicillin Binding Proteins)(Figure 14). These enzymes came to be known as  $\beta$ -lactamases. The resistance to  $\beta$ -lactam antibiotics in many species of bacteria is due to the wide spread of genes encoding  $\beta$ -lactamases. It has been proposed that the origin of these genes lies with the penicillin-sensitive D-alanyl-D-alanyl peptidases (34). Huletsky has made significant progress toward answering the question of how the class A  $\beta$ -lactamases have evolved by studying the phylogeny of the SHV-2  $\beta$ -lactamase (35).

Over 80  $\beta$ -lactmases have been identified, and are divided into three categories based on size, sequence homology, and activity (36). The class A  $\beta$ -lactamases include the RTEM  $\beta$ -lactamases (RTEM-1, 2 and 3) of *Escherichia coli* (37), *Staphylococcus aureus* PC1 (38), *Bacillus licheniformis* 749/C (39), and *Bacillus cereus* 569/HI (40). All of these enzymes have a molecular weight of around 30 kilodaltons and exhibit considerable sequence homology (~30%). There are only two class B  $\beta$ -lactamases, those of *B. cereus* and *Proteus maltophilia* (41). The class B  $\beta$ -lactamases are smaller (molecular weights of approximately 23 kD) and form metalloenzyme complexes with zinc. The class C  $\beta$ -lactamases are the largest at 40 kD and include *Enterobacterium cloacae* P99 and *Escherichia*

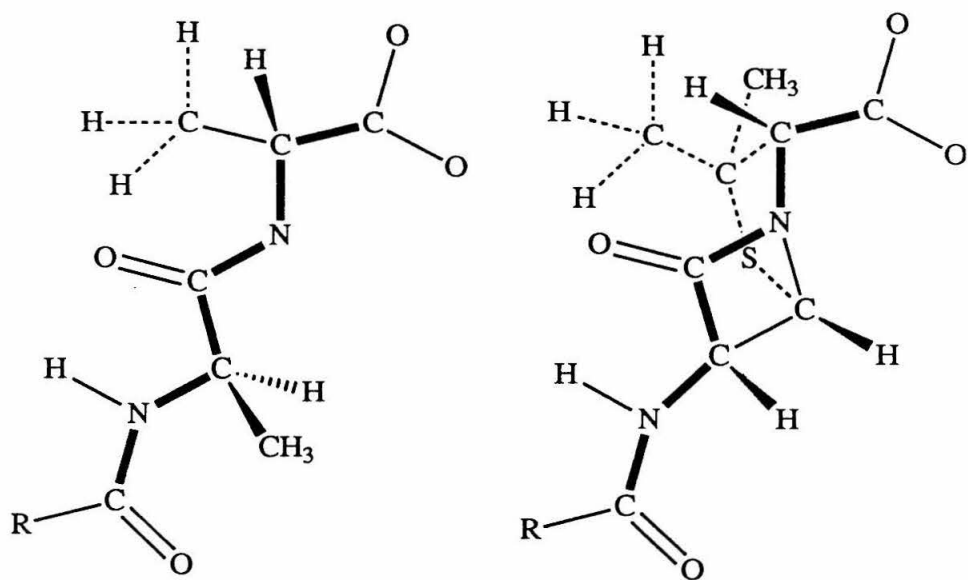


Figure 13. Chemical structures emphasizing the close structural analogy of the  $\beta$ -lactam antibiotics (right) with the D-Ala-D-Ala dipeptide (left). Hydrolysis of the lactam bond leads to a conformation which is nearly superimposable with the peptide.

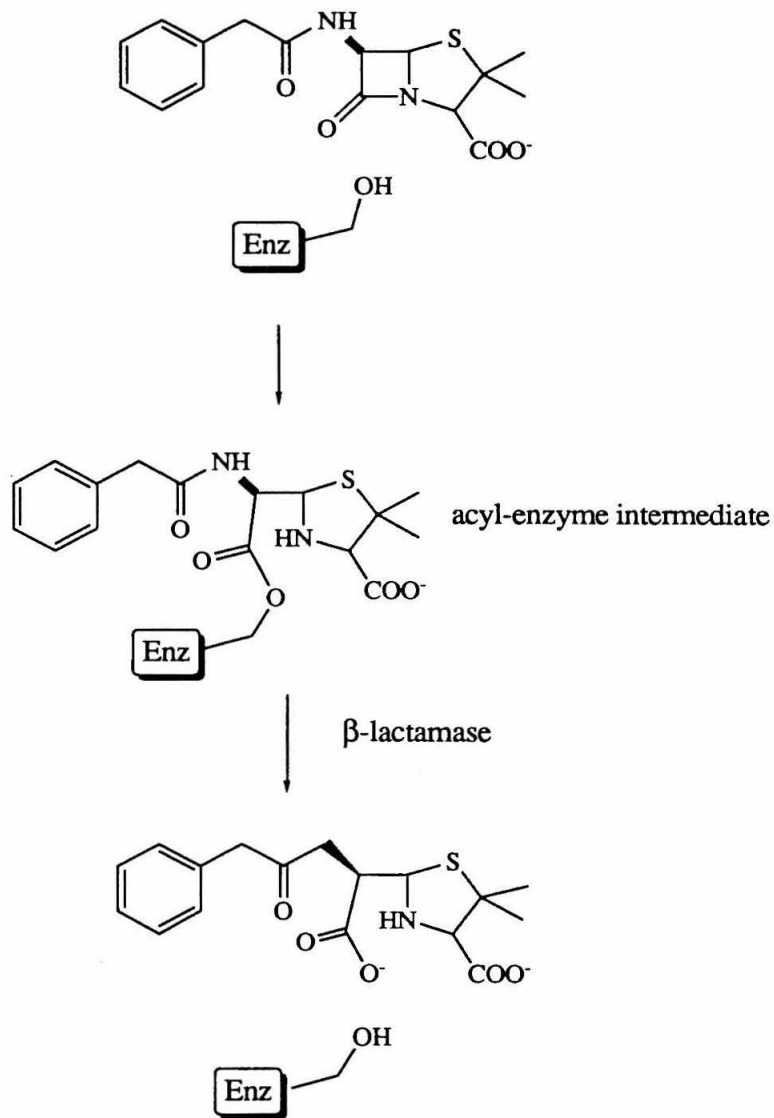


Figure 14. Interaction of the  $\beta$ -lactamases with  $\beta$ -lactam antibiotics results in an acyl-enzyme intermediate which is rapidly hydrolyzed by a bound water molecule.

*coli* K12 (42). In addition to size, the three classes also differ in substrate specificity. The class A  $\beta$ -lactamases preferentially hydrolyze penams, while the other two classes prefer cephem antibiotics.

Analysis of the primary sequences of class A  $\beta$ -lactamases indicated a number of conserved residues (Figure 15). The active site serine, Ser 70 (Ambler numbering, 36) is conserved, along with other residues such as Glu 166, Lys 73, and the so called SDN loop (Ser 130, Asp 131, Asn 132). With the publication of a crystal structure of a class A  $\beta$ -lactamase, that of *Staphylococcus aureus* PC1, the location of many of these conserved residues in the active site was confirmed (Figure 16)(43). The structure displays a two-domain structural motif, with one domain consisting solely of  $\alpha$ -helices, and the second domain having a mixed structure, containing a minimum five-stranded  $\beta$ -sheet sandwiched between two sets of  $\alpha$ -helices. The active site is defined by the interface between the two domains, bordered on one side by the  $\beta$ -7 strand and on the other by the  $\alpha$ -2 and  $\alpha$ -10 helices, with the active site serine residing at the amino-terminal end of the  $\alpha$ -2 helix, in the bottom of the active site cleft.

RTEM-1  $\beta$ -lactamase is a 28.5kD soluble protein isolated from *E. coli*. It differs from RTEM-2  $\beta$ -lactamases by one residue (residue 39) and from RTEM-3 by three residues (residues 39, 104, and 238)(44). Like the other class A  $\beta$ -lactamases, RTEM preferentially hydrolyzes penam antibiotics over cepheims (Figure 10). The rate of penam hydrolysis approaches diffusion control limits, with a second-order rate constant on the order of  $10^8 \text{ M}^{-1}\text{s}^{-1}$ (13). The  $\beta$ -lactam substrate is subjected to nucleophilic attack on the lactam carbonyl group by the active site serine (Ser 70 in RTEM). Nucleophilic attack proceeds through a tetrahedral intermediate which is proposed to be stabilized by an oxyanion hole (43), similar to that observed in the serine proteases (45). The resulting acyl-enzyme intermediate is rapidly hydrolyzed by a bound water, which is activated by Glu 166 (46), leading to an inactive antibiotic (Figure 17).

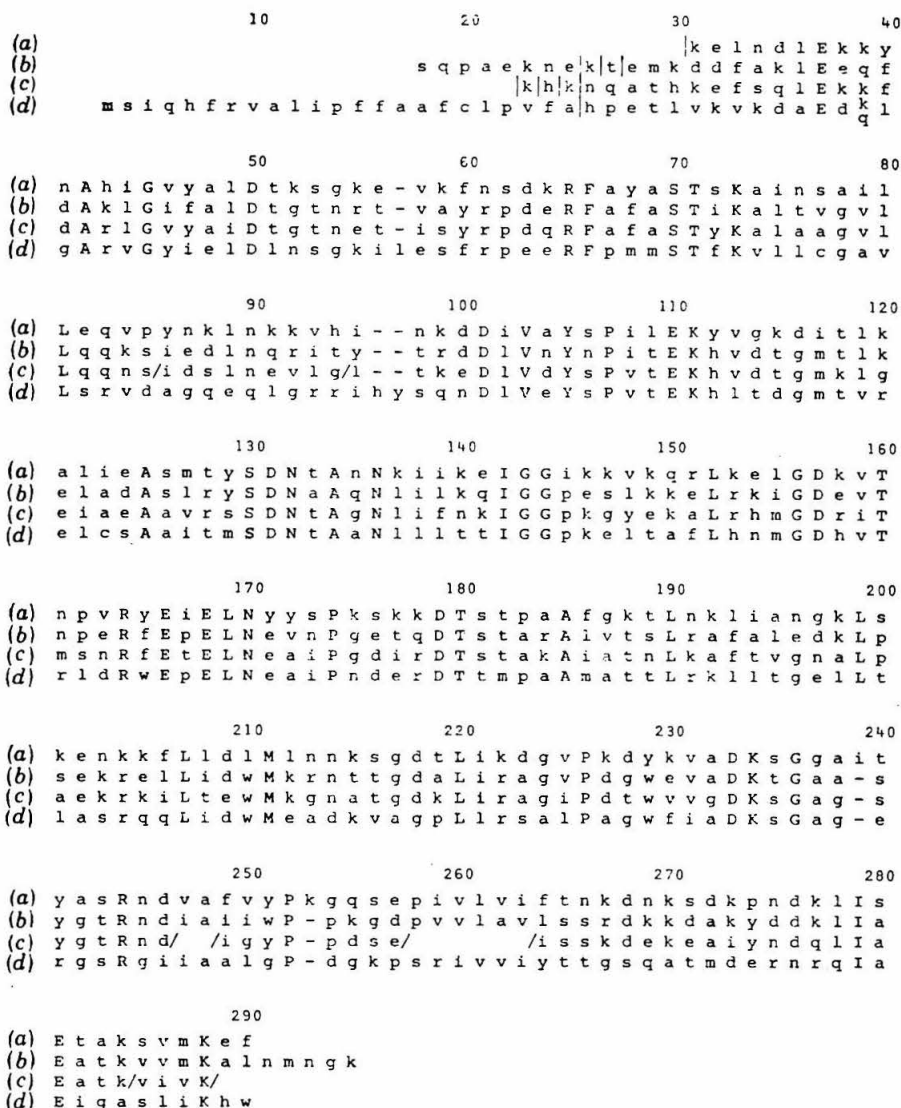


Figure 15. Sequence alignment of Class A  $\beta$ -lactamases. the sequences are: (a) *Staphylococcus aureus* PC1; (b) *Bacillus licheniformis* 749/C; (c) *Bacillus cereus* 569/H lactamase 1; (d) *Escherichia coli* pBR322 RTEM-1. Numbering starts from the n-terminus of the longest form of the *B. licheniformis* enzyme that has been isolated, and takes into account the gaps postulated in the currently known sequences to obtain optimal matching. the vertical bars show the n-termini of naturally released enzymatically active molecules.

Residues that are identical in all four molecules are shown in capitals (1).



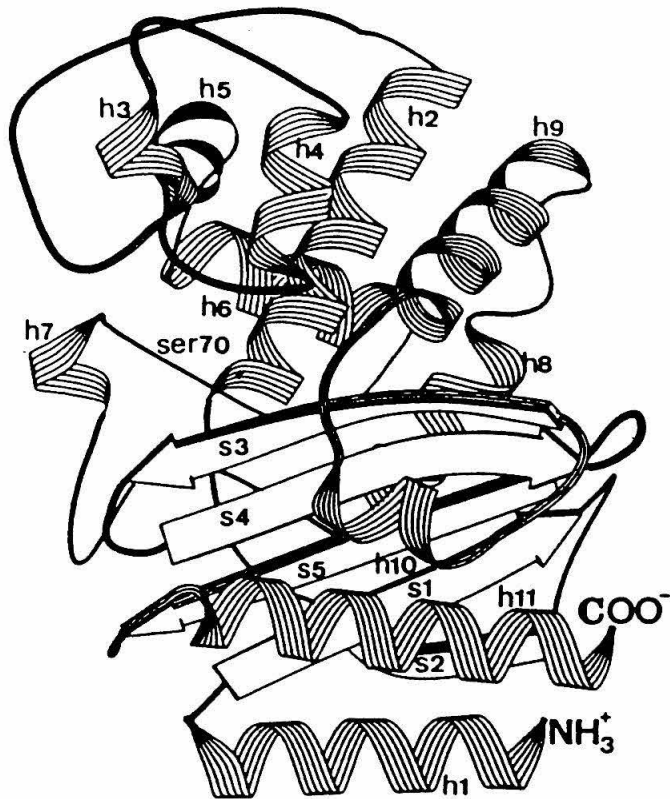


Figure 16. Structure of RTEM-1  $\beta$ -lactamase

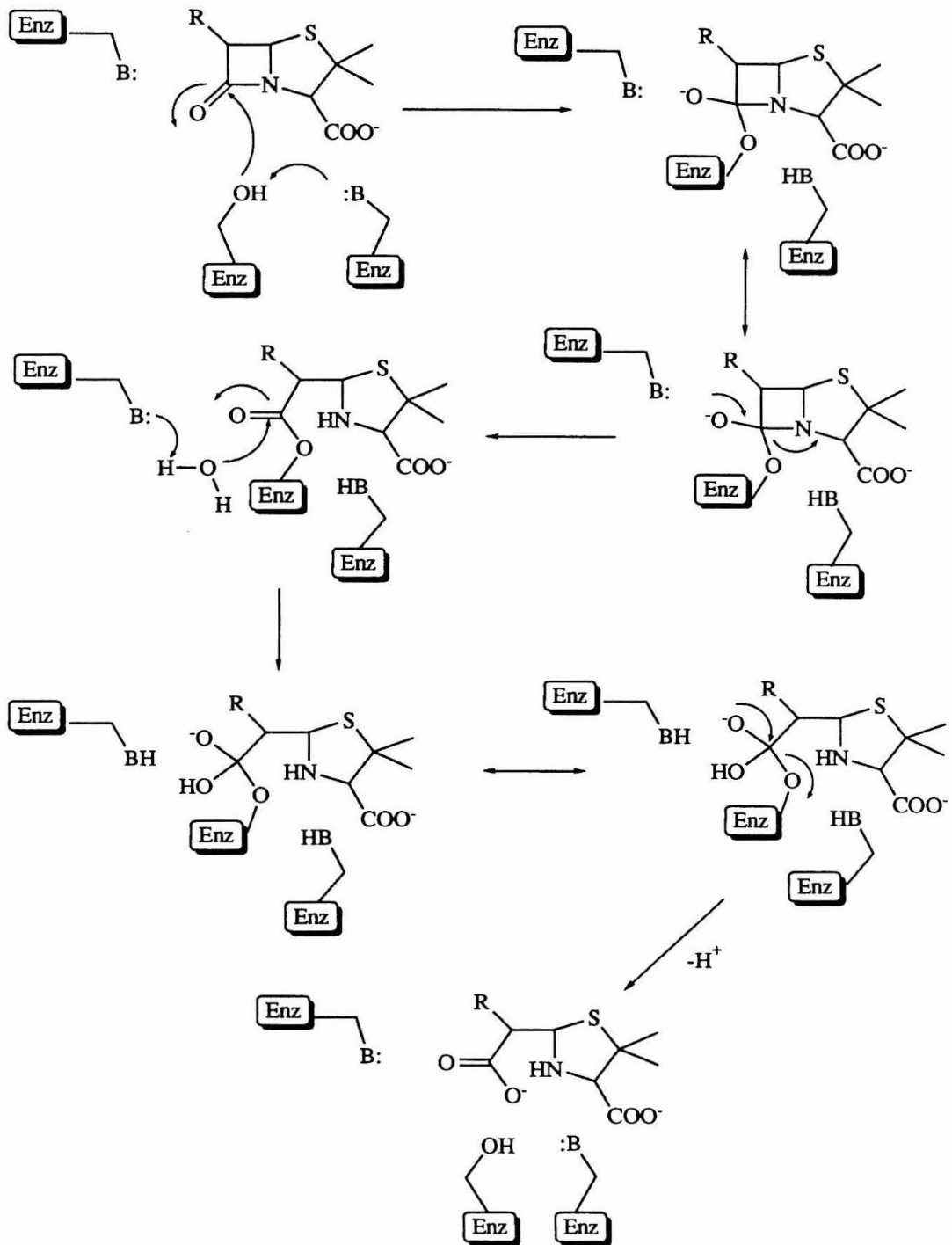


Figure 17. Detailed mechanism postulated for  $\beta$ -lactam hydrolysis catalyzed by  $\beta$ -lactamase.

Much research has been performed in our laboratory to investigate the roles of several important residues in RTEM-1  $\beta$ -lactamase including site-saturation of residues Thr 71(47), Lys 73 (48), Glu 166 (49), Lys (50), Ala 237 (51), Ser 130 (52), and residues 237-240 (53). Other research has been directed towards the generation of mutants at Ser 70 (54, 55). In spite of the wealth of information concerning catalysis in RTEM-1  $\beta$ -lactamase, questions still persist. This thesis concerns some of the remaining puzzles in the RTEM-1 active site. The function of Asn 132, a strictly conserved residue among the class A  $\beta$ -lactamases was not known. Similarly, the details of residues 73 and 166, and any possible interactions was yet investigated. And finally, the nature of activation of the active site serine nucleophile was unknown.

Site directed mutagenesis has been shown to be an effective tool for the study of enzyme structure/function relationships (56). To further investigate the structural requirements for catalysis in RTEM-1  $\beta$ -lactamase, new mutants have been generated, and some existing mutants have been studied using different approaches. Chapter 2 looks at the function of Asn 132 as studied by site-saturation mutagenesis. A technique known as combinatorial mutagenesis is described in Chapter 3, and is used to study interactions between residues 73 and 166, with 400 mutants being generated and easily screened for activity. Finally, the question of whether Lys 73 functions as a general base, activating Ser 70, is investigated via sequential site-directed mutagenesis, chemical modification, and NMR spectroscopy. The goal of this research is to gain a better understanding of the structural basis for catalysis in enzyme systems.

## REFERENCES

1. Stryer, L. (1988) "Biochemistry." Freeman and Company, New York.
2. Fersht, A.R. (1971) *J. Am. Chem. Soc.* **93**, 3504.
3. Pauling, L. (1960) "The Nature of the Chemical Bond," Cornell University Press.
4. Silverman, R.B. (1992) "The Organic Chemistry of Drug Design and Drug Action." Academic Press, San Diego.
5. Kuntz, I.D. (1972) *J. Am. Chem. Soc.* **94**, 4009.
6. Richardson, J.S. (1981) *Adv. Protein Chem.* **34**, 167.
7. Sumner, J.B. (1926) *J. Biol. Chem.* **69**, 435.
8. Kraut, J. (1988) *Science* **242**, 533.
9. Haldane, J.B.S. (1930) "Enzymes." Longmans, Green, London, 1930 (reprinted in 1965 by MIT Press, Cambridge, Massachusetts).
10. Eyring, H. (1935) *J. Phys. Chem.* **3**, 107.
11. Pauling, L. (1946) *Chem. Eng. News* **24**, 1375; Pauling, L. (1948) *Am. Sci.* **36**, 51.
12. Richards, F.M. (1977) *Annu. Rev. Biophys. Bioeng.* **6**, 151.
13. Blacklow, S.C., Raines, R.T., Lim, W.A., Zamore, P.D., and Knowles, J.R. (1988) *Biochemistry* **27**, 1158.
14. Jencks, W.P. (1969) "Catalysis in Chemistry and Enzymology," Chaps. 1-3, and 5. McGraw-Hill, New York.
15. Jenks, W.P. (1975) *Adv. Enzymol.* **43**, 219.
16. Wolfenden, R., and Frick, L. (1987) "Enzyme Mechanisms" (Page, M. I., and Williams, A., eds.), p. 97. Royal Society of Chemistry, London.
17. Bruice, T.C., and Pandit, U.K. (1960) *J. Am. Chem. Soc.* **82**, 5858.
18. Kirby, A.J. (1980) *Adv. Phys. Org Chem.* **17**, 183.
19. Schmidt, D.E. Jr., and Westheimer, F.H. (1971) *Biochemistry* **10**, 1249.

20. Gerlt, J.A., Kozarich, J.W., Kenyon, G.L., and Gassman, P.G. (1991) *J. Am. Chem. Soc.* **113**, 9667.
21. Keil, B. (1971) *The Enzymes* **3**, 249.
22. Blow, D.M., Birktoft, J.J., and Hartley, B.S. (1969) *Nature (London)* **221**, 811.
23. March, J. (1985) "Advanced Organic Chemistry," 3rd ed., p. 268. Wiley, New York.
24. Bryan, P., Pantoliano, M.W., Quill, S.G., Hsaio, H.Y., and Poulos, T. (1986) *Proc. Natl. Acad. Sci. U.S.A.* **83**, 3743.
25. Carter, P., and Wells, J. A. (1988) *Nature (London)* **332**, 564.
26. Warshel, A., Naray-Szabo, G., Sussman, F., and Hwang, J.K. (1989) *Biochemistry* **28**, 3629.
27. Fleming, A. (1929) *Br. J. Exp. Path.* **10**, 26.
28. Georgopapadakou, N.H. and Sykes, R.B. (1983) In "Antibiotics Containing the  $\beta$ -lactam Structure, Part II," Demain, A. L. and Solomon, N. A., eds., Springer-Verlag, Berlin.
29. Frere, J.M., and Joris, B. (1985) *CRC Crit. Rev. Microbiol.* **11**, 299.
30. Georgopapadakou, N.H., Liu, F.Y., Ryono, D.E., Neubeck, R., and Ondetti, M.A. (1981) *Eur. J. Biochem.* **115**, 53.
31. Tipper, D.J., and Strominger, J.L. (1965) *Proc. Natl. Acad. Sci. U.S.A.* **54**, 1133.
32. Tipper, D.J., and Strominger, J.L. (1968) *J. Biol. Chem.* **243**, 3169.
33. Abraham, E.P. and Chain, E. (1940) *Nature (London)* **145**, 837.
34. Kelly, J.A., Dideborg, O., Charlier, P., Wery, J.P., Libert, M., Meows, P.C., Knox, J.R., Duez, C., Fraipont, C., Joris, B., Dusart, J., Frere, J.M., Ghuysen, J.M. (1986) *Science* **231**, 1429.
35. Huletsky, A., Couture, F., and Levesque, R.C. (1990) *Antimicrob. Agents Chemother.* **34**, 1725.
36. Ambler, R.P. (1980) *Phil. Trans. Roy. Soc. Lond. B* **289**, 321.

37. Sutcliffe, J.G. (1978) *Proc. Natl. Acad. Sci. U.S.A.* **75**, 3737.
38. Ambler, R.P. (1975) *Biochem J.* **151**, 197.
39. Neugebauer, K., Sprengel, R. and Schaller, H. (1981) *Nucleic Acids Res.* **9**, 2577.
40. Madgwick, P.J. and Waley, S.G. (1987) *Biochem J.* **248**, 657.
41. Bicknell, R. and Waley, S.G. (1985) *Biochemistry* **24**, 6876.
42. Knot-Hunziker, V., Peursson, S., Waley, S.G., Jarrin, B., and Grundstrom, T. (1982) *Biochem J.* **207**, 315.
43. Hertzberg, O. and Moulton, J. (1987) *Science* **236**, 694.
44. Matagne, A., Misselyn-Baudin, A.M., Joris, B., Erpicum, T., Granier, B., and Frere, J.M. (1990) *Biochem J.* **265**, 131.
45. Fujinaga, M., Read, R.J., Sielecki, A., Laskowski, M. Jr., and James, M.N.G. (1982) *Proc. Natl. Acad. Sci. U.S.A.* **79**, 4868.
46. Adachi, H., Ohta, T. and Matsuzawa, H. (1990) *J. Biol. Chem.* **266**, 3186.
47. Schultz, S.C. and Richards, J.H. (1986) *Proc. Natl. Acad. Sci. U.S.A.* **83**, 1588.
48. Carroll, S.S. (1987) Ph.D. Thesis, California Institute of Technology.
49. Healy, W.J. (1989) Ph.D. Thesis, California Institute of Technology.
50. Long, D.M. (1991) Ph.D. Thesis, California Institute of Technology.
51. Healy, W.J., Labgold, M.R., and Richards, J.H. (1989) *Proteins* **6**, 275.
52. Emerling, M.R. (1992) Ph.D. Thesis, California Institute of Technology.
53. Hollenbaugh, D.L. (1991) Ph.D. Thesis, California Institute of Technology.
54. Dalbadie-McFarland, G., Riggs, A.D., Morin, C., Itakura, K., and Richards, J.H. (1982) *Proc. Natl. Acad. Sci. U.S.A.* **79**, 6409.
55. Sigal, I.S., Degradó, W.F., Thomas B.J., and Pelleway, J.R. (1984) *J. Biol. Chem.* **259**, 5327.
56. Richards, J.H. (1986) *Nature (London)* **323**, 11.

## **Chapter 2**

### **Site-Saturation of Residue 132 in RTEM-1 $\beta$ -lactamase**

## INTRODUCTION

RTEM-1  $\beta$ -lactamase is one of a group of related enzymes characterized by their ability to confer resistance to penam and cephem antibiotics such as penicillin and cephalothin (1)(Figure 1). This bacterial resistance is the result of enzyme catalyzed hydrolysis of the  $\beta$ -lactam ring, which renders the antibiotic inactive (2). The mechanism is proposed to involve an active site serine responsible for nucleophilic attack on the  $\beta$ -lactam ring, leading to an acyl-enzyme intermediate which is subsequently hydrolyzed by a bound water molecule (Figure 2).

The  $\beta$ -lactamases are classified based upon molecular weight, requirement of metal ions, substrate specificity, and sequence homology (3). RTEM-1 is a member of the class A  $\beta$ -lactamases which consists of enzymes of molecular weight approximately 29 kD, and possessing a serine as an active site nucleophile (1). Sequence homology, between 30 to 50%, is high among the class A enzymes. Other class A  $\beta$ -lactamases include those from *Staphylococcus aureus* (PC1)(4), *Bacillus licheniformis* (749/C)(5), *Bacillus cereus* (569/H)(6) and *Escherichia coli* (RTEM-1 and RTEM-2)(7).

RTEM-1  $\beta$ -lactamase is the enzyme encoded by the ampicillin resistance gene in the *E. coli* plasmid pBR322. It is synthesized as a 286 amino acid pre-protein, with a 23 amino acid leader sequence cleaved during export to the periplasm, giving a molecular weight of the mature enzyme of 28.5 kD (8). RTEM-1 has been the subject of much study due to the fact that its gene is easily manipulated. This has led to studies in protein excretion (9), expression of fusion proteins (10), and use as a selectable marker (11). Our laboratory has studied  $\beta$ -lactamase primarily as a model enzyme for examining the structural basis of catalysis (12-19).

With the publication of the crystal structure of a class A  $\beta$ -lactamase, that of *Staphylococcus aureus*, it was possible to choose residues for study based on both their locations in the enzyme and their proposed roles in catalysis (20) (Figure 3). Although no



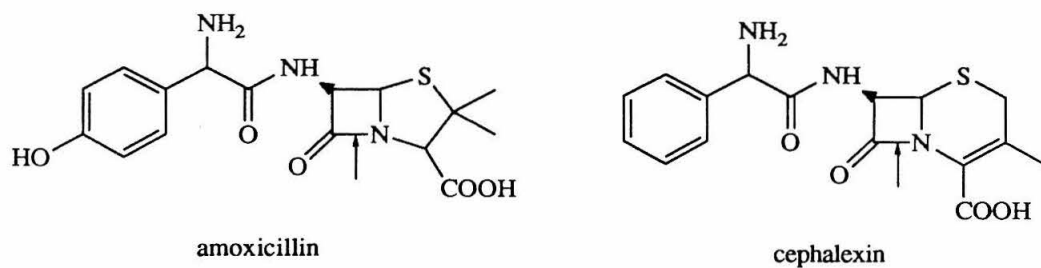


Figure 1. Representative  $\beta$ -lactam antibiotics. Amoxicillin is a member of the penam family, cephalixin is a cephem. Arrow points to bond broken during hydrolysis.

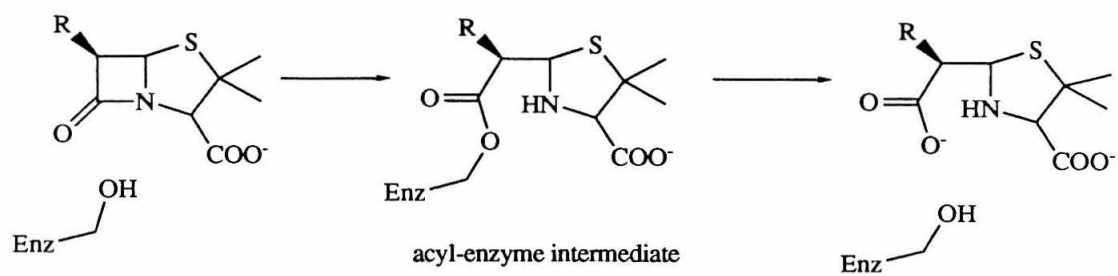


Figure 2. Overall reaction catalyzed by  $\beta$ -lactamase

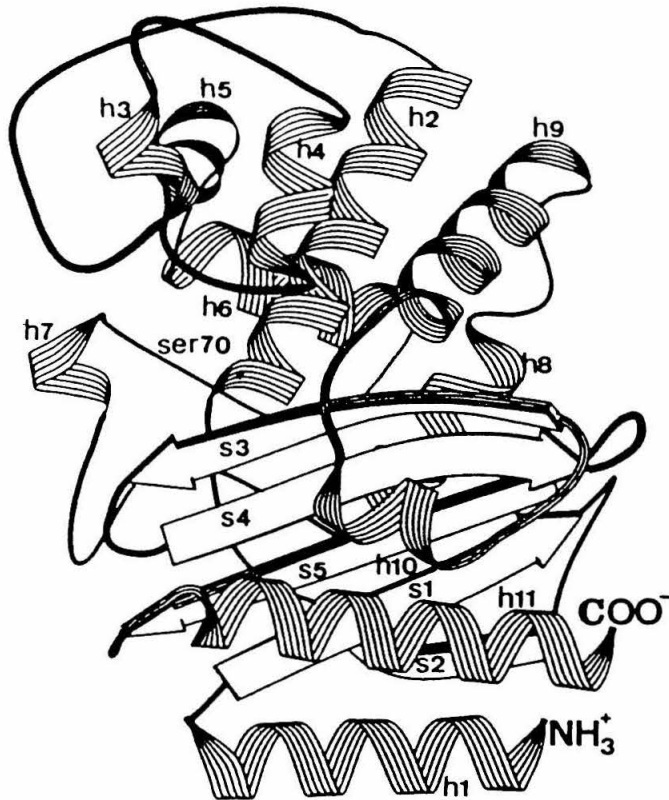


Figure 3. Structure of RTEM-1  $\beta$ -lactamase.

structure of an enzyme-substrate co-crystal had been solved, model building with ampicillin indicated that only a few modes of binding are possible. Hertzberg *et al* (20) proposed that Lys 73 and Glu 166 were involved in the catalytic mechanism along with Ser 70. These residues are separated by 2.2 Å and are both conserved among class A  $\beta$ -lactamases. Sequence alignments of the class A  $\beta$ -lactamases showed a number of conserved residues, including the so called SDN loop of residues 130-132 (Ser 130, Asp 131, Asn 132, Figure 4)(21). Further analysis of the crystal structure indicated that Asn 132, was in or near the putative active site (Figure 5).

Mutagenesis of Glu 166 showed that this residue is involved in deacylation, illustrated by the detection of a stable acyl-enzyme intermediate (22). One of these deacylation-deficient mutants, E166N, was used by Strynadka *et al.* to crystallize the acyl-enzyme intermediate (23). Analysis of this structure, the first  $\beta$ -lactamase structure with substrate in the active site, revealed the identity of many other residues involved in substrate binding and/or catalysis, and suggested a catalytic mechanism (Figure 6).

Asn 132 was proposed to be important in binding substrate and also function as a hydrogen bond acceptor, orienting the amine functionality of Lys 73. Since Lys 73 has been suggested as being the general base responsible for assisting Ser 70 in acylation, any residue interacting with Lys 73 should influence catalysis. Thus changes at position 132 should affect both substrate binding and acylation. A previous study by Jacob *et al.* generated two mutations at position 132 (21). To further probe the function of residue 132, site-saturation mutagenesis was performed, generating all 20 possible amino acids at position 132. Subsequent analysis of these mutants indicate that residue 132 does indeed participate in substrate binding and acylation

(a) 124-A a i t m S D **N** t A a N l l t-136  
 (b) 124-A s m t y S D **N** t A n N k i i-140  
 (c) 124-A s l r y S D **N** a A q N l i l-140  
 (d) 124-A a v r s S D **N** t A g N l i f-140

Figure 4. Amino acid sequence alignment of four class A  $\beta$ -lactamases in the region of Asn 132 (in bold). The sequences are: (a) *Escherichia coli* pBR322 RTEM-1; (b) *Staphylococcus aureus* PC1; (c) *Bacillus licheniformis* 749/C; (d) *Bacillus cereus* 569/H. The numbering starts from the *n*-terminus of the longest form of the *B. licheniformis* enzyme that has been isolated, and takes account of the gaps postulated in the currently known sequences to obtain optimal matching (1).

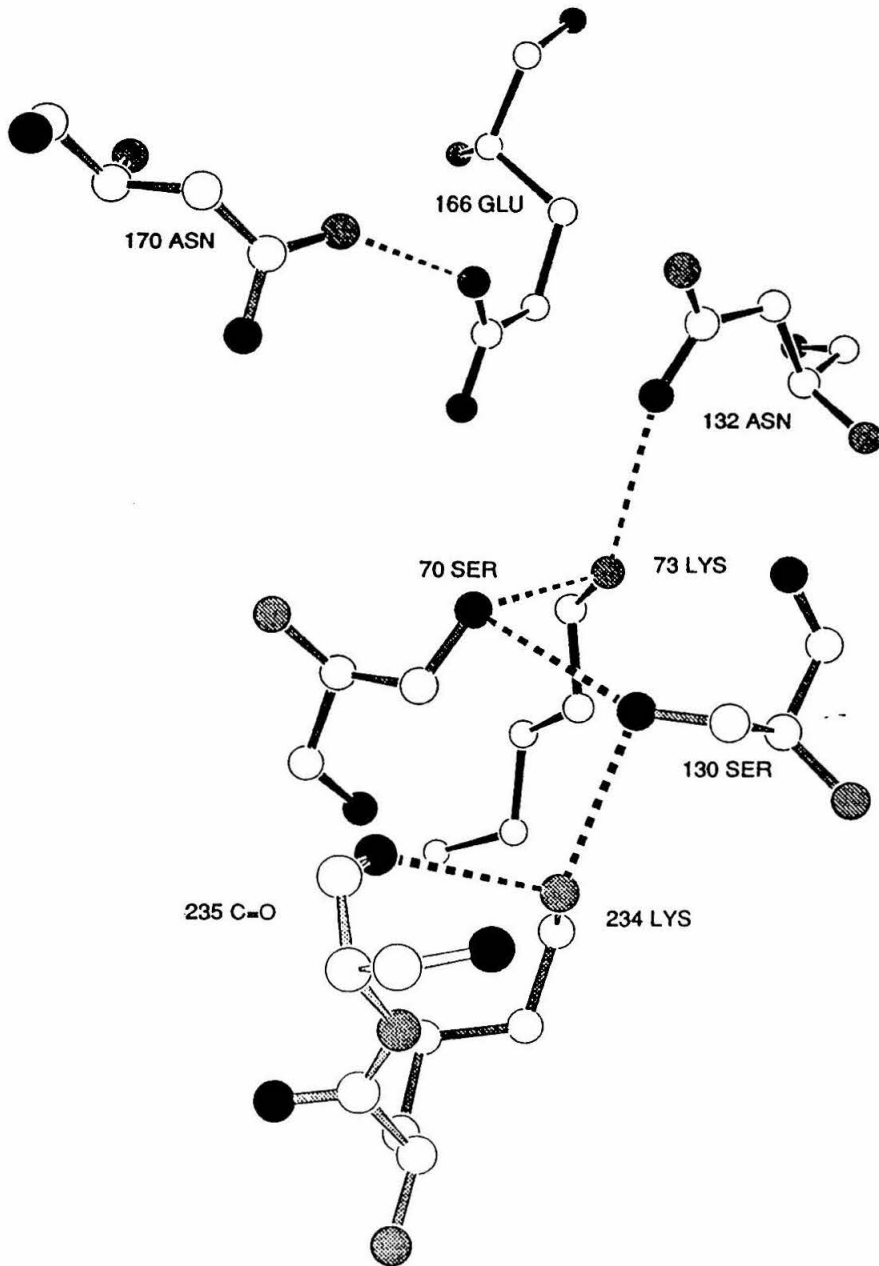


Figure 5. Arrangement of residues in the active site of RTEM-1  $\beta$ -lactamase

## MATERIALS AND METHODS

*Enzymes and Chemicals.* Enzymes were purchased from Boehringer Mannheim Biochemicals, New England Biolabs, and Promega. Antibiotics were from Sigma. Radioactive compounds were supplied by Amersham. Isopropyl- $\beta$ -thiogalactoside (IPTG) was from International Biotechnologies Inc. (IBI). Molecular biology grade reagents agarose, acrylamide, phenol, chloroform, ammonium persulfate were from Bio Rad.

*Bacterial Strains.* *Escherichia coli* were used in all experiments. Plasmid DNA was grown in strain HB101 (24); the pJN expression vector was grown in strain D1210, which is lac<sup>iQ</sup>. Culture media was L broth unless otherwise indicated. Cells were made competent for transformation of plasmid DNA using a process adapted from Hanahan (25).

*DNA.* Oligonucleotides were synthesized by the Caltech Microchemical Facility using phosphoramidite chemistry (26) on an Applied Biosystems automated DNA synthesizer 380A. Degenerate oligonucleotides were made equimolar in A, C, G, and T at positions 1 and 2 of the codon, and in C and G at position 3. These oligonucleotides were purified by preparative polyacrylamide gel electrophoresis.

Wild-type plasmid pBR322 and bacteriophage M13 mp18 replicative form (RF) DNA were purchased from Bethesda Research Laboratories. Mutant plasmids and RF phage were purified from *E. coli* by alkaline lysis method (27). Single-stranded phage DNA was prepared from phage supernatant by precipitation with 20% polyethylene glycol-6000/2.5 M NaCl (28) followed by phenol/chloroform extraction and ethanol precipitation.

Restriction digest typically used 10-20  $\mu$ g plasmid DNA, 2-5 units of restriction enzyme, and 2  $\mu$ l 10X digest buffer in 20  $\mu$ l at 37°C for 1-2 hours. DNA restriction fragments were run in 1.2% low melt agarose gels, visualized with ethidium bromide, and

isolated by established procedures (29).

*Oligonucleotide-directed Mutagenesis.* Two new restriction endonuclease sites were added to facilitate cassette mutagenesis and screening. Oligonucleotide-directed mutagenesis (Figure 6) of the existing  $\beta$ -lactamase gene in a modified pBR322 plasmid (30) was used to create a *Sac* I site at 3748 bases (Ambler numbering), and a *Ksp* I (*Sac* II) site at 3712. This was accomplished using the *in vitro* mutagenesis system<sup>TM</sup> by Amersham (31). After cloning the 2958 bp *Pst* I/*Sal* I fragment from pBR322 into RF M13 mp18 using standard procedures (29), single stranded phage was isolated and annealed to the oligonucleotides coding for creation of silent mutations creating *Sac* I and *Ksp* I restriction sites by heating to 95°C and slowly cooling to room temperature. Mutagenesis was then done using the Eckstein protocol (28). Twenty plaques were tested and sequenced using the Sanger dideoxy method (32). DNA having the desired mutations were subcloned back into pBR322 to produce pJN-Sax (Figure 7). The presence on the *Sac* I and *Ksp* I sites were then confirmed by restriction mapping.

*DNA Sequencing.* Plasmid DNA was sequenced using a modification of the Sanger dideoxy method for denatured, double-stranded DNA (32). Plasmid DNA together with sequencing primer was boiled for 5 min., then snap frozen in dry ice/ethanol. Chain extension reactions were performed with a SEQUENASE<sup>TM</sup> kit from United States Biochemical (33). Radioactive labeling was accomplished with  $\alpha$ -<sup>35</sup>S-dATP. Labeled DNA was separated on 8% polyacrylamide sequencing gels, and resulting gels were dried *in vacuo*. Kodak AR x-ray film was then exposed in the presence of the sequencing gel for 12 hours.

*Cassette Mutagenesis.* Cassette mutagenesis is a technique wherein mutations can be introduced into a gene of interest using complementary synthetic oligonucleotides in conjunction with restriction endonucleases, followed by ligation (Figure 8). Provided that convenient restriction site are available in the gene, mutagenesis of one or more residues



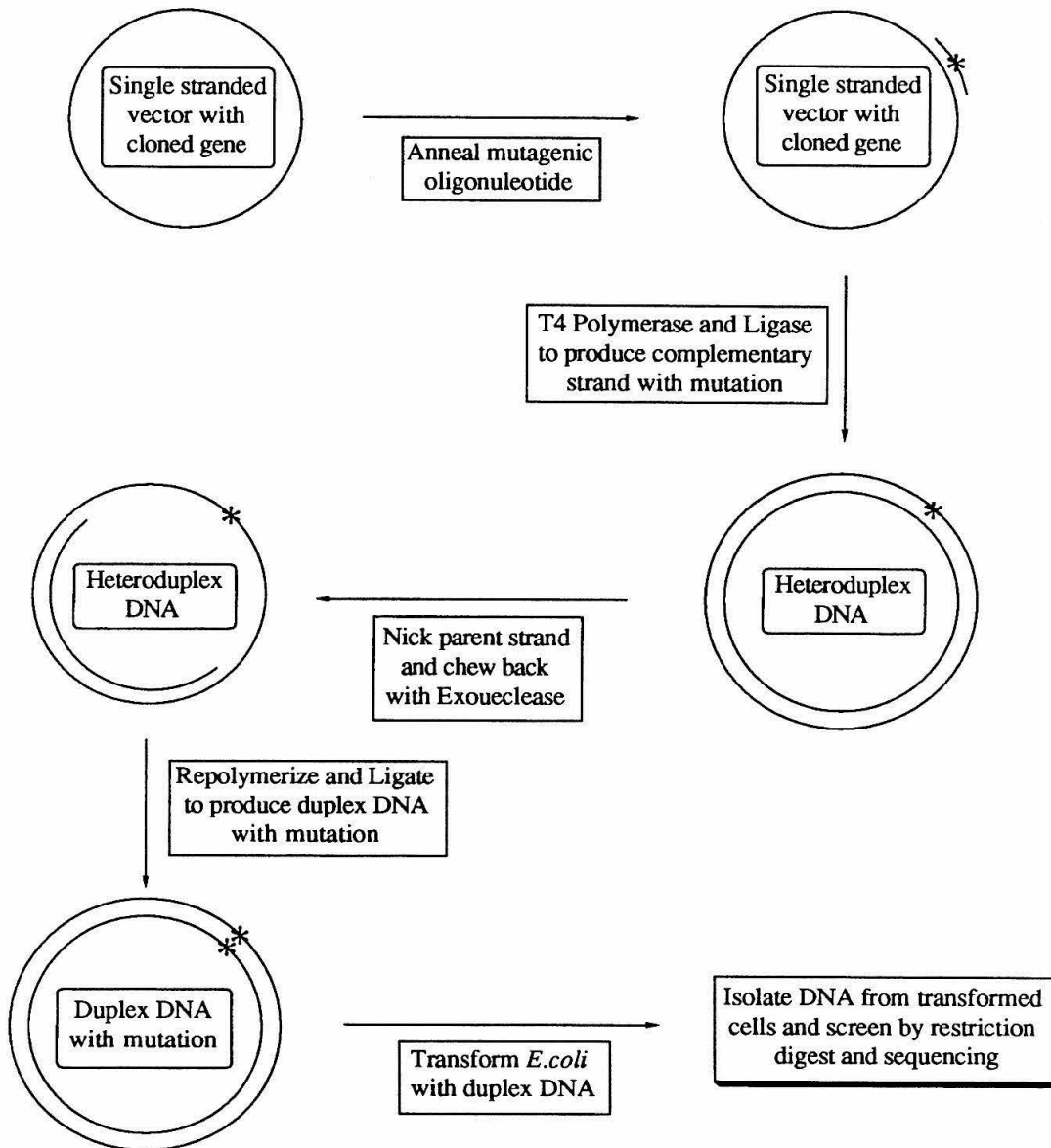


Figure 6. Scheme for introduction of unique restriction sites by site directed mutagenesis.

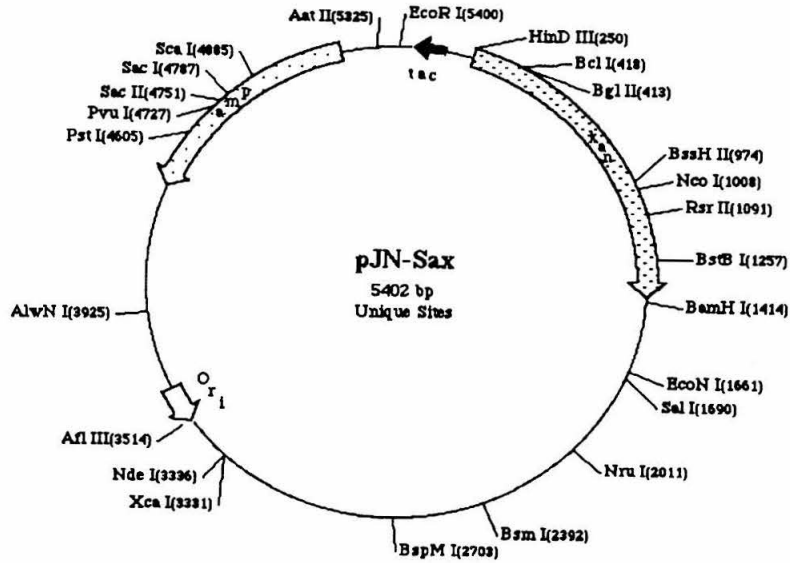


Figure 7. Map of pJN-Sax vector.

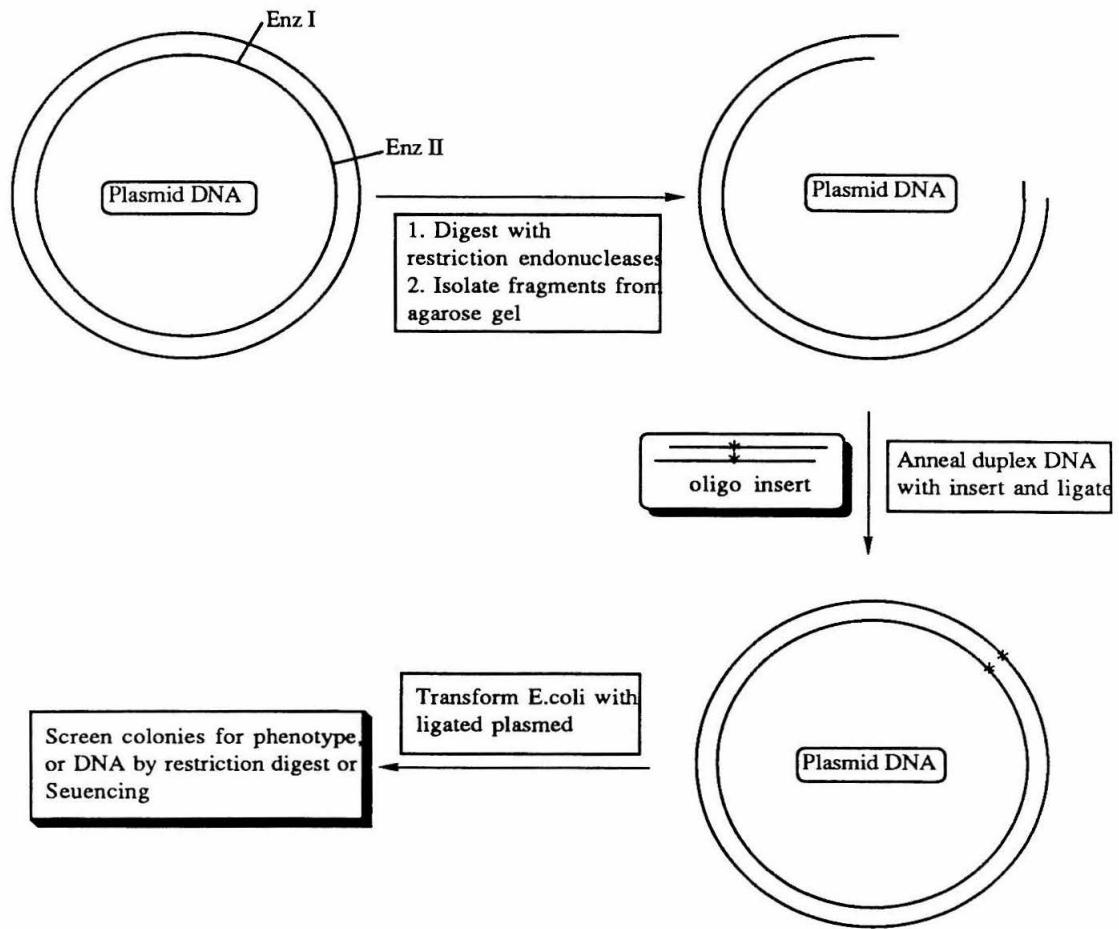


Figure 8. A schematic overview of cassette mutagenesis.

can be accomplished with out the use of a single stranded vector or subcloning routines. The complementary synthetic oligonucleotides containing a degenerate codon at residue 132 and overhangs corresponding to *Sac* I and *Pvu* I restriction endonuclease sites (Figure 10) were kinased by standard procedures (29) and annealed by heating to 95°C in 10 mM Tris-HCl, pH 7.5, 10 mM MgCl<sub>2</sub>, 50 mM NaCl, and then slowly cooled to room temperature. A three fragment ligation was then carried out as follows: pJN-Sax was linearized with *Bam*H I and isolated from a low melting agarose gel (29). The linear DNA was then digested with *Pvu* I (tube 1) and *Sac* I (tube 2). The 3313 bp piece from the *Pvu* I digest and the 2029 bp fragment from the *Sac* I digest were isolated from a low melt agarose gel. These two fragments were mixed with equimolar concentrations of the synthetic cassette insert, and ligated in a mixture of 10 mM Tris-HCl, pH 8.0, 5 mM MgCl<sub>2</sub>, 5 mM DTT, 1 mM ATP, and 1 unit T4 DNA ligase for 2 hours at room temperature. 10 µl of this ligation mixture were transformed directly into competent *E. coli*. strain D1210 and cells were spread onto L plates containing 50 µg/ml kanamycin. The plasmid DNA was isolated by alkaline lysis, and subjected to restriction analysis and sequencing. Successful insertion of the cassette results in the removal of the *Ksp* I site, therefore allowing a quick screen for positive mutants.

*Phenotypic Screening.* Following identification of all 19 mutants, each was grown to late log phase in LB/kan. 10 µl of cells were diluted 10<sup>5</sup> and plated onto L plates with varying concentrations of ampicillin, benzyl penicillin, and cephalothin (25, 50, 75, 100, 200, 400, 800, 1200, 1600, 2000 µg/ml). These plates were incubated at 37°C for 12 hours, and presence or absence of colony growth for each mutant noted.

*Western Blots.* The levels of mutant β-lactamase present in the cells were assayed by Western blot analysis of whole-cell lysates prepared in the following manner: *E. coli* were grown in LB containing kanamycin (50 µg/ml) to late log phase (OD<sub>u</sub> = 1) at 37°C. 1.5 ml of each culture was centrifuged to pellet the cells, which were then resuspended in



100  $\mu$ l of protein loading buffer and heated to 95°C for 10 minutes to lyse the cells. Aliquots of 20  $\mu$ l each were loaded onto a 15 cm 15% polyacrylamide gel (4% stack) and electrophoresed at 5 mA for 12-16 hours. Protein was then transferred from the gel onto DEAE nitrocellulose using a Bio-Rad Transblot cell (120 V for 6 hours).  $\beta$ -lactamase was visualized following binding of rabbit anti- $\beta$ -lactamase (34) using the highly sensitive Vectastain ABC immunoperoxidase system (35).

*Protein Expression and Purification.* To facilitate expression, the mutant  $\beta$ -lactamases were subcloned into pJN, an expression vector which was developed in this lab (36). It contains the  $\beta$ -lactamase gene under control of the tac promoter (37), and well as a kanamycin gene for a selection marker. Synthesis of  $\beta$ -lactamase is induced by the addition of IPTG.

One liter cultures of *E.coli* D1210 containing mutant plasmid were grown in X broth (25 g Tryptone, 7.5 g yeast extract, 20 ml 1 M MgSO<sub>4</sub>, 50 ml 1 M Tris-HCl pH 7.5 per liter) containing 50  $\mu$ g/ml kanamycin for 12-14 hours at 37°C. IPTG was added to a final concentration of 0.1 mM and growth continued for 1 hour at 37°C. Cells were centrifuged in 250 ml bottles in a GSA rotor for 10 minutes at 10,000 rpm.  $\beta$ -lactamase, which is located in the periplasm, was released by osmotic extrusion (38). Briefly, pelleted cells were resuspended in 1/10 of the culture volume in a sucrose solution (450 g. sucrose, 0.5 g. EDTA, 25 mM Tris pH 8.0, per liter). This was shaken for 30 minutes, followed by centrifugation at 7000 rpm for 30 minutes. The cells were then resuspended in cold water (equal volume to sucrose solution) and shaken at 4°C for thirty minutes. Centrifugation at 12000 rpm for 45 minutes afforded relatively cell free periplasmic lysate. The sample containing the periplasmic proteins was reduced to ~1 ml using a Diaflow cell (Amicon) under nitrogen. The resulting solution was then filtered through a Schleicher and Schuell 0.22 mm Uniflow filter to remove any cellular debris.

Further purification was carried out using FPLC (fast protein liquid

chromatography) first with a HR16/10 Fast Flow MonoQ™ column, followed by a HR10/10 MonoQ™, both by Pharmacia. Crude protein was loaded onto the fast flow column, and the column was washed in 100% A (25 mM triethanolamine (TEA), pH 7.65). Then crude  $\beta$ -lactamase was eluted with 20%B (25 mM TEA, 1M NaCl). This protein was loaded onto the HR 10/10 column in 25 mM TEA and eluted with a salt gradient. The gradient used was: t=0, 100% A, t=5, 100% A, t=35, 80%A, 20%B, t=45, 100% B. The flow rate was 1.0 ml/minutes. Elution was monitored by A280. Peak fractions were pooled and dialyzed versus 50 mM potassium phosphate, pH 7.0. Protein concentrations were estimated from OD<sub>280</sub> using an extinction coefficient of 29,400 M<sup>-1</sup>cm<sup>-1</sup>(2). Samples were run on 15% polyacrylamide gels (as in western blot ) and stained with Coomassie blue to gauge purity.

*Kinetics.* Michaelis-Menten kinetic parameters ( $k_{cat}$ ,  $K_M$ , and  $k_{cat}/K_M$ ) for mutant  $\beta$ -lactamases were determined by Hanes plots using initial rates (39). Reactions were carried out at 30°C in 50 mM potassium phosphate pH 7.0. All reagent were maintained at 30°C prior to beginning the assay to avoid error from temperature flux. An HP 8420 spectrophotometer was used for the assays, with quartz cells of pathlength 1 cm at wavelength 232 nm.

*Identification of Acyl-enzyme Intermediate.* If the deacylation step is primarily affected by the mutation at 132, acyl-enzyme would build up. Previous studies on residue 166 in RTEM-1  $\beta$ -lactamase have shown that this acyl-enzyme can be detected using <sup>14</sup>C-benzyl penicillin (22). <sup>14</sup>C-benzyl penicillin (Amersham) was reacted with concentrated osmotic extrusion from 10 mls of saturated cells according to published procedures (22). The mutant E166V was run as a positive control, as it has been shown that this mutation causes acyl-enzyme to build up (40). Reactions were loaded onto 15% polyacrylamide gels and electrophoresed as in western blot. The gels were fixed (40% MeOH:10%HOAc:50%H<sub>2</sub>O), followed by treatment with Amplify™ (Amersham)

according to manufacturers directions. The gel was dried *in vacuo*, and Kodak AR film was exposed in the presence of the gel.

## RESULTS

*Mutagenesis.* Oligonucleotide-directed mutagenesis was used to create unique *Sac* I and *Ksp* I sites within the existing  $\beta$ -lactamase gene (from pBR322) in M13. Restriction endonuclease (Figure 11) and sequencing analysis (Figure 12) confirmed the presence of these sites. Site-saturation of residue 132 was accomplished using cassette mutagenesis with oligonucleotides degenerate at codon 132. The cassette DNA contained sticky ends complimentary to *Pvu* I and *Sac* I sites. A three fragment ligation with these two enzymes along with *Bam*H I was used to insert the cassette into the  $\beta$ -lactamase gene (Figure 13). Following ligation and transformation, colonies were picked, their plasmid DNA isolated, screened by restriction digest with *Ksp* I, and positive colonies sequenced. 60 colonies were sequenced, with 17 mutants found (Figure 14). The mutations N132I, N132Q, N132V were not found. Oligonucleotide cassettes were then synthesized coding specifically for each of these mutants (N132I-ATC, N132Q-CAG, N132V-GTG), and a similar three piece ligation was performed. Colonies were isolated, plasmid DNA sequenced, and identity of the mutants confirmed.

*Phenotypic Screening.* Each of the mutants were grown to late log phase and plated on varying concentrations of antibiotic following dilution. The results of these experiments are shown in Figure 15. Only four mutants, N132C, N132D, N132E, N132Q showed any appreciable activity. Most of these would be considered conservative changes, with the exception of N132C. These experiments were repeated under a number of dilution conditions to insure repeatable results.

*Stability of Mutant Enzymes.* The stability of mutant enzymes produced were assayed by Western blot analysis. All mutants exhibited expression and stability's



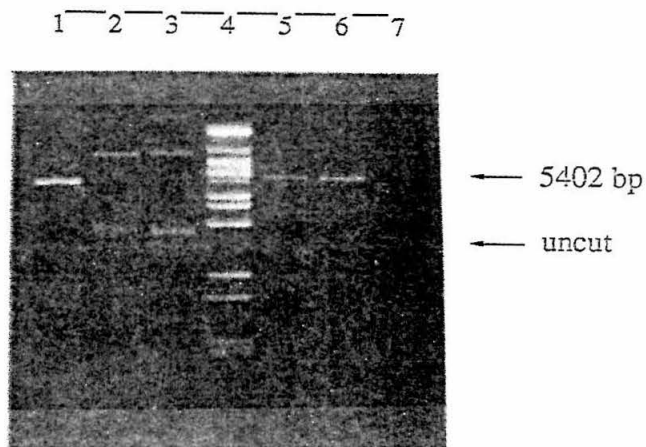


Figure 10. Agarose gel showing the presence of *Sac* I and *Sac* II restriction sites in pJN-Sax. Lane 1, pJN-N132C cut with *Sac* I. Lane 2, pJN-N132C cut with *Sac* II. Lane 3, uncut pJN-N132C. Lane 4, molecular weight marker. Lane 5, pJN-Sax cut with *Sac* I. Lane 6, pJN-Sax cut with *Sac* II. Lane 7, uncut pJN-Sax. Successful ligation of N132X with synthetic cassette removes *Sac* II site.

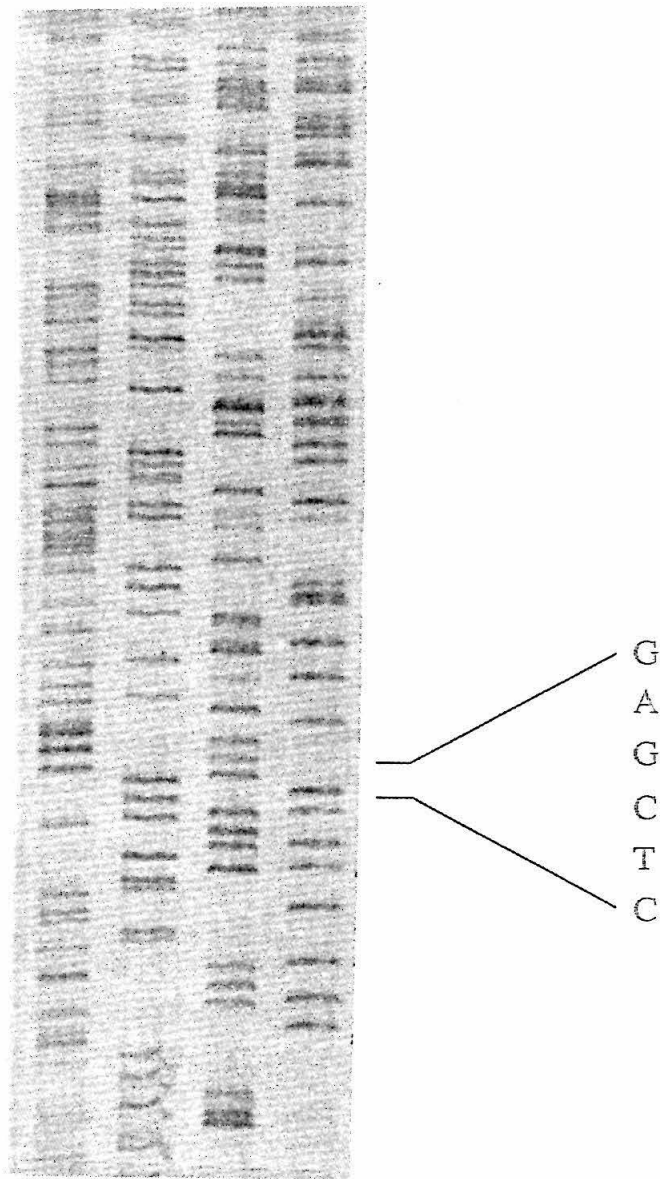


Figure 11. Sequencing gel showing presence of *Sac* I site (GAGCTC) in pJN-Sax.

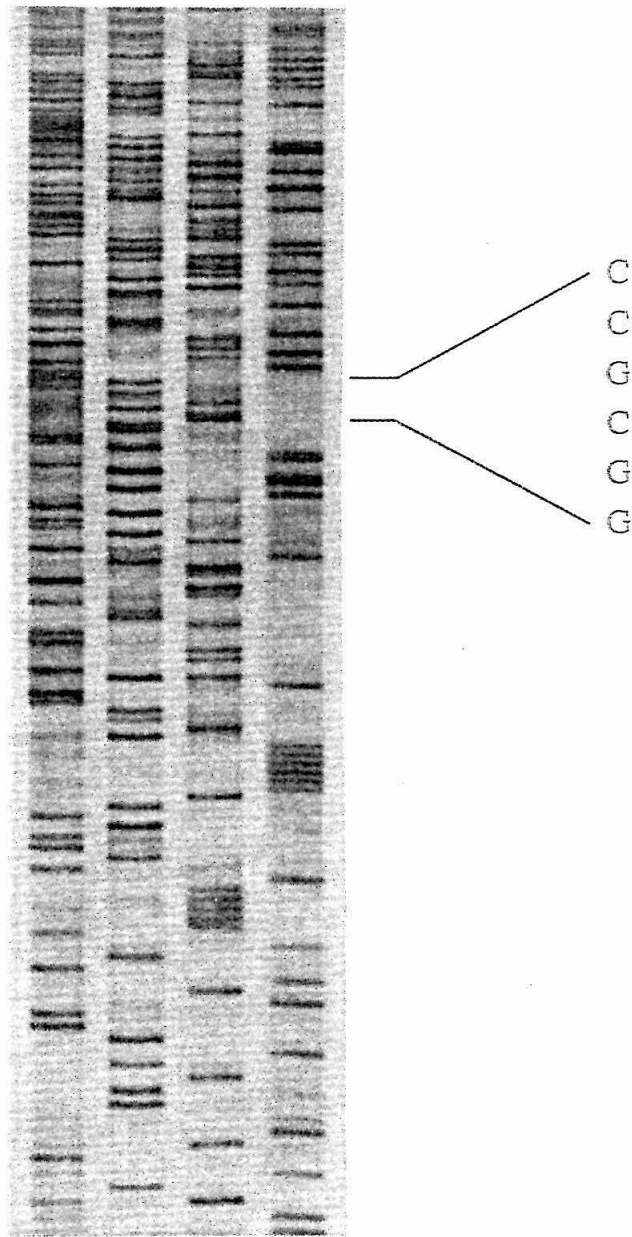


Figure 12. Sequencing gel showing the presence of *Sac* II site (CCGCGG) in pJN-Sax.

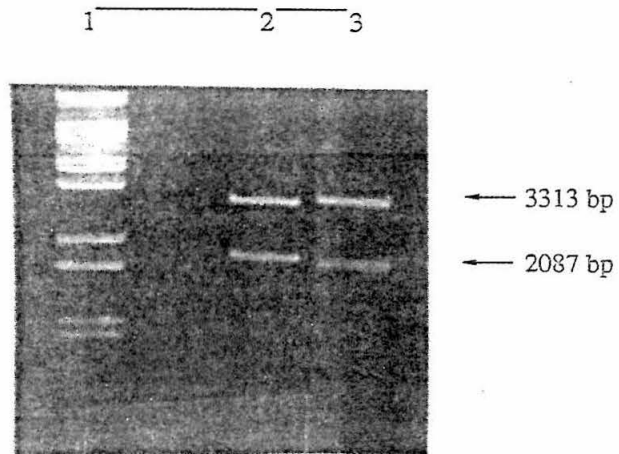


Figure 13. Agarose gel showing fragments used in cassette mutagenesis of residue 132. Lane 1, molecular weight marker. Lane 2, pJN-Sax cut with *Bam*H I and *Pvu* I. Lane 3, pJN-Sax cut with *Bam*H I and *Sac* I.

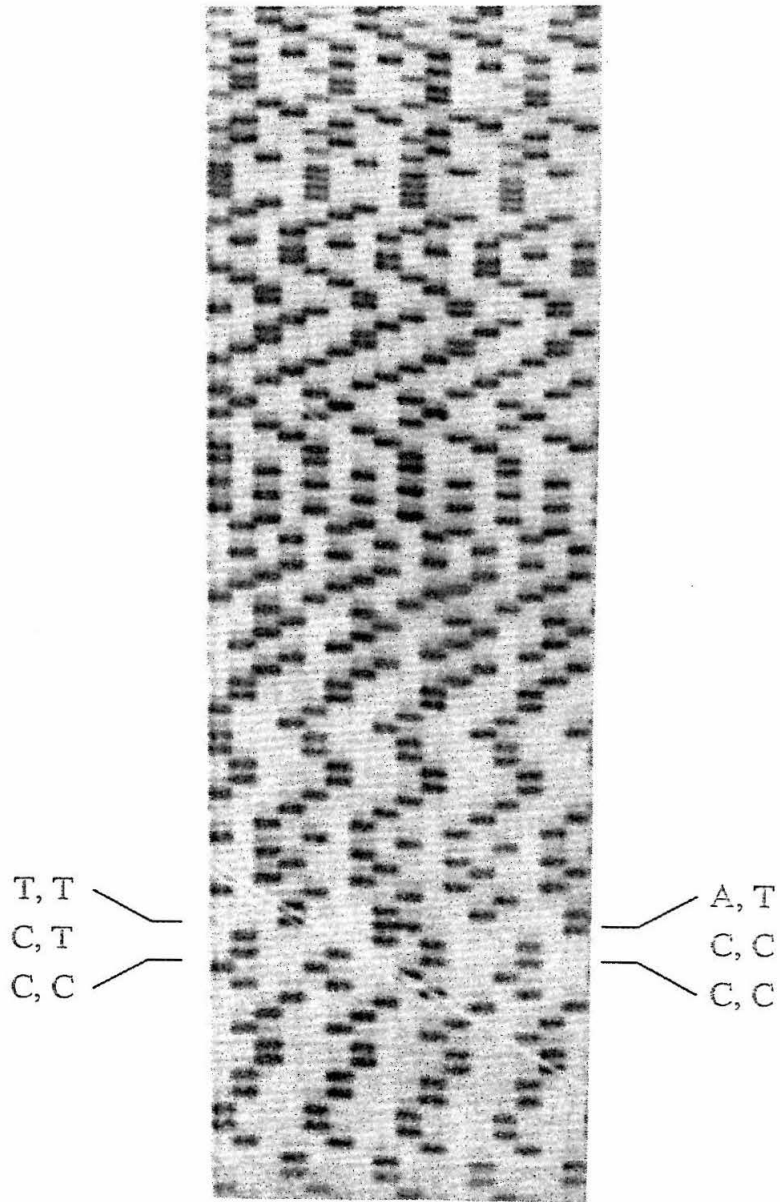


Figure 14. Sequencing gel of four N132X colonies; TCC (Ser), TCC (Phe), ACC (Thr), and TCC (Ser).

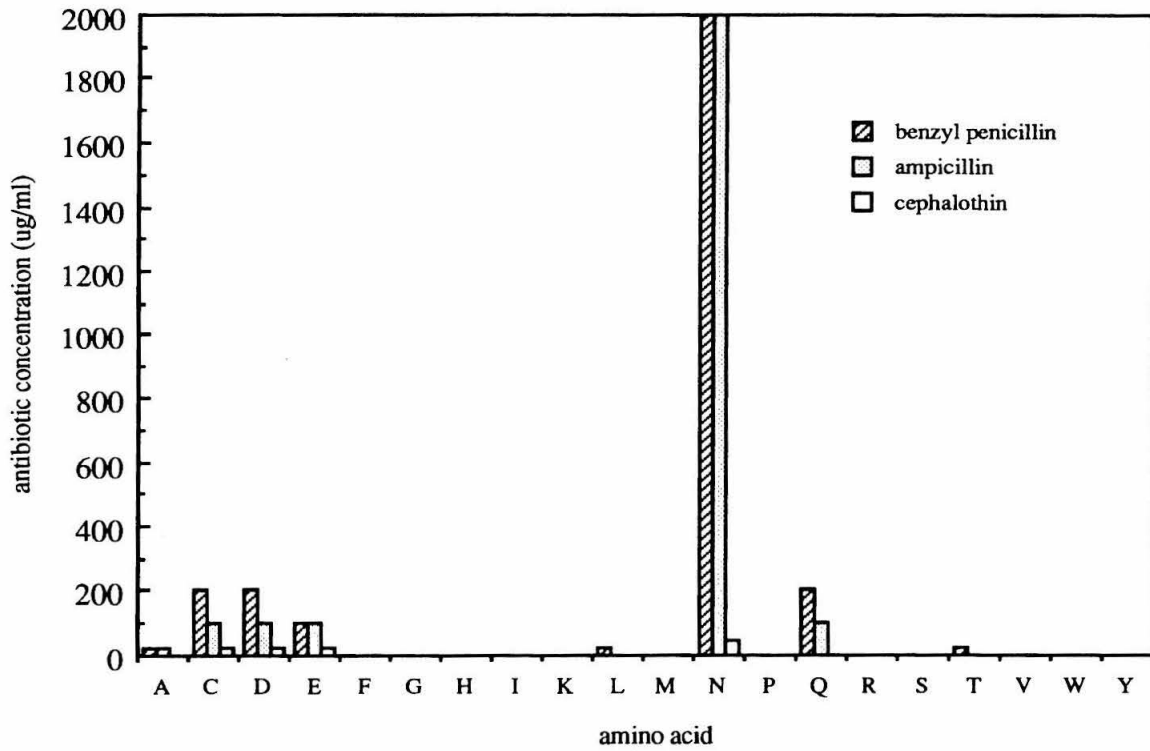


Figure 15. Plot of phenotypic resistance for N132X mutants.

comparable to wild-type (data not shown). This indicates that the lack of activity of the mutants is due to structural changes in the protein rather than instability, incorrect folding, or lack of protein expression.

*Isolation of Mutant Enzymes.* Three mutants (N132C, N132D, N132Q) were chosen for kinetic analysis, as these appeared to possess significant enough activity to assay by spectrophotometric means. Two liters of media with proper antibiotic were grown to saturation at 37°C. IPTG was added (24 mg/l) and incubation continued for 1 hour. Following osmotic extrusion, concentration in an Amicon unit afforded ~10ml of crude protein. This was chromatographed first by FPLC on a HR16/10 Fast Flow column with the 20%B cut retained. After dialysis into Buffer A and concentration by Amicon,  $\beta$ -lactamase was purified on a Mono Q<sup>TM</sup> column by FPLC (Figure 16). Fractions containing  $\beta$ -lactamase and purity were identified by PAGE (Figure 17).

*Kinetics.* Steady-state kinetic analysis of three mutants (N132C, N132D, N132Q) was undertaken, with the kinetic scheme shown in Figure 18. The hydrolysis reaction is followed by decrease in absorbance at 232 nm, which indicates the opening of the  $\beta$ -lactam ring (Figure 19). The results are shown in Table 1. Increases in  $K_M$  for the three mutants indicate that residue 132 is important in binding substrate. The dramatic decrease in  $k_{cat}$  ( $\sim 10^{-4}$ ) indicates that 132 is significantly involved in catalysis, most probably acylation.

*Presence of Acyl-Enzyme Intermediate.* Previous experiments in our lab and elsewhere have indicated that residue 166 is involved in deacylation, functioning as a general base (22, 41). Mutations at residue 166 give rise to a stable acyl-enzyme intermediate which can be trapped. Reaction of 166 mutants with <sup>14</sup>C-benzyl penicillin lead to accumulation of radio-labeled  $\beta$ -lactamase, which can be identified by PAGE and autoradiography. This assay was used to probe for stable acyl-enzyme intermediates with 132 mutants, which would indicate the participation of residue 132 in deacylation. A

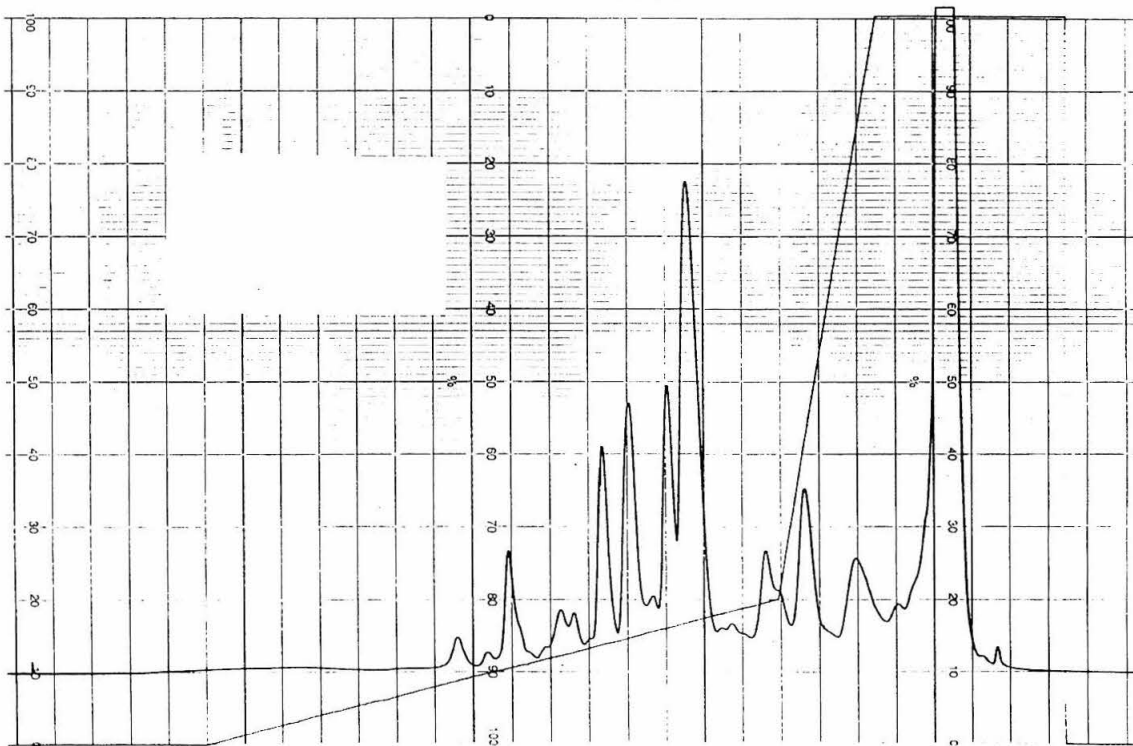


Figure 16. FPLC trace for purification of N132C mutant.  $\beta$ -lactamase is peak @ 15% B



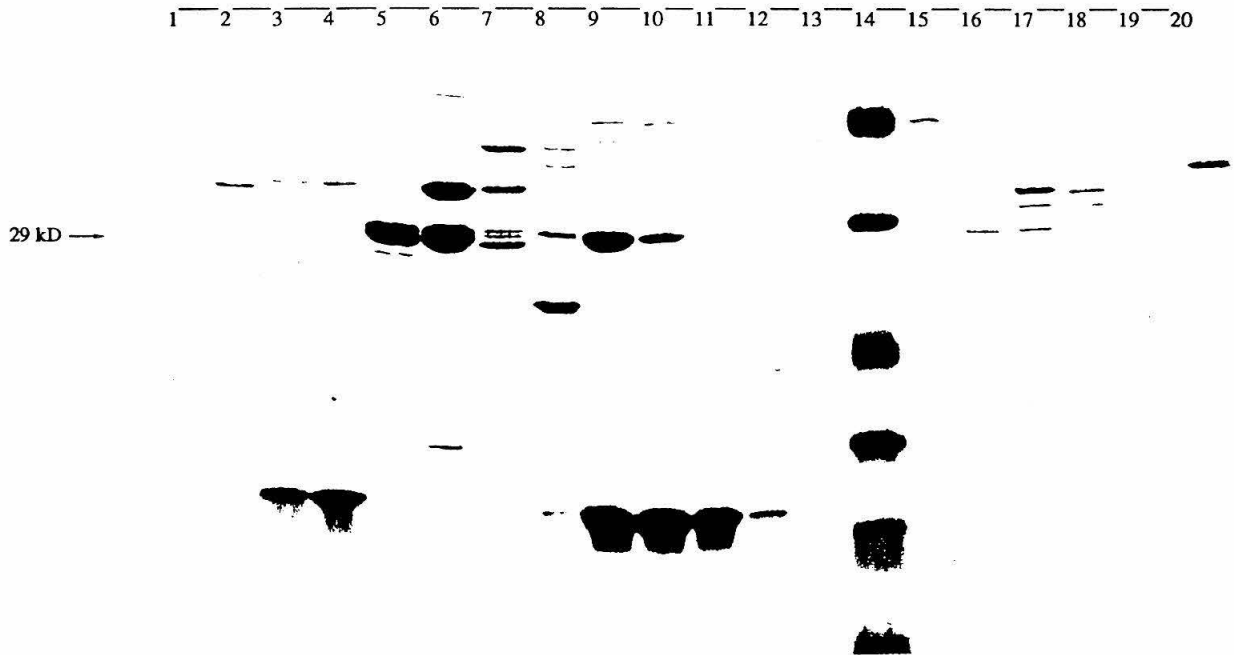


Figure 17. PAGE analysis of FPLC fractions for purification of N132C mutant. Fractions 5 and 6 contain  $\beta$ -lactamase.

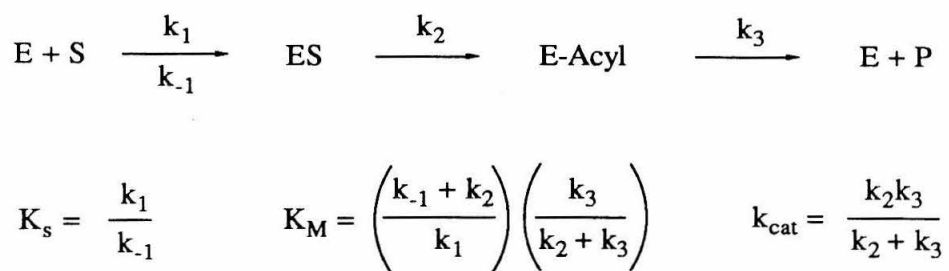


Figure 18. Kinetic scheme for  $\beta$ -lactam hydrolysis catalyzed by  $\beta$ -lactamase.

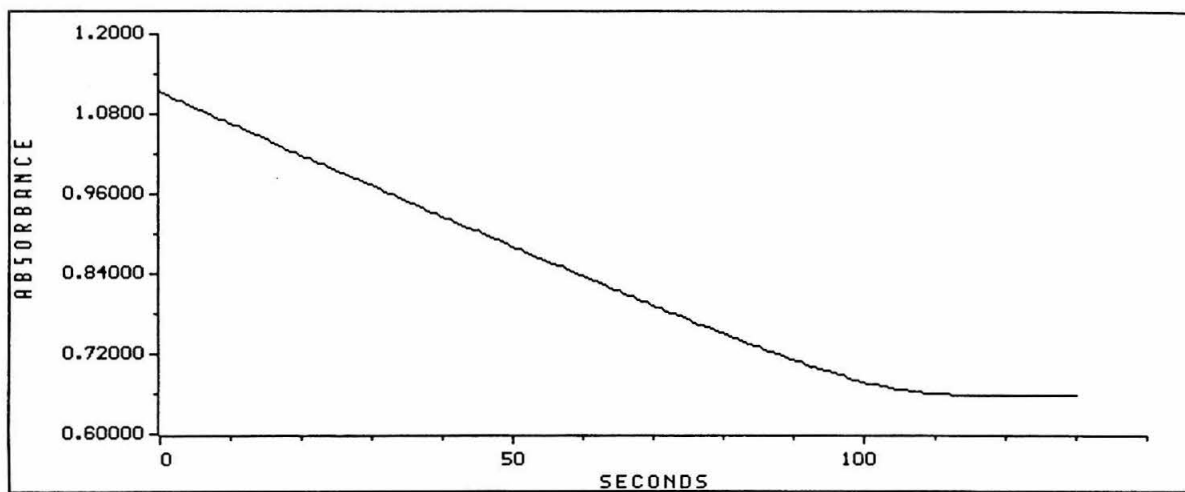


Figure 19. Plot of absorbance vs. time for the hydrolysis of benzyl penicillin catalyzed by N132C  $\beta$ -lactamase. Decrease in absorbance at 232 nm follows ring opening.

	<u><math>k_{cat}</math> (s<sup>-1</sup>)</u>	<u><math>K_M</math> (μM)</u>	<u><math>k_{cat}/K_M</math> (s<sup>-1</sup>M<sup>-1</sup>)</u>	<u>relative rate</u>
WT	980	42	$2.5 \times 10^7$	1
N132Q	2.0	400	$5.0 \times 10^3$	$2.2 \times 10^{-4}$
N132C	0.43	130	$3.3 \times 10^3$	$1.4 \times 10^{-4}$
N132D	0.11	120	$9.2 \times 10^2$	$4.0 \times 10^{-5}$

Table 1. Kinetic parameters for hydrolysis of benzylpenicillin catalyzed by RTEM-1 β-lactamase

number of 132 mutants (A, C, D, F, G, M, Q, S) were assayed along with E166V as a positive control. Repeated attempts to see stable intermediates with 132 mutants were unsuccessful (Figure 20). This negative result indicates that mutations at position 132 either affect acylation only, or acylation and deacylation equally.

## DISCUSSION

The level of understanding of enzymatic mechanisms has increased greatly over the past 15 years, largely due to crystallographic and mutagenesis studies. However, the subtleties of catalysis remain elusive. In the past our lab has investigated many of the catalytically important residues by site-saturation mutagenesis. We have utilized site-saturation for a number of reasons including ease of mutation, cloning efficiencies and screening. But primarily, generation of all 20 amino acids at a specific residue has led to results not anticipated *a priori*. For example, site-saturation of glutamate 166, the residue believed to be responsible for deacylation of the acyl-enzyme intermediate, gave three mutants with activity; aspartate, histidine and tyrosine (42). Previous reports of mutagenesis at residue 166 did not include the E166H and E166Y mutations (22). The activity of these unexpected functional mutations leads to a greater understanding of the structural requirements of catalysis. Thus, site-saturation mutagenesis has assumed an important role in our lab's investigations of  $\beta$ -lactamase activity.

Asn 132 was originally chosen as a target following analysis of the *B. licheniformis* structure by Moews *et al.* (43). The asparagine side chain amide appeared to be strategically positioned to function as a hydrogen bond donor and/or acceptor for substrate binding and/or catalysis. Site-saturation of residue 132 shows that only four amino acid substitutions give appreciable activity.

Phenotypic screening is the initial test for mutants generated. Resistance to antibiotics indicates activity of the mutant  $\beta$ -lactamase enzyme. Again site-saturation yielded some

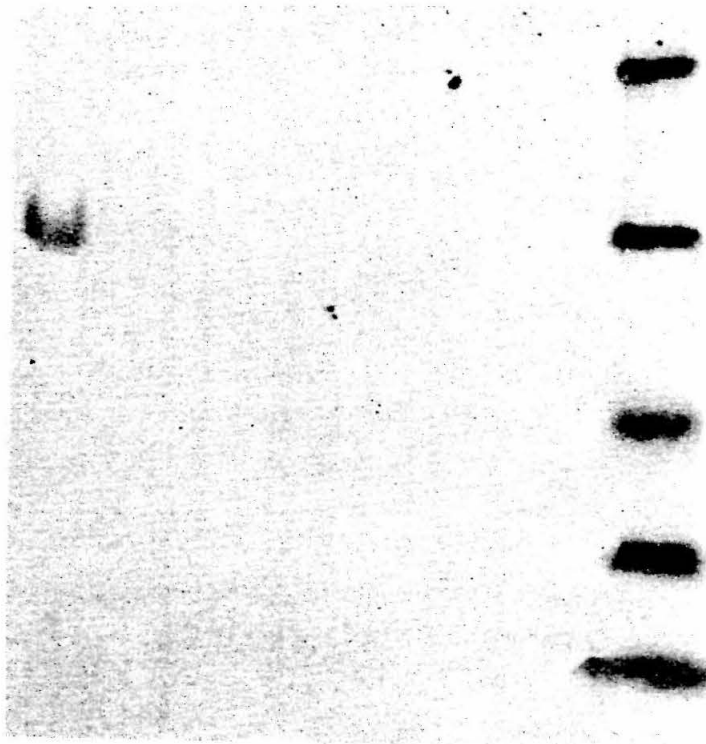


Figure 20. Autoradiograph of PAGE using N132X mutants and  $^{14}\text{C}$ -benzyl penicillin. Lane 1, E166V positive control. Lane 2, N132A. Lane 3, N132C. Lane 4, N132D. Lane 5, N132N (negative control). Lane 6, N132S. Lane 7, molecular weight marker.

surprise. the N132Q mutant showed activity; this is not surprising as this is a conservative change, only increasing the side-chain length by one CH<sub>2</sub> unit. Similarly, the activity of N132D and N132E were not unexpected. This result does indicate that the side chain group is probably functioning as a hydrogen bond acceptor. If it were a donor, the carboxylate side chains, which should be deprotonated at pH 7 ( $pK_a \sim 4$ ), would not possess a hydrogen atom to donate. The activity of N132C is at first surprising, especially considering the inactivity of N132S. However this result can be rationalized, again if residue 132 is considered to be a hydrogen bond acceptor. Two factors could be influencing the difference in activities of N132C and N132S. A steric argument could be put forth, as the sulfur of cysteine is larger than the oxygen of serine. Thus the cysteine side chain would extend slightly further into the active site than serine. Secondly, and possibly more importantly, the  $pK_a$  of the thiol is significantly lower than the serine hydroxyl ( $pK_a \sim 8$  vs.  $pK_a \sim 12$ ). Thus the cysteine thiol could be largely deprotonated at pH 7, serving as a much better hydrogen bond acceptor.

Further study on the active mutants involved steady-state kinetic analysis. To a gross approximation, increases in  $K_M$  would indicate a decrease in binding efficiency, indicating disruption of enzyme-substrate interactions. The three mutants investigated, N132C, N132D, N132Q all show increased  $K_M$ 's, although none by more than an order of magnitude. This suggests that residue 132 does influence substrate binding, but not to a large degree.

Mutations at 132 do have a large influence on the pseudo first-order rate constant,  $k_{cat}$ . All three mutants show  $k_{cat}$  down by at least  $10^3$ . Therefore it appears that the side-chain of residue 132 does influence catalysis. Due to the nature of the mechanism of  $\beta$ -lactamase, there are two catalytic steps that could be involved: acylation and deacylation. It has been shown that residue 166 is involved in deacylation, as illustrated by the buildup of acyl-enzyme intermediate in glutamate 166 mutants. If residue 132 is involved in

deacylation as well, a similar phenomenon would be expected. However repeated attempts to trap acyl-enzyme intermediate with 132 mutants were unsuccessful. This suggests two possibilities: either both steps are equally affected or acylation only is affected. The later explanation is more attractive, due to a number of reasons. First, the active site is separated by the substrate into two halves, with acylation taking place on one face of the substrate, and deacylation taking place on the other. Thus one would assume that a mutation would affect either one step or the other. Secondly, the recent crystal structure of the acyl-enzyme intermediate suggests that 132 is interacting with Lys 73, a residue which is thought to be directly responsible for acylation.

The publication of the acyl-enzyme structure shed light onto the intricacies of the active site, and suggested roles for many of the residues surrounding the substrate. The main feature of the mechanism put forth by Strynadka *et al* not suggested by other groups is the involvement of the amine side chain of Lys 73 in acylation; specifically that it functions as a general base, extracting a proton from the active site nucleophile Ser 70 (Figure 5). The structure also showed Asn 132 to interact with Lys 73, either serving to orient the amine base, or perhaps to help lower the  $pK_a$  of Lys 73, a necessity for it to function as a general base. Thus the mechanism suggests a catalytic importance for residue 132 specific for the acylation reaction, and our results are in line with this hypothesis (Figure 21).

It is obvious from these results that the interactions in the active site of an enzyme are many and often subtle. Identification of the main players in catalysis are often easy to identify, particularly with good crystal structures available. But the intricacies are often more elusive, as illustrated by the function of residue 132. Site-saturation shows that acceptable interactions of amino acids are difficult to predict.





## REFERENCES

1. Ambler, R. (1980) *Phil. Trans. R. Soc. Lond.* **289**, 321.
2. Datta, N., and Kontomichalou, P. (1965) *Nature* **208**, 239.
3. Sykes, R.J. (1982) *J. Infect. Dis.* **145**, 762.
4. Ambler, R. (1975) *Biochem J.* **151**, 197.
5. Meadway, R. (1969) *Biochem J.* **115**, 12.
6. Thatcher, D. (1975) *Biochem. J.* **137**, 313.
7. Sutcliffe, J. (1978) *Proc. Nat. Acad. Sci. U.S.A.* **75**, 3732.
8. Ambler, R., (1978) *Proc. Nat. Acad. Sci. U.S.A.* **75**, 3732.
9. Koshland, D., and Botstein, D. (1980) *Cell* **20**, 749.
10. Palva, I., Sarvas, M., Lechtovaara, P., Sibalow, M., and Kaariainen, L. (1982) *Proc. Nat. Acad. Sci. U.S.A.* **79**, 5582.
11. Roggenkamp, R., Kustermann-Kuhn, B., and Hollenberg, K.C. (1981) *Proc. Nat. Acad. Sci. U.S.A.* **78**, 4466.
12. Dalbadie-McFarland, G., Cohen, L.W., Riggs, A.D., Morin, C., Itakura, K., and Richards, J.H. (1982) *Proc. Natl Acad. Sci. U.S.A.* **79**, 6409.
13. Schultz, S.C. and Richards, J.H. (1986) *Proc. Natl. Acad. Sci. U.S.A.* **83**, 1588.
14. Dalbadie-McFarland, G., Neitzel, J.J., and Richards, J.H. (1986) *Biochemistry* **25**, 332.
15. Richards, J.H. (1986) *Nature (London)* **323**, 187.
16. Carroll, S.S. and Richards, J.H. (1987) *Ann. Rep. Med. Chem.* **22**, 293.
17. Schultz, S.C., Dalbadie-McFarland, G., Neitzel, J.J., and Richards, J.H. (1987) *Prot. Struc. Func. Gen.* **2**, 290.
18. Chang, Y, Labgold, M.R., and Richards, J.H. (1990) *Proc. Natl. Acad. Sci. U.S.A.* **87**, 2823.

19. Healy, W.J., Labgold, M.R., and Richards, J.H. (1989) *Prot. Strc. Func. Gen.* **1**,
20. Hertzberg, O. and Moulton, J. (1987), *Science* **236**, 694.
21. Jacob, F., Joris, B., Lepage, S., Dusart, J., Frere J. M. (1990) *Biochem J.* **271**, 399.
22. Adachi, H., Ohta, Takahisa, and Matsuzawa, H. (1991) *J. Biol. Chem.* **266**, 3186.
23. Strynadka, N.C., Adachi, H, Jensen, S.E., Johns, K., Sielecki, A., Betzel, C., Sutoh, K., James, M.N.G. (1992) *Nature (London)* **359**, 700.
24. Boyer, H. and Roullard-Dussoix, D. (1969) *J. Mol. Biol.* **41**, 459.
25. Hanahan, D. (1983) *J. Mol. Biol.* **166**, 557.
26. Beaucage, S.L. and Carruthers, M.H. (1981) *Tet. Lett.* **22**, 1859.
27. Ish-Horowitz, D., Burke, J. (1981) *Nucl. Acids Res.* **9**, 2989.
28. Nakmaye, K., Eckstein, F. (1986) *Nucl. Acids Res.* **14**, 9679.
29. Maniatis, T., Fritsch, E., Sambrook, J. (1982) "Molecular Cloning, A laboratory Manual." Cold Spring Harbor, N.Y., Cold Spring Harbor Laboratory.
30. Bolivar, S., and Backman, R. (1977) *Gene* **2**, 95.
31. Amersham (1988) "Oligonucleotide-directed In Vitro Mutagenesis System Manual," Arlington Heights, IL, Amersham Corp.
32. Sanger, F. Nicklen, S., Coulson, A. (1977) *Proc. Natl. Acad. Sci. U.S.A.* **74**, 5463.
33. U.S. Biochemicals (1988) "Sequenase Manual," Cleveland, OH, U.S. Biochemical.
34. Dalbadie-McFarland, G., Neitzel, J., and Richards, J.H. (1986), *Biochemistry* **25**, 332.
35. Vector Laboratories (1977) "Vectastain ABC Kit Manual," Burlingame CA.
36. Neitzel, J. (1987) PhD Thesis, California Institute of Technology.
37. De Boer, H.A., Comstock, L.J., and Vasser, M. (1983) *Proc. Natl. Acad. Sci. U.S.A.* **80**, 21.
38. Fisher, J., Belasco, J. Khosla, S., Knowles, J. (1980) *Biochemistry* **19**, 2895.
39. Hanes, J. (1932) *Biochem. J.* **26**, 1406.
40. Richmond, T.A., Long, D.M., Emerling, M.R., Carroll, S.S., Cho, W., Healy, W.J.,

and Richards, J.H., in preparation

41. Hollenbaugh, D.L., unpublished results.
42. Healy, W.J. (1988) Ph.D. Thesis, California Institute of Technology.
43. Moews, P.C., Knox, J.R., Dideberg, O., Charlier, P., Frer, J.M. (1990) *Prot. Struc. Func. Gen.* **7**, 156.

## **Chapter 3**

### **Combinatorial Mutagenesis of Residues 73 and 166 in RTEM-1 $\beta$ -lactamase**

## INTRODUCTION

The  $\beta$ -lactamases are a group of related enzymes characterized by their ability to confer resistance to penam and cephem antibiotics such as penicillin and cephalothin (1)(Figure 1). The antibiotic is rendered inactive by enzyme catalyzed hydrolysis of the  $\beta$ -lactam (2). The mechanism is proposed to involve an active site serine responsible for nucleophilic attack on the  $\beta$ -lactam ring, leading to an acyl-enzyme intermediate which is subsequently hydrolyzed by a bound water molecule (Figure 2).

Over 80  $\beta$ -lactamases have been identified, and divided into three categories based on sequence homology, size, and activity (3). The class A  $\beta$ -lactamases include the RTEM  $\beta$ -lactamases (RTEM-1, 2 and 3) of *Escherichia coli* (4), *Staphylococcus aureus* PC1 (5), *Bacillus licheniformis* 749/C (6), and *Bacillus cereus* 569/HI (7). All of these enzymes exhibit considerable sequence homology (~30%) and have a molecular weight of around 30 kD. There are only two class B  $\beta$ -lactamases, those of *B. cereus* and *Proteus maltophilia* (8). The class B  $\beta$ -lactamases differ from the class A  $\beta$ -lactamases in that they have molecular weights of approximately 23 kD and form a metalloenzyme complex with zinc. The class C  $\beta$ -lactamases are the structurally largest at 40 kD and include *Enterobacterium cloacae* P99 and *Escherichia coli* K12 (9). In addition to size, the three classes also differ in substrate specificity. The class A  $\beta$ -lactamases preferentially hydrolyze penams, while the other two classes target the cephem antibiotics. Sequence alignments of the class A  $\beta$ -lactamases have indicated a number of strictly conserved residues, including Lys 73 and Glu 166 (Figure 3)(1).

RTEM-1  $\beta$ -lactamase is a 28.5 kD soluble protein isolated from *E. coli*. Like the other class A  $\beta$ -lactamases, RTEM preferentially hydrolyzes penam antibiotics over cepheims. The rate of penam hydrolysis approaches diffusion control limits, with a second-order rate constant on the order of  $10^8$  (10). The  $\beta$ -lactam substrate is subjected to nucleophilic attack on the lactam carbonyl group by an active site serine (Ser 70 in

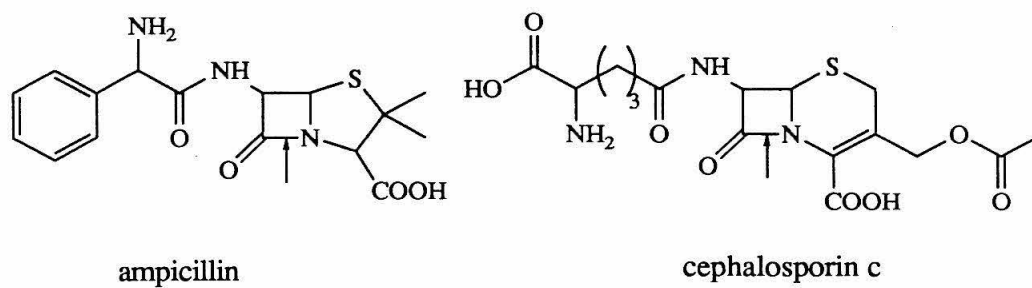


Figure 1. Representative  $\beta$ -lactam antibiotics. Ampicillin is a member of the penam family, cephalosporin c is a cephem. Arrow points to bond broken during hydrolysis.

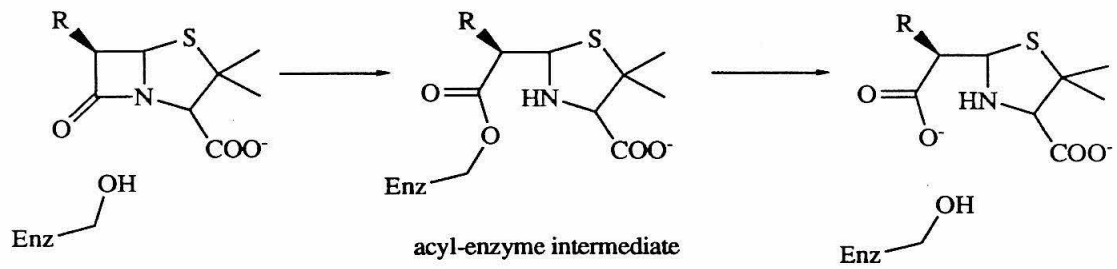


Figure 2. Overall reaction catalyzed by  $\beta$ -lactamase.



(a) 63-e R F p m m **S** T f **K** v l l c g a v L s-83  
 (b) 63-k R F a y a **S** T s **K** a i n s a i l L e-83  
 (c) 63-e R F a f a **S** T i **K** a l t v g v l L q-83  
 (d) 63-q R F a f a **S** T y **K** a l a a g v l L q-83

(a) 156-D h v T r l d R w **E** p E L N e a i P n-176  
 (b) 156-D k v T n p v R y **E** i E L N y y s P k-176  
 (c) 156-D e v T n p e R f **E** p E L N e v n P g-176  
 (d) 156-D r i T m s n R f **E** t E L N e a i P g-176

Figure 3. Amino acid sequence alignment of four class A  $\beta$ -lactamases in the regions of Lys 73 and Glu 166 (in bold). The sequences are: (a) *Escherichia coli* pBR322 RTEM-1; (b) *Staphylococcus aureus* PC1; (c) *Bacillus licheniformis* 749/C; (d) *Bacillus cereus* 569/H. The numbering starts from the *n*-terminus of the longest form of the *B. licheniformis* enzyme that has been isolated, and takes account of the gaps postulated in the currently known sequences to obtain optimal matching.

RTEM). Nucleophilic attack proceeds through a tetrahedral intermediate which is proposed to be stabilized by an oxyanion hole (11), similar to that observed in the serine proteases (12). The resulting acyl-enzyme intermediate is rapidly hydrolyzed, leading to an inactive antibiotic (13).

A considerable amount of research has been performed in our laboratory to investigate the roles of several important residues in RTEM-1  $\beta$ -lactamase including Thr 71(14), Lys 73 (15), Glu 166 (16), Lys 234 (17), Ala 237 (18), Ser 130 (19), and residues 237-240 (20). Other research has been directed towards the generation of mutants at Ser 70 (21, 22). In spite of the wealth of information concerning catalysis in RTEM-1  $\beta$ -lactamase, questions still persist.

Initial crystallographic studies indicated that two conserved active site residues, Lys 73 and Glu 166, could interact in a salt bridge or hydrogen bonding scheme, and were important for catalysis (Figure 4)(11). Previous studies in our labs analyzed these sites singly by site saturation techniques (15, 16). Any changes at residue 73 resulted in serious reductions in catalysis. Site 166 however showed that some alterations were tolerated, with mutations to Asp, His and Tyr giving phenotypic resistance.

An attempt to change the polarity of this putative salt bridge was made by the generation of the double mutant K73E/E166K. This mutant showed no phenotypic activity. It was thought that perhaps some other combination of mutations at sites 73 and 166 could give competent enzyme. The technique of combinatorial mutagenesis can be used to generate large numbers of combinatorial mutants providing proper restriction sites exist in the gene of interest (Figure 5). Since site saturations at residues 73 and 166 had been previously accomplished, the 400 possible combinations could be attained using a convenient *Pvu* I site. Screening for low levels of ampicillin resistance allows rapid detection of any functional mutants.

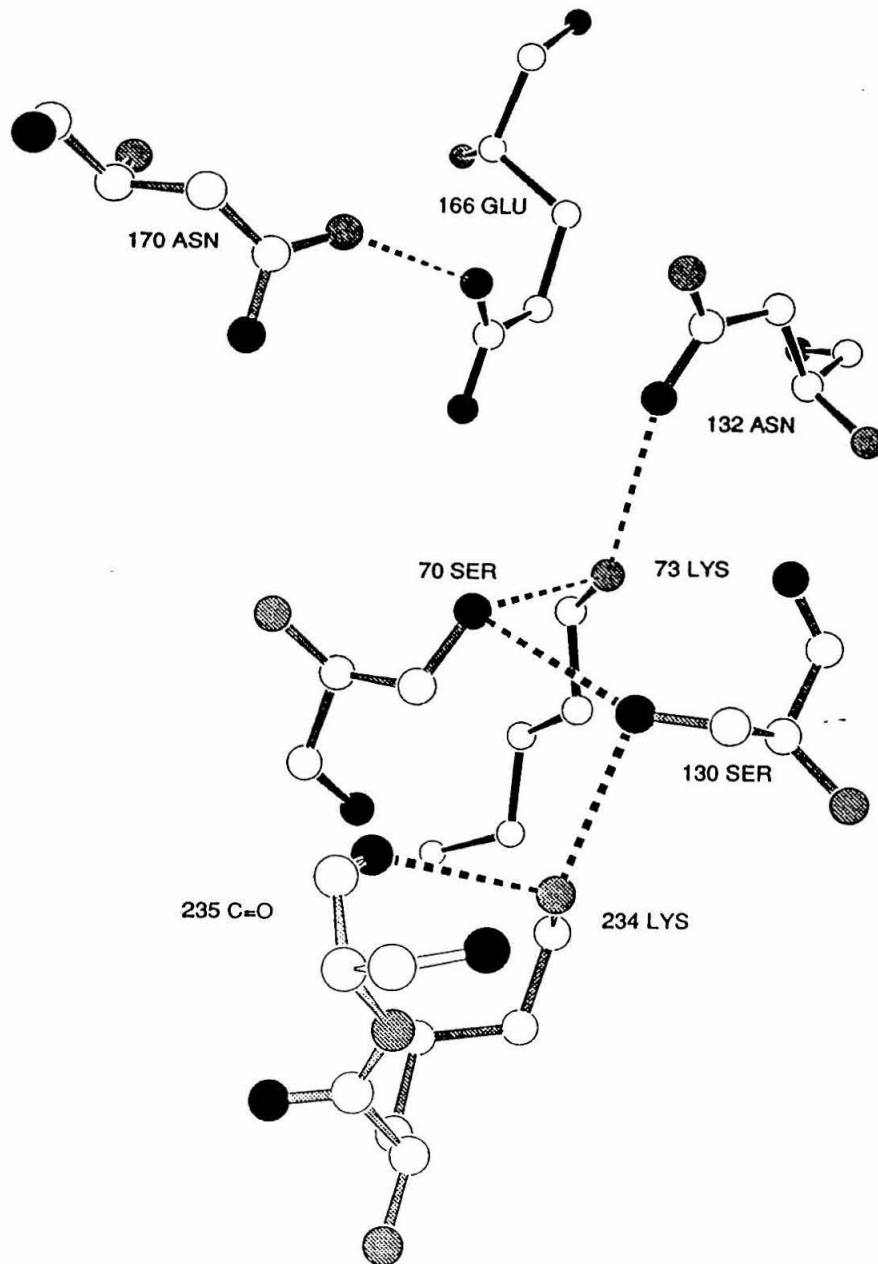


Figure 4. Active site structure showing positions of residues 73 and 166.

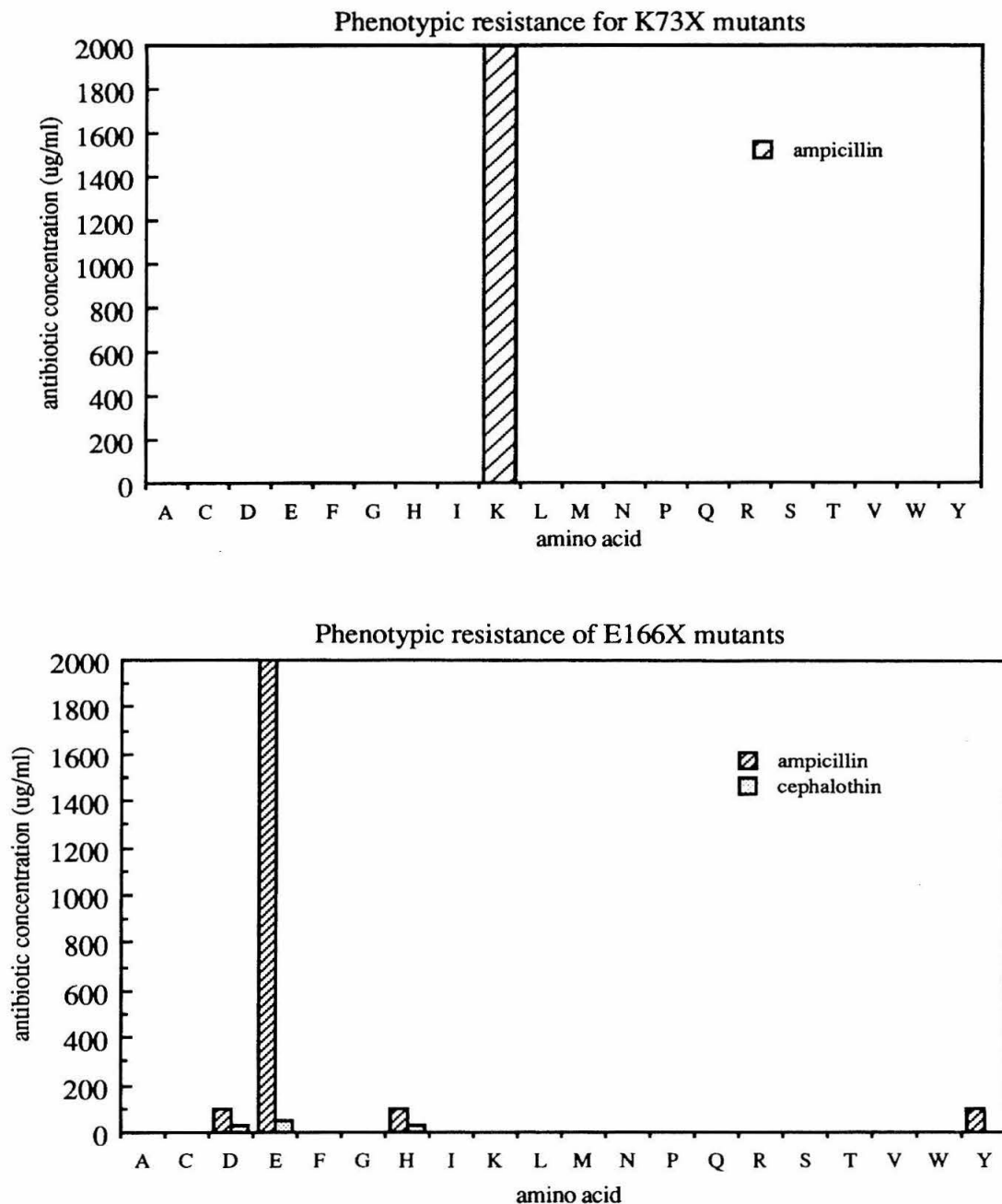


Figure 5. Plots of phenotypic resistance for K73X and E166X mutants.

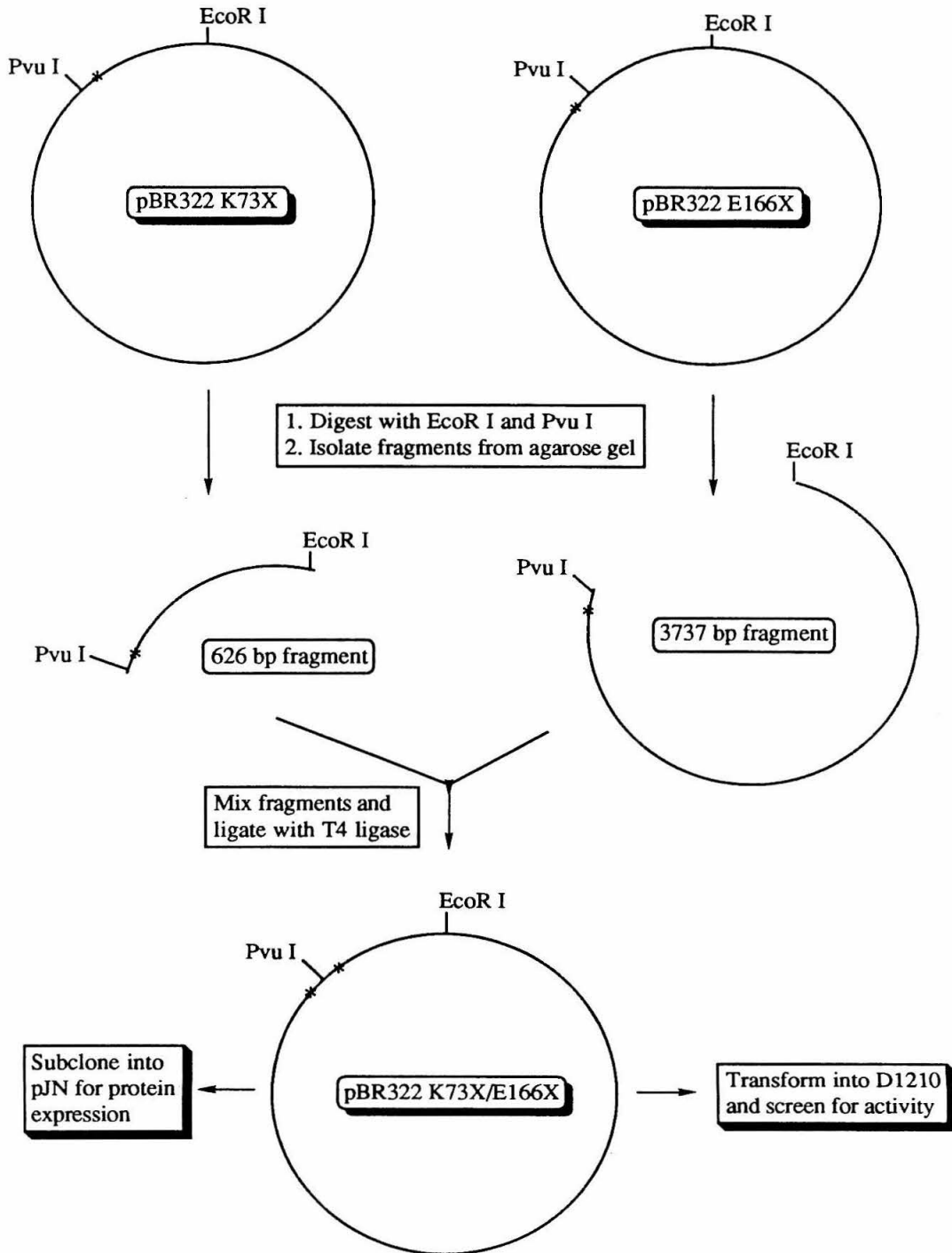


Figure 6. Combinatorial mutagenesis scheme

## MATERIALS AND METHODS

*Enzymes and Chemicals.* Enzymes were purchased from Boehringer Mannheim Biochemicals, New England Biolabs, and Promega. Antibiotics were from Sigma. Radioactive compounds were supplied by Amersham. Isopropyl- $\beta$ -thiogalactoside (IPTG) was from International Biotechnologies Inc. (IBI). Molecular biology grade reagents agarose, acrylamide, phenol, chloroform, ammonium persulfate were from Bio Rad.

*Bacterial Strains.* *Escherichia coli* were used in all experiments. Plasmid DNA was grown in strain HB101 (23); the pJN expression vector was grown in strain D1210, which is lac <sup>i</sup>Q. Culture media was L broth unless otherwise indicated. Cells were made competent for transformation of plasmid DNA using a process adapted from Hanahan (24).

*DNA.* Oligonucleotides were synthesized by the Caltech Microchemical Facility using phosphoramidite chemistry (25) on an Applied Biosystems automated DNA synthesizer 380A. Degenerate oligonucleotides were made equimolar in A, C, G, and T at positions 1 and 2 of the codon, and in C and G at position 3. These oligonucleotides were purified by preparative polyacrylamide gel electrophoresis.

Wild-type plasmid pBR322 and bacteriophage M13 mp18 replicative form (RF) DNA were purchased from Bethesda Research Laboratories. Mutant plasmids and RF phage were purified from *E. coli* by alkaline lysis method (26, 27). Single-stranded phage DNA was prepared from phage supernatant by precipitation with 20% polyethylene glycol-6000/2.5 M NaCl (28) followed by phenol/chloroform extraction and ethanol precipitation.

Restriction digest typically used 10-20  $\mu$ g plasmid DNA, 2-5 units of restriction enzyme, and 2  $\mu$ l 10X digest buffer in 20  $\mu$ l at 37°C for 1-2 hours. DNA restriction fragments were run in 1.2% low melt agarose gels, visualized with ethidium bromide, and isolated by established procedures (27).

*Oligonucleotide-directed Mutagenesis.* Two new restriction endonuclease sites were added previously to facilitate cassette mutagenesis and screening (26). Oligonucleotide-directed mutagenesis of the existing  $\beta$ -lactamase gene in a modified pBR322 plasmid (29) was used to create a *Sca* I site, and an *Ava* I site for cassette mutagenesis of position 73. Cassette mutagenesis of position 166 was made possible by the creation of unique *Mlu* I, *Sba* I, and *Sac* I sites (16). This was accomplished using the *in vitro* mutagenesis system<sup>TM</sup> by Amersham (30).

*DNA Sequencing.* Plasmid DNA was sequenced using a modification of the Sanger dideoxy method for denatured, double-stranded DNA (31). Plasmid DNA together with sequencing primer was boiled for 5 minutes, then snap frozen in dry ice/ethanol. Chain extension reactions were performed with a SEQUENASE<sup>TM</sup> kit from United States Biochemical (32). Radioactive labeling was accomplished with  $\alpha$ -<sup>35</sup>S-dATP. Labeled DNA was separated on 8% polyacrylamide sequencing gels, and resulting gels were dried *in vacuo*. Kodak AR x-ray film was then exposed in the presence of the sequencing gel for 12 hours.

*Cassette Mutagenesis of Position 73* Site saturation of residue 73 was accomplished by Steve S. Carroll in our laboratories previously (Figure 7)(15). Briefly, complementary synthetic oligonucleotides containing a degenerate codon at residue 73 and overhangs corresponding to *Ava* I and *Sca* I sites were kinased and annealed by standard procedures (27). Plasmid pBR-CR7 (15) was digested with *Sca* I and *Sal* I, and the 3286 bp fragment was isolated from a low melt agarose gel (27). Plasmid pBR322-XN1 (15) was digested with *Ava* I and *Sal* I, and the 1042 bp fragment isolated from a low melt agarose gel. These two fragments were mixed in equimolar concentrations with a five-fold excess of the synthetic cassette insert, and ligated and transformed directly into competent *E. coli* strain HB101 and cells were spread onto L plates containing 15  $\mu$ g/ml tetracycline. The plasmid DNA was isolated by alkaline lysis, and subjected to

restriction analysis and sequencing.

*Cassette Mutagenesis of Position 166.* Site saturation of residue 166 was accomplished previously by William J. Healy in our labs (16). Briefly, complementary synthetic oligonucleotides degenerate at position 166 with overhangs corresponding to *Mlu* I and *Sac* I sites were kinased and annealed as above. Plasmid pBR322-*Mlu* (16) was digested with *Mlu* I and *Sal* I, with the 1335 bp fragment isolated. Plasmid pBR322-*Sac* (16) was digested with *Sac* I and *Sal* I, with the 3000 bp fragment isolated. These fragments were ligated with synthetic cassette as above and transformed into HB101 *E. coli* and plated on L plates containing 15 µg/ml tetracycline.

*Combinatorial Mutagenesis.* Combinatorial mutagenesis is a technique that uses existing site saturation mutations to generate combinations of mutations at multiple sites (Figure 6). Equimolar mixtures of pBR322 plasmids containing the site-saturations from 73 and 166 were made. These mixtures were digested with *Eco*R I and *Pvu* I according to standard procedures (27), and the resulting fragments isolated from a low melting agarose gel. The 626 bp piece from the K73X mixture was ligated with the 3737 bp piece from the E166X mixture. The ligation mixture was then transformed directly into competent *E. coli* strain D1210, with the cells plated out on low (10-25 µg/ml) concentration ampicillin plates also containing tetracycline. Colonies that grew were sequenced by dideoxy methods.

*Phenotypic Screening.* Following identification of all 19 mutants, each was grown to late log phase in LB/kan. 10 µl of cells were diluted  $10^5$  and plated onto L plates with varying concentrations of ampicillin, benzyl penicillin, and cephalothin (25, 50, 75, 100, 200, 400, 800, 1200, 1600, 2000 µg/ml). These plates were incubated at 37°C for 12 hours, and presence or absence of colony growth for each mutant noted.

*pJN Subcloning.* To facilitate expression, the mutant β-lactamases were subcloned into pJN, an expression vector which was developed in this lab (Figure 7) (33).



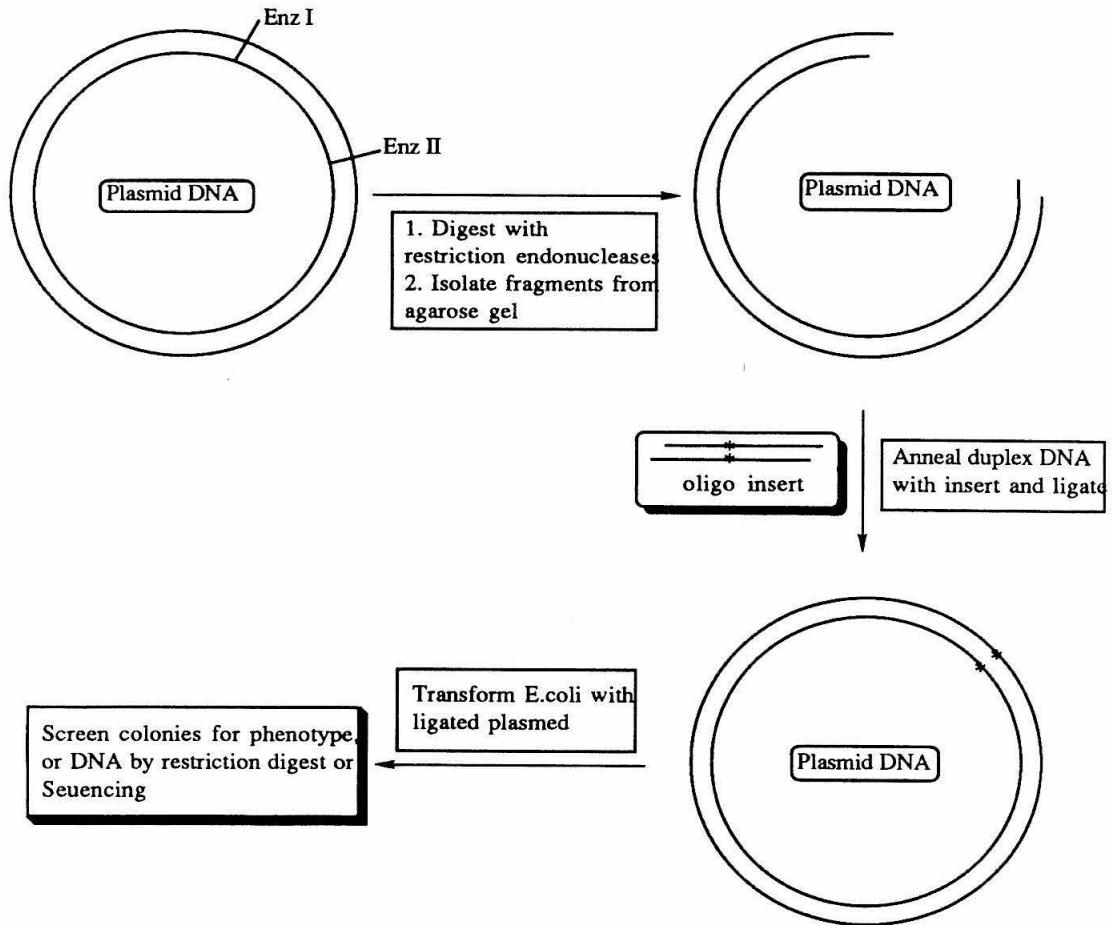


Figure 7. A schematic overview of cassette mutagenesis.

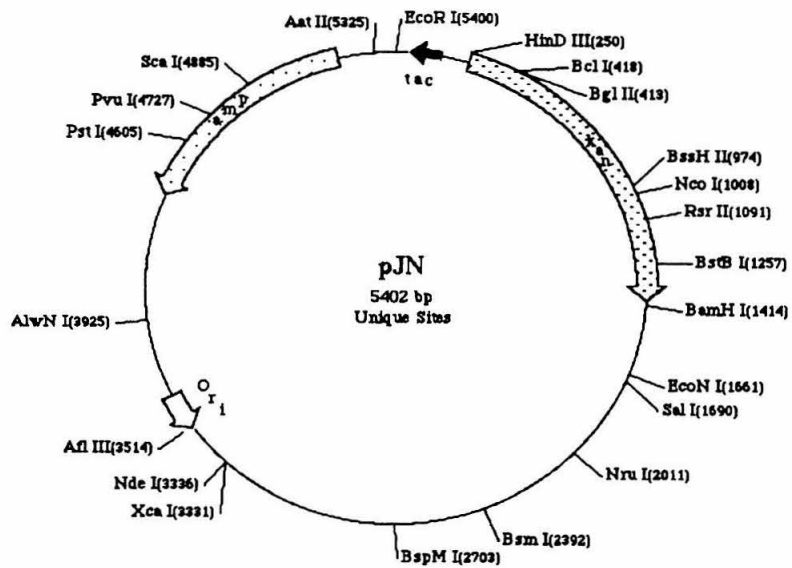


Figure 8. pJN expression vector.

It contains the  $\beta$ -lactamase gene under control of the *tac* promoter (34), and well as a kanamycin gene for a selection marker. Synthesis of  $\beta$ -lactamase is induced by the addition of IPTG. The subcloning scheme is shown in Figure 8. Plasmid DNA from active combinatorial mutants was isolated as described above, and digested with *EcoR* I and *Bam* HI, with the resulting 3986 bp fragment isolated from a low melt agarose gel. The pJN expression vector plasmid DNA was similarly digested with *EcoR* I and *Bam*H I, with the resulting 1416 bp fragment isolated. These two fragments were mixed in equimolar amounts with T4 DNA ligase and proper buffer at room temperature for 2 hours, followed by transformation and plating onto L plates with 50  $\mu$ g/ml kanamycin as described above.

*Protein Expression and Purification.* One liter cultures of *E.coli* D1210 containing mutant plasmid were grown in X broth containing 50  $\mu$ g/ml kanamycin for 12-14 hours at 37°C. IPTG was added to a final concentration of 0.1 mM and growth continued for 1 hour at 37°C. Cells were centrifuged in 250 ml bottles in a GSA rotor for 10 minutes at 10,000 rpm.  $\beta$ -lactamase, which is located in the periplasm, was released by osmotic extrusion (10). The sample containing the periplasmic proteins was reduced to ~1 ml using a Diaflow cell (Amicon) under nitrogen. The resulting solution was then filtered through a Schleicher and Schuell 0.22 m Uniflow filter to remove any cellular debris.

Further purification was carried out using FPLC (fast protein liquid chromatography) first with a HR16/10 Fast Flow MonoQ<sup>TM</sup> column, followed by a HR10/10 MonoQ<sup>TM</sup>, both by Pharmacia. Crude protein was loaded onto the fast flow column, and the column was washed in 100% A (25 mM triethanolamine (TEA), pH 7.65). Then crude  $\beta$ -lactamase was eluted with 20%B (25 mM TEA, 1M NaCl). This protein was loaded onto the HR 10/10 column in 25 mM TEA and eluted with a salt gradient. The gradient used was: t=0, 100% A, t=5, 100% A, t=35, 80%A, 20%B, t=45, 100% B. The flow rate was 1.0 ml/min. Elution was monitored by A280. Peak fractions

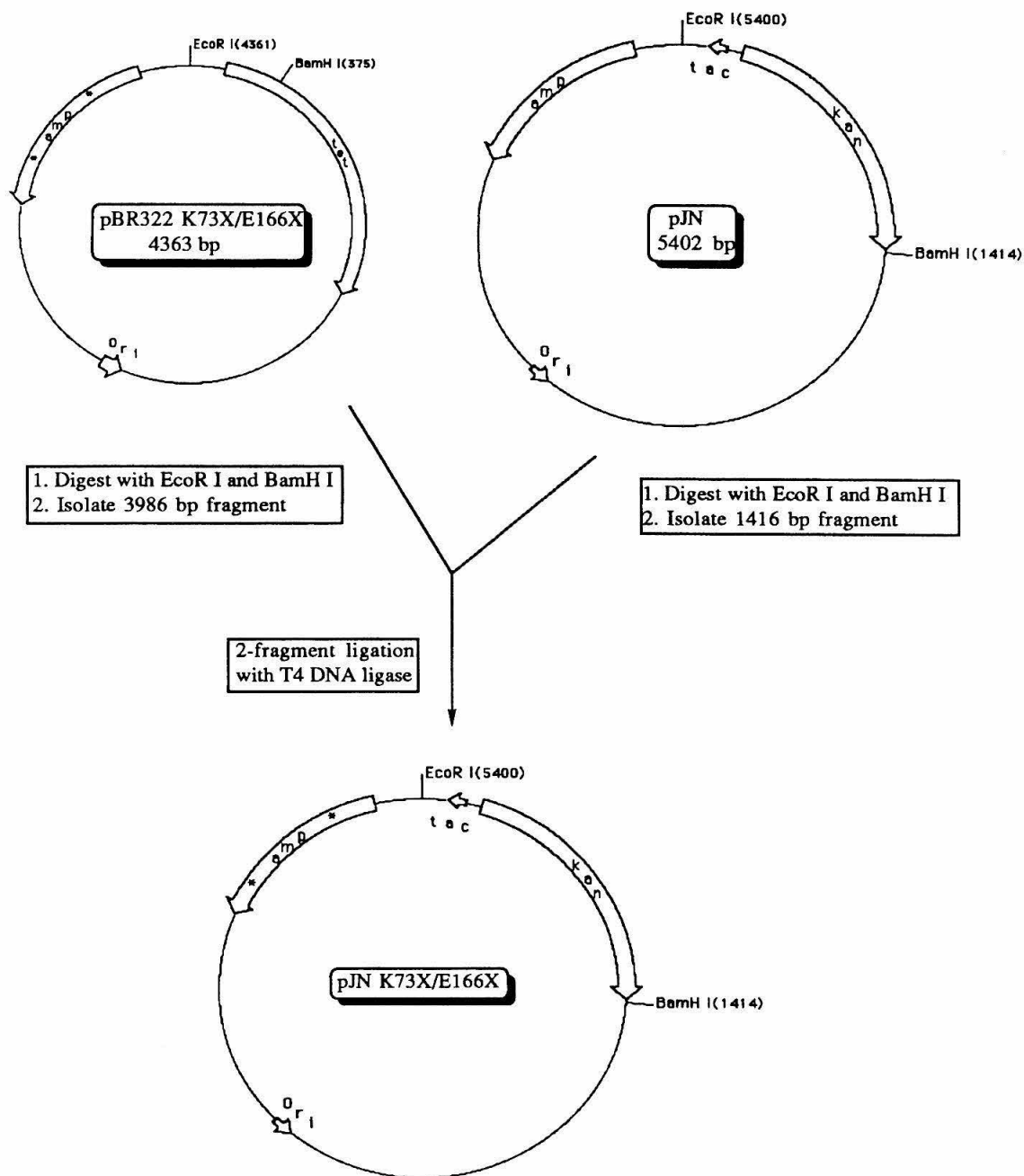


Figure 9. Scheme for subcloning mutants into pJN expression vector.

were pooled and dialyzed versus 100 mM potassium phosphate, pH 7.0. Protein concentrations were estimated from OD<sub>280</sub> using an extinction coefficient of 29,400 M<sup>-1</sup>cm<sup>-1</sup>(2). Samples were run on 15% polyacrylamide gels (as in western blot ) and stained with Coomassie blue to gauge purity.

*Kinetics.* Michaelis-Menten kinetic parameters ( $k_{cat}$ ,  $K_M$ , and  $k_{cat}/K_M$ ) for mutant  $\beta$ -lactamases were determined by Hanes plots (35) using initial rates. Reactions were carried out at 30°C in 100 mM potassium phosphate pH 7.0. All reagent were maintained at 30°C prior to beginning the assay to avoid error from temperature flux. An HP 8420 spectrophotometer was used for the assays, with quartz cells of pathlength 1 cm at wavelength 232 nm.

## RESULTS

*Mutagenesis.* Oligonucleotide-directed mutagenesis was used by Steve S. Carroll in our group to create unique *Ava I* and *Sca I* sites within the existing  $\beta$ -lactamase gene (from pBR322) in M13 (15). Sequencing and restriction endonuclease analysis confirmed the presence of these sites. Site-saturation of residue 73 was accomplished using cassette mutagenesis with oligonucleotides degenerate at codon 73 (15). Oligonucleotide-directed mutagenesis was used by William J. Healy in our group to create unique *Mlu I*, *Sba I*, and *Sac I* sites within the existing  $\beta$ -lactamase gene (from pBR322) in M13 (16). Sequencing and restriction endonuclease analysis confirmed the presence of these sites. Site-saturation of residue 166 was accomplished using cassette mutagenesis with oligonucleotides degenerate at codon 166 (16).

Combinatorial mutagenesis used the previously created site saturation's to generate 400 possible combinations of amino acids at two conserved residues in the RTEM-1  $\beta$ -lactamase gene. Equimolar amounts of plasmid DNA coding for all 20 amino acids at sites 73 and 166 was digested with *EcoR I* and *Pvu I*, followed by isolation from

low melt agarose gel (Figure 9). Ligation reactions with equimolar amounts of digested plasmid DNA were repeatedly transformed into competent D1210 *E. coli*, and plated on L plates with 50 µg/ml kanamycin and 10 to 25 µg/ml ampicillin to screen for active mutants. A total of 23 colonies were isolated and their plasmid DNA sequenced (Figure 10). Only three mutants were found (along with wild-type)-K73K/E166D, K73K/E166H, K73K/E166Y (data not shown).

*Phenotypic Screening.* Each of the site saturation mutants were grown to late log phase and plated on varying concentrations of antibiotic following dilution in previous experiments (15, 16). The results of these experiments are shown in Figure 11. For residue 73, none of the mutants showed any appreciable activity (<0.5% that of wild-type) towards usual substrates. A few mutants at position 166 showed activity, specifically E166D, E166H, and E166Y.

*Stability of Mutant Enzymes.* The stability of mutant enzymes produced were previously assayed by Western blot analysis. All K73X mutants exhibited expression and stability's comparable to wild-type (data not shown)(15). This indicates that the lack of activity of the mutants is due to structural changes in the protein rather than instability, incorrect folding, or lack of protein expression. All E166X mutants, with the exception of E166R and E166K, exhibited stability comparable to wild-type (data not shown)(16).

*Isolation of Mutant Enzymes.* The active combinatorial mutants (K73K/E166D and K73K/E166H) were chosen for kinetic analysis, as these appeared to possess significant enough activity to assay by spectrophotometric means. Two liters of media with proper antibiotic were grown to saturation at 37°C. IPTG was added (24 mg/ml) and incubation continued for 1 hour. Following osmotic extrusion, concentration in an Amicon unit afforded ~10 ml of crude protein. This was chromatographed first by FPLC on a HR16/10 Fast Flow column with the 20%B cut retained. After dialysis into Buffer A and concentration by Amicon, β-lactamase was purified on a Mono Q column by FPLC

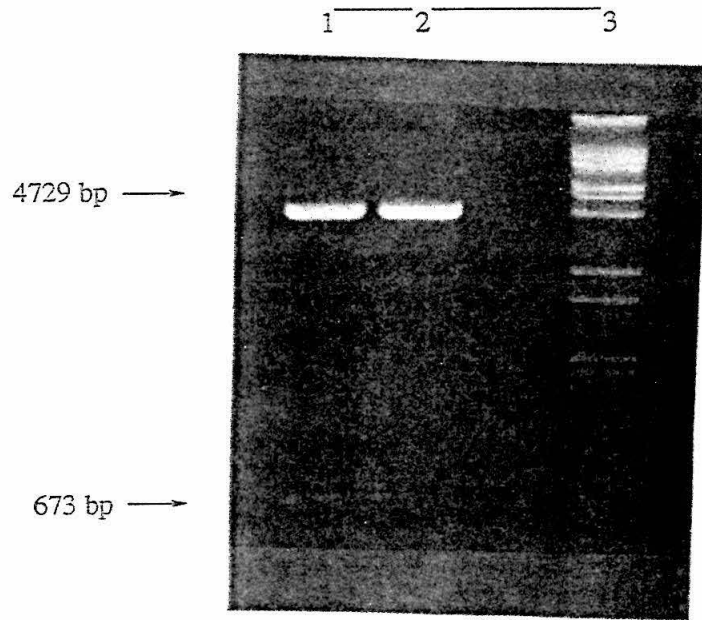


Figure 10. Agarose gel showing restriction digests and fragments used in combinatorial mutagenesis. Lane 1, pBR322-K73X cut with *EcoR* I and *Pvu* I. Lane 2, pBR322-E166X cut with *EcoR* I and *Pvu* I. Lane 3, Molecular weight marker.

(Figure 11). Fractions containing  $\beta$ -lactamase and purity were identified by PAGE.

*Kinetics.* Steady-state kinetic analysis of three mutants (E166D, E166H, E166Y) was undertaken, with the kinetic scheme shown in Figure 12. The hydrolysis reaction is followed by decrease in absorbance at 232 nm, which indicates the opening of the  $\beta$ -lactam ring. The results are shown in Table 1. Decreases in  $k_{\text{cat}}$  for the mutants indicate that residue 166 is important in catalysis, while  $K_M$  values near that of wild-type show that residue 166 has little effect on substrate binding. The pH profiles for the two mutants are nearly identical to those for wild-type (Figure 13).

## DISCUSSION

In the past our lab has investigated many of the catalytically important residues by site-saturation mutagenesis. We have utilized site-saturation's for a number of reasons including ease of mutation, cloning efficiencies and screening. But primarily, generation of all 20 amino acids at a specific residue leads to results not anticipated *a priori*. For example, site-saturation of Glu 166, the residue believed to be responsible for deacylation of the acyl-enzyme intermediate, gave three mutants with activity; aspartate, histidine and tyrosine (16). Previous reports of mutagenesis at residue 166 did not include the E166H and E166Y mutations (36). The activity of these unexpected functional mutations leads to a greater understanding of the structural requirements of catalysis. Thus, site-saturation mutagenesis has assumed an important role in our lab's investigations of  $\beta$ -lactamase activity.

Early crystallographic studies identified a number of residues in the area of the active site. Our lab has studied a number of these sites, including Lys 73 and Glu 166. Computer modeling of the active site indicated a possible mode of binding for the  $\beta$ -lactam substrate, as well as the catalytic functions of certain residues (17). As stated above, the carboxylate side chain of Glu 166 was implicated as a general base in the



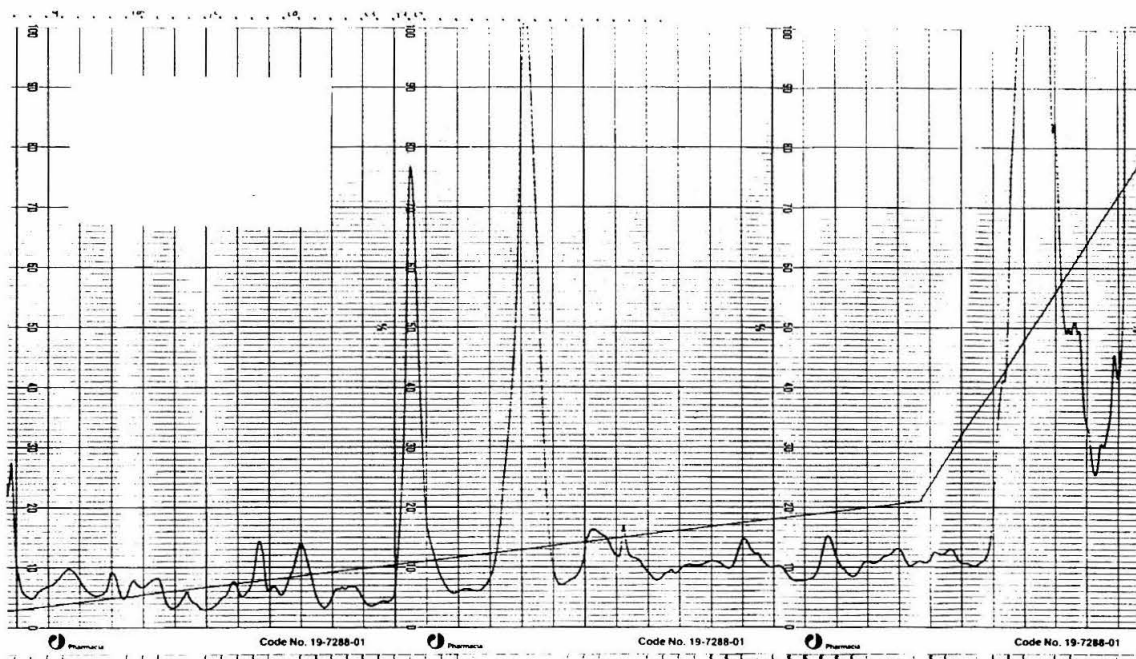


Figure 11. FPLC trace for purification of K73K/E166D mutant.  $\beta$ -lactamase is found in peak @ 11% B.

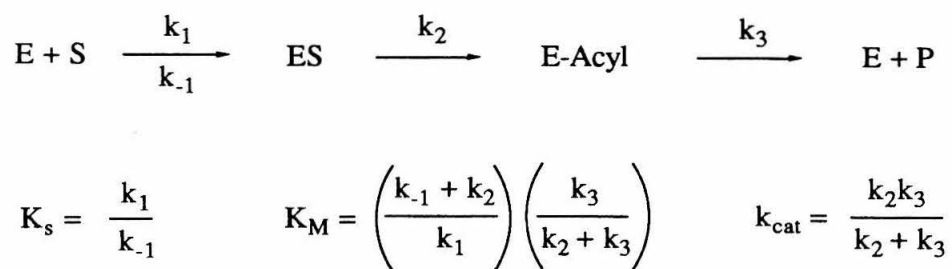


Figure 12. Kinetic scheme for  $\beta$ -lactam hydrolysis catalyzed by  $\beta$ -lactamase.

	<u><math>k_{cat}</math></u> ( $s^{-1}$ )	<u><math>K_M</math></u> ( $\mu M$ )	<u><math>k_{cat}/K_M</math></u> ( $s^{-1}M^{-1}$ )	<u>relative rate</u>
WT	980	42	$2.5 \times 10^7$	1
K73R	0.3	43	$6.9 \times 10^3$	
K73C	0.2	21	$1.2 \times 10^4$	
E166D	25	22	$1.1 \times 10^6$	0.044
E166H	13	22	$5.9 \times 10^5$	0.024

Table 1. Kinetic parameters for hydrolysis of benzylpenicillin catalyzed by RTEM-1  $\beta$ -lactamase

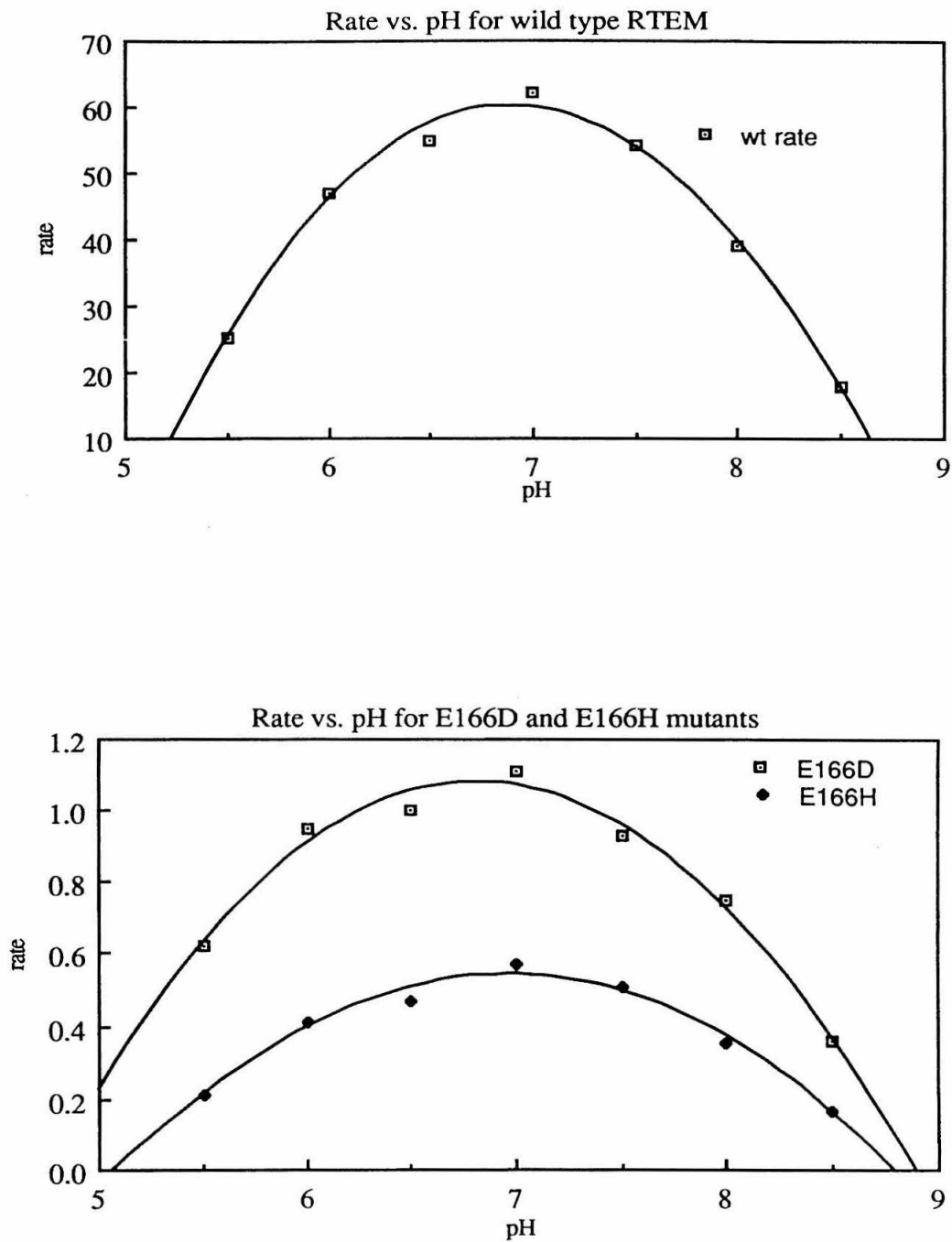


Figure 13. pH profiles for K73K/E166D and K73K/E166H mutants.

deacylation step of enzyme catalysis (Figure 14). Mutagenesis studies support this hypothesis, and also helps to define the structural requirements for catalysis. The conservative mutation E166D is functional, with  $K_M$  nearly identical to wild-type, but  $k_{cat}$  down by  $\sim 2$  orders of magnitude. The pH studies show catalytic behavior similar to wild-type. This illustrates that the residue is important for catalysis, but probably not directly involved in formation of the ES complex. The removal of one  $\text{CH}_2$  unit in the E166D mutant shortens the side chain by  $\sim 1\text{\AA}$ , thereby pulling the carboxylate functionality away from the substrate (as acyl-enzyme) and the water implicated in deacylation. This explains the reduction in rate.

The mutation E166H also gives a functional enzyme, with kinetic parameters comparable to the E166D mutant. It would appear that the active site environment around the 166 residue is such that the imidazole side chain of histidine is deprotonated, and can thus also function as a general base. However it is difficult to determine if the rate decrease is a function of different basicities, geometry changes, or a combination of the two. Another factor concerns the formation of a positive charge on the imidazole upon protonation. This charge could be somewhat undesirable in that particular area of the active site, and could act to raise the  $\text{p}K_a$ , therefore decreasing the rate.

Attempts were made to study the catalytic behavior of the E166Y mutant. Unfortunately, this enzyme did not seem to obey Michaelis-Menten kinetics. It is possible to envision an altered mechanism for this mutation, where the phenolic side chain of the tyrosine is deprotonated. This anion could function as a base, but it could also function as a nucleophile, directly attacking the acyl-enzyme intermediate, giving a second acyl-enzyme intermediate (Figure 15). This second intermediate would then need to be hydrolyzed for enzyme turnover. The nucleophilicity of phenoxide is rather high, with a  $n$  value of 3.5, equivalent to  $\text{Br}^-$  (37), and the leaving group ability of the phenolic group (Tyr 166) is greater than that of the hydroxyl (Ser 70)(38). This more complex

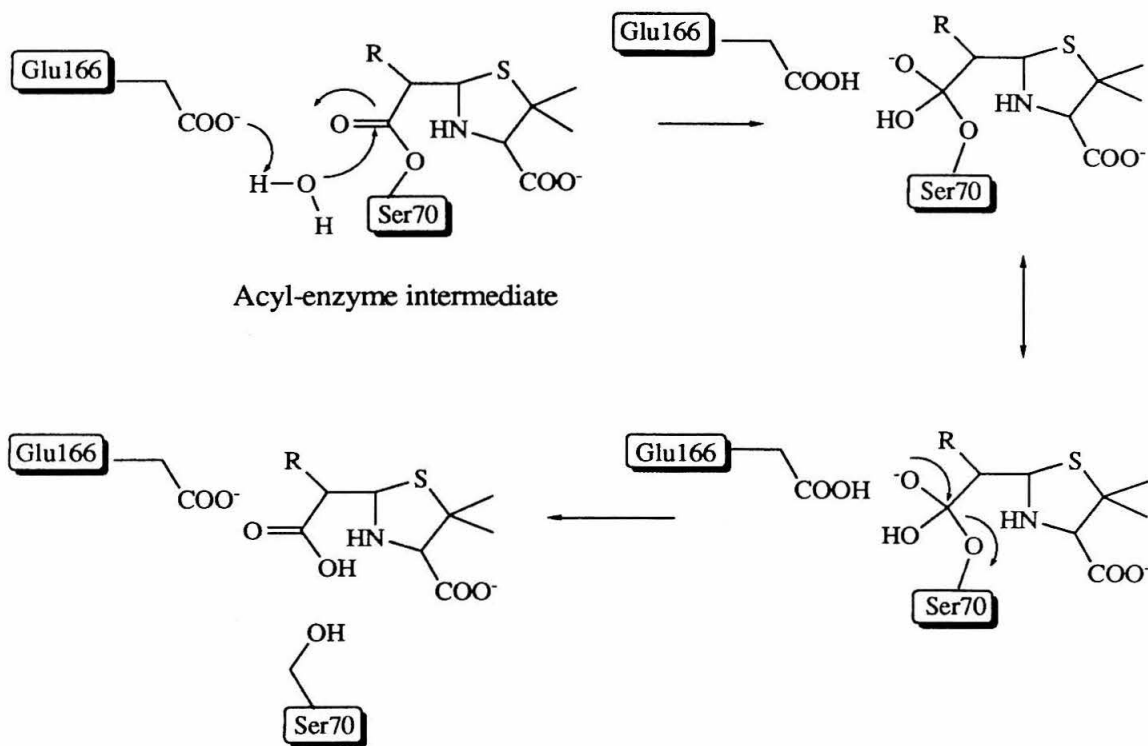


Figure 14. Deacylation reaction with Glu 166 functioning as a general base.

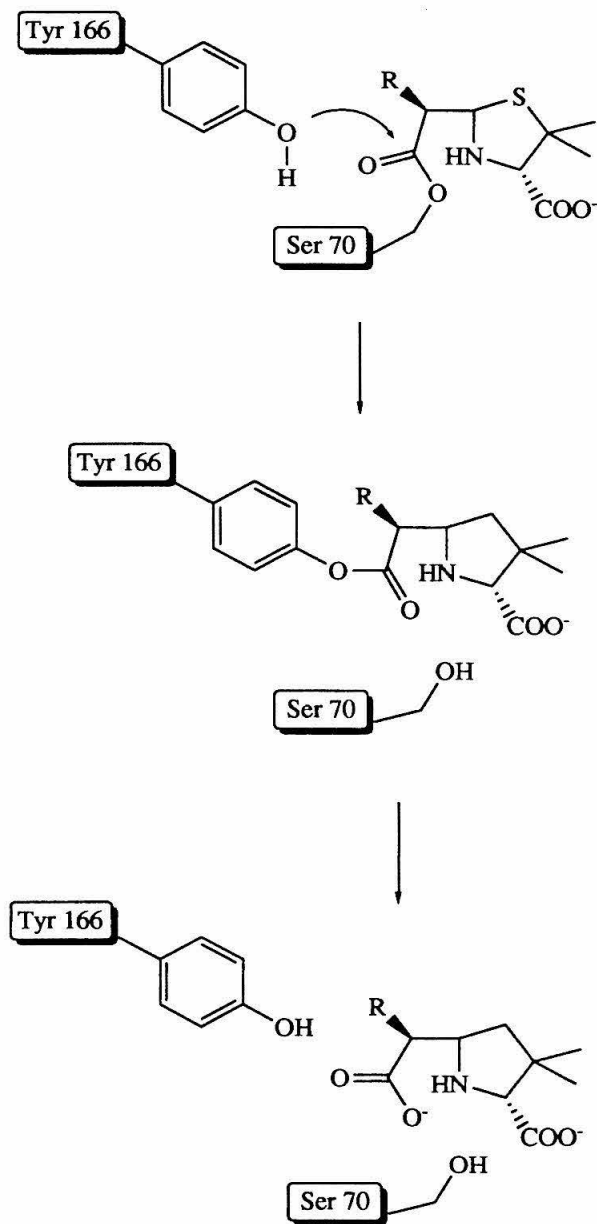


Figure 15. Possible mechanism for deacylation reaction for E166Y mutant.

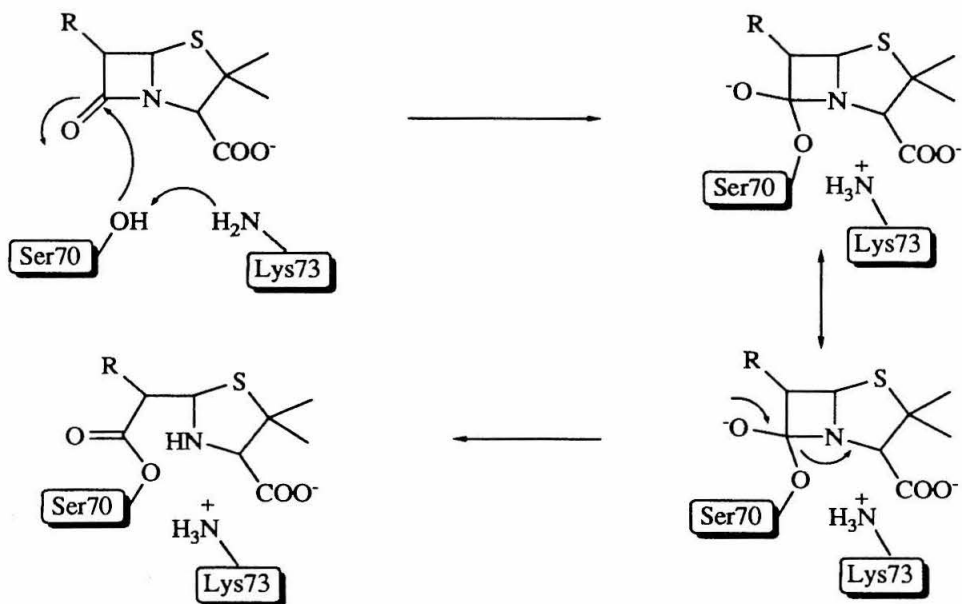
mechanism would be slower, but could be facile enough to confer phenotypic resistance.

The details of the acylation step in  $\beta$ -lactamase catalyzed hydrolysis are still not well understood. It has been suggested that Lys 73 is a key player in the kinetic scheme, either directly as a general base, or indirectly by electrostatic interactions (Figure 16)(refs). Site saturation mutagenesis studies unfortunately do not shed much light on this dilemma. It is obvious that no other amino acid at position 73 gives functional enzyme. Yet some generalizations can be suggested. If Lys 73 were interacting solely by electrostatics, it would be expected that the mutant K73R would have some activity, as this side chain is positively charged. The geometry differences between the two could cause some problems, but since electrostatic interactions are basically non-directional, it would be expected that the Arg side chain would give an enzyme with some activity.

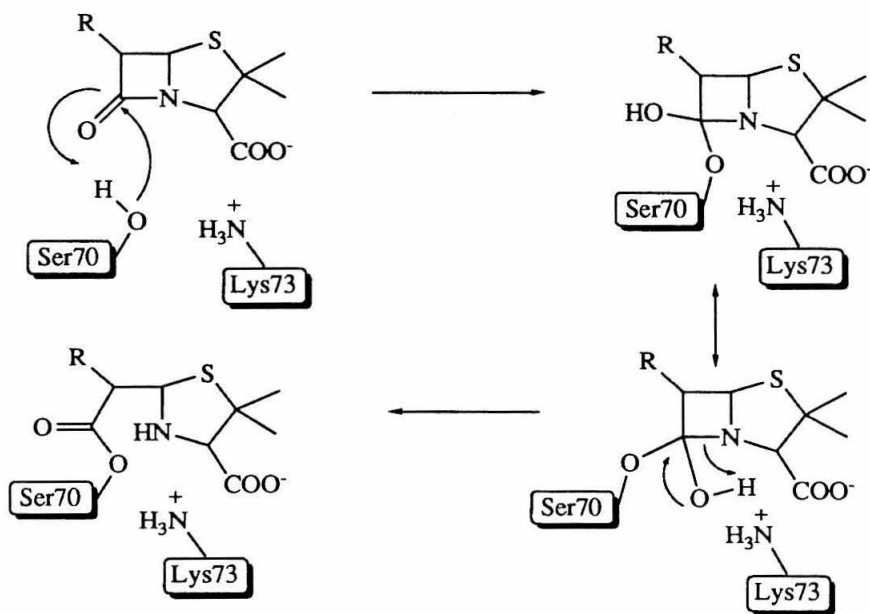
The fact that other amino acids known to function as general bases (His, Asp, Glu) similarly give inactive enzyme would seem to suggest that the function of Lys 73 is not basic in nature. However this hypothesis overlooks geometric concerns. None of the other basic side chains would extend into the active site cleft like Lys. Therefore, the mutant basic side chains would be fairly far removed from the correct position and orientation for proton abstraction. The lack of active combinatorial mutants indicates that there can be no compensation for the loss of amine functionality by residue 166, and it appears that the reasons are primarily geometric in nature.

There is no way to generate a mutant at site 73 that positions a basic side chain far enough into the active site, save mutagenesis using unnatural amino acids or chemical modification techniques (Figure 17). These experiments could indicate the function of Lys 73. For instance, if an amino acid with a butanionic side chain could be inserted, the carboxylate should be closer to the correct position for proton abstraction. Similarly, chemical modification of the K73C mutant could also give a mutant with a potential base closer to the putative deacylating water. These experiments unfortunately cannot address





Formation of acyl-enzyme intermediate with Lys 73 functioning as a general base



Formation of acyl-enzyme intermediate with Lys 73 giving "electrostatic assistance"

Figure 16. Possible roles of Lys 73 in acylation step.

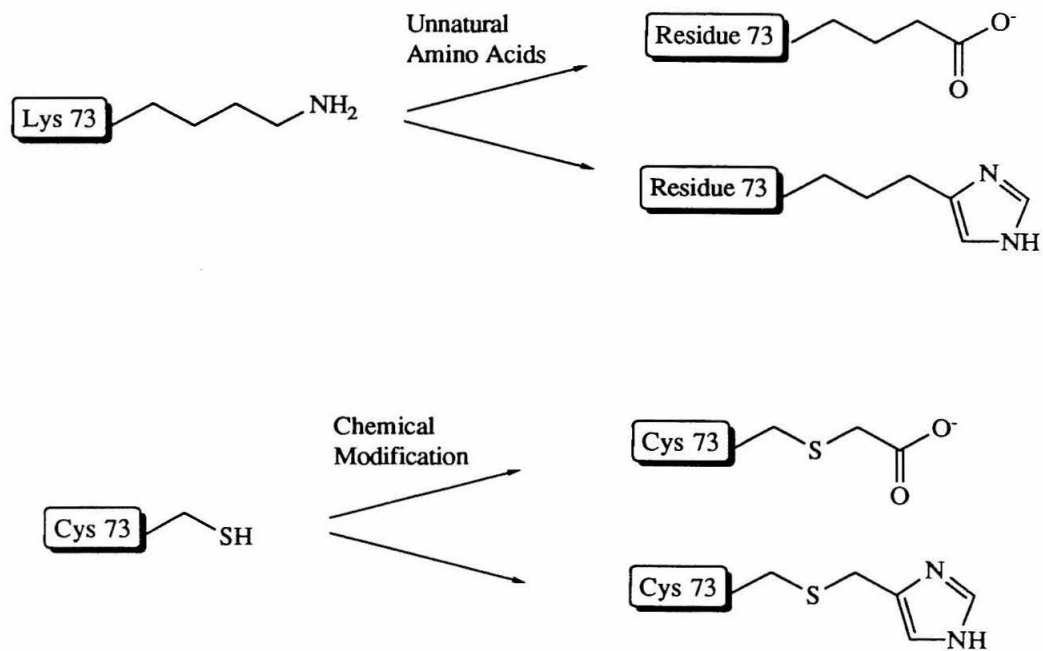


Figure 17. Possible scheme for changing functional group at residue 73.

the  $pK_a$  necessary to do the job. For instance a carboxylate may not be basic enough to deprotonate the water; it may be that an amine is the optimal functional group considering the surrounding environment. The next chapter discusses what could be the definitive experiment to determine the  $pK_a$  of Lys 73, and the probable function of this conserved active site residue.

## REFERENCES

1. Ambler, R. (1980) *Phil. Trans. R. Soc. Lond.* **289**, 321.
2. Datta, N., and Kontomichalou, P. (1965) *Nature* **208**, 239.
3. Ambler, R., (1978) *Proc. Natl. Acad. Sci. U.S.A.* **75**, 3732.
4. Sutcliffe, J.G. (1978) *Proc. Natl. Acad. Sci. U.S.A.* **75**, 3737.
5. Ambler, R.P. (1975) *Biochem J.* **151**, 197.
6. Neugebauer, K., Sprengel, R. and Schaller, H. (1981) *Nucleic Acids Res.* **9**, 2577.
7. Madgwick, P.J. and Waley, S.G. (1987) *Biochem J.* **248**, 657.
8. Bicknell, R. and Waley, S.G. (1985) *Biochemistry* **24**, 6876.
9. Knot-Hunziker, V., Peursson, S., Waley, S.G., Jarrin, B., and Grundstrom, T. Ambler, R. (1975) *Biochem J.* **151**, 197-218.
10. Fisher, J., Belasco, J., Khosla, S., and Knowles, J., (1980) *Biochemistry* **19**, 2895.
11. Hertzberg, O. and Moulton, J. (1987) *Science* **236**, 694.
12. Fujinaga, M., Read, R.J., Sielecki, A., Laskowski, M. Jr., and James, M.N.G. (1982) *Proc. Natl. Acad. Sci. U.S.A.* **79**, 4868.
13. Adachi, H., Ohta, T. and Matsuzawa, H. (1990) *J. Biol. Chem.* **266**, 3186.
14. Schultz, S.C. and Richards, J.H. (1986) *Proc. Natl. Acad. Sci. U.S.A.* **83**, 1588.
15. Carroll, S.S. (1987) Ph.D. Thesis, California Institute of Technology.
16. Healy, W.J. (1989) Ph.D. Thesis, California Insitute of Technology.
17. Long, D.M. (1991) Ph.D. Thesis, California Institute of Technology.
18. Healy, W.J., Labgold, M.R., and Richards, J.H. (1989) *Proteins* **6**, 275.
19. Emerling, M.R. (1992) Ph.D. Thesis, California Institute of Technology.
20. Hollenbaugh, D.L. (1991) Ph.D. Thesis, California Institute of Technology.
21. Dalbadie-McFarland, G., Riggs, A.D., Morin, C., Itakura, K., and Richards, J.H. (1982) *Proc. Natl. Acad. Sci. U.S.A.* **79**, 6409.

22. Sigal, I.S., Degrado, W.F., Thomas B.J., and Pelleway, J.R. (1984) *J. Biol. Chem.* **259**, 5327.
23. Boyer, H., Roullard-Dussoix, D. (1969) *J. Mol. Biol.* **41**, 459.
24. Hanahan, D. (1983) *J. Mol. Biol.* **166**, 557.
25. Beaucage, S.L., Carruthers, M.H. (1981) *Tet. Lett.* **22**, 1859.
26. Ish-Horowitz, D, Burke, J. (1981) *Nucl. Acids Res.* **9**, 2989.
27. Maniatis, T., Fritsch, E., Sambrook, J. 1982, "Molecular Cloning, A Laboratory Manual". Cold Spring Harbor, NY, Cold Spring Harbor Laboratory.
28. Nakmaye, K., Eckstein, F. (1986) *Nucl. Acids Res.* **14**, 9679.
29. Amersham 1988, "Oligonucleotide-directed In Vitro Mutagenesis System Manual," , Arlington Heights, IL, Amersham Corp.
30. Sanger, F. Nicklen, S., Coulson, A. (1977) *Proc. Natl. Acad. Sci U.S.A.* **74**, 5463.
31. U.S. Biochemicals 1988, "Sequenase Manual," Cleveland, OH, United States Biochemical.
32. Neitzel, J. 1987, PhD Thesis, California Institute of Technology.
33. De Boer, H.A., Comstock, L.J., Vasser, M. (1983) *Proc. Natl. Acad. Sci U.S.A.* **80**, 21.
34. Hanes, J. (1932) *Biochem. J.* **26**, 1406.
35. Adachi, H., Ohta, Takahisa, Matsuzawa, H. (1991) *J. Biol. Chem.* **266**, 3186.
36. March, J. (1985) "Advanced Organic Chemistry." Wiley-Interscience, New York, p. 309.
37. March, J. (1985) "Advanced Organic Chemistry." Wiley-Interscience, New York, p. 315.
38. Hertzberg, O., Moul, J. (1987) *Science* **236**, 694.
39. Moews, P.C., Knox, J.R., Dideberg, O., Charlier, P., Frer, J.M. (1990) *Prot. Struc. Func. Gen.* **7**, 156.

40. Strynadka, N.C.J., Adachi, H., Jensen, S.E., Johns, K., Sielecki, A., Betzel, C., Sutoh, K., James, M.N.G. (1992) *Nature (London)* **359**, 700.

## Chapter 4

Attempts to Determine the  $pK_a$  of an Active Site Residue in RTEM-1  $\beta$ -lactamase via  
Site-Directed Mutagenesis, Chemical Modification, and NMR Spectroscopy

## INTRODUCTION

The class A  $\beta$ -lactamases all have a molecular weight around 30 kilodaltons and catalyze  $\beta$ -lactam cleavage which confers bacterial resistance to cephem and penam antibiotics (Figure 1)(1). This class includes the RTEM-1  $\beta$ -lactamase of *E. coli* (2), *Staphylococcus aureus* PC1 (3), *Bacillus licheniformis* 749/C (4), and *Bacillus cereus* 569/HI(5). Sequence homologies between members of this class are considerable, ranging from 26 to 65 % (6). The class B  $\beta$ -lactamases consist of only two enzymes, from *B. cereus* and *Proteus maltophilia*, and differ considerable from the class A enzymes in molecular weight and catalytic mechanism. These enzymes, which contain a metalloenzyme complex with either zinc(II) or cobalt (III) at the catalytic center, appear to function as general base catalysts, with no indication of an acyl-enzyme intermediate formation during the hydrolysis (7). The third  $\beta$ -lactamase class, the class C enzymes, consist of the largest enzymes and utilize a nucleophilic serine in the active site (8). Both the class B and C  $\beta$ -lactamase preferentially hydrolyze cepheems.

The class A and class C  $\beta$ -lactamases attack the  $\beta$ -lactam of penam and cephem antibiotics through a nucleophilic serine, in a mechanism similar to that of the penicillin binding proteins (Figure 2). A class A  $\beta$ -lactamase of particular interest is the RTEM-1 enzyme from *E. coli* (9). This enzyme has been extensively studied, in part due to its availability as a resistance marker on the ubiquitous plasmid pBR322. RTEM-1 is a soluble protein of 28.5 kD. It is synthesized as a 286 amino acid preprotein, with a 23 residue leader sequence cleaved off during export of the protein into the periplasm of the cell. The RTEM-1 enzyme has been used in the examination of protein secretion (10), expression of fusion proteins (11), and as a selectable marker (12). Like most class A  $\beta$ -lactamases, RTEM-1 preferentially hydrolyze penam antibiotics at rates approaching evolutionary perfection. The apparent second-order rate constant,  $k_{cat}/K_M$ , is on the order of  $10^8 \text{ M}^{-1}\text{s}^{-1}$ , nearly the rate of a diffusion controlled mechanism.



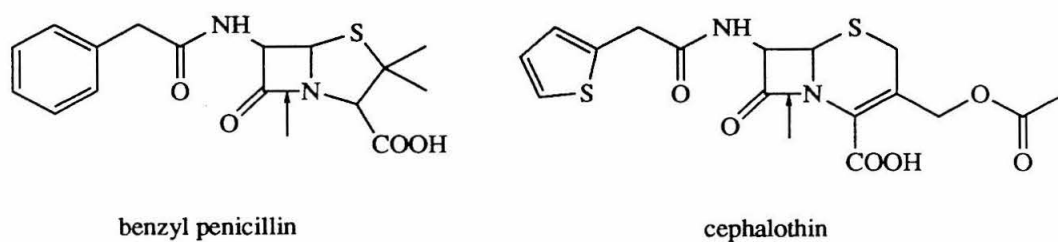


Figure 1. Representative  $\beta$ -lactam antibiotics. Benzyl penicillin is a member of the penam family, cephalothin is a cephem. Arrow points to bond broken during hydrolysis.

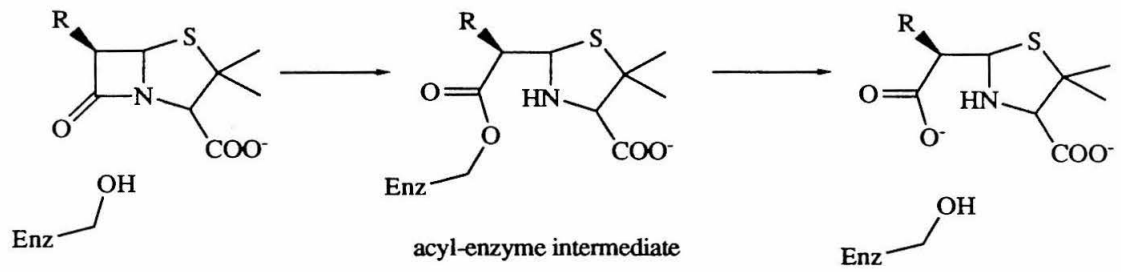


Figure 2. Overall reaction catalyzed by  $\beta$ -lactamase

Though the overall mechanism of  $\beta$ -lactamase activity is understood, the role of many specific residues has not been well characterized. A detailed understanding of the catalytic mechanism of these enzymes would not only further the understanding of the structure/function relationships of enzymatic processes in general, but would also aid in the rational design of new antibiotics.

To date the most elusive aspect of the detailed mechanism of action of  $\beta$ -lactamase is the nature of activation of the active site serine hydroxyl. Figure 3 shows the arrangement of residues in the active site. It has been assumed that a proton shuttle mechanism akin to the serine proteases is at work in the active site of  $\beta$ -lactamase. An alternative explanation was put forth by Hertzberg *et al.* with the publication of their crystal structure (13). The authors implicated Lys 73 as influencing Ser 70, but through electrostatic assistance of the Lys 73 positively charged ammonium group. An alternate explanation was suggested by Strynadka *et al.* in a paper describing the crystal structure of the acyl-enzyme intermediate of a deacylation defective mutant (14). These authors predicted that Lys 73 functioned as a general base, removing the proton from Ser 70, thus increasing its nucleophilicity (Figure 4). For this to be plausible, the  $pK_a$  of Lys 73 would have to be depressed approximately three to four pH units from the typical  $pK_a$  of  $\sim 10$ . This is not unheard-of, as  $pK_a$ 's of lysine side chains in proteins have been measured as low as 5.9 (15). Unfortunately, normal crystal structure analysis does not give information about protons, so no further evidence for this mode of action was available.

In order to test this hypothesis, the  $pK_a$  of Lys 73 would need to be determined some way. Mutagenesis experiments in our laboratories showed that any changes at position 73 resulted in severely impaired enzyme. Further, the mutation K73C gave enzyme that was down  $\sim 10^4$  from wild-type (16). However, upon reaction with ethyleneimine, activity of the K73C mutant was restored to near wild-type levels (17). The newly competent enzyme was deemed to have an aminoethylated cysteine residue at

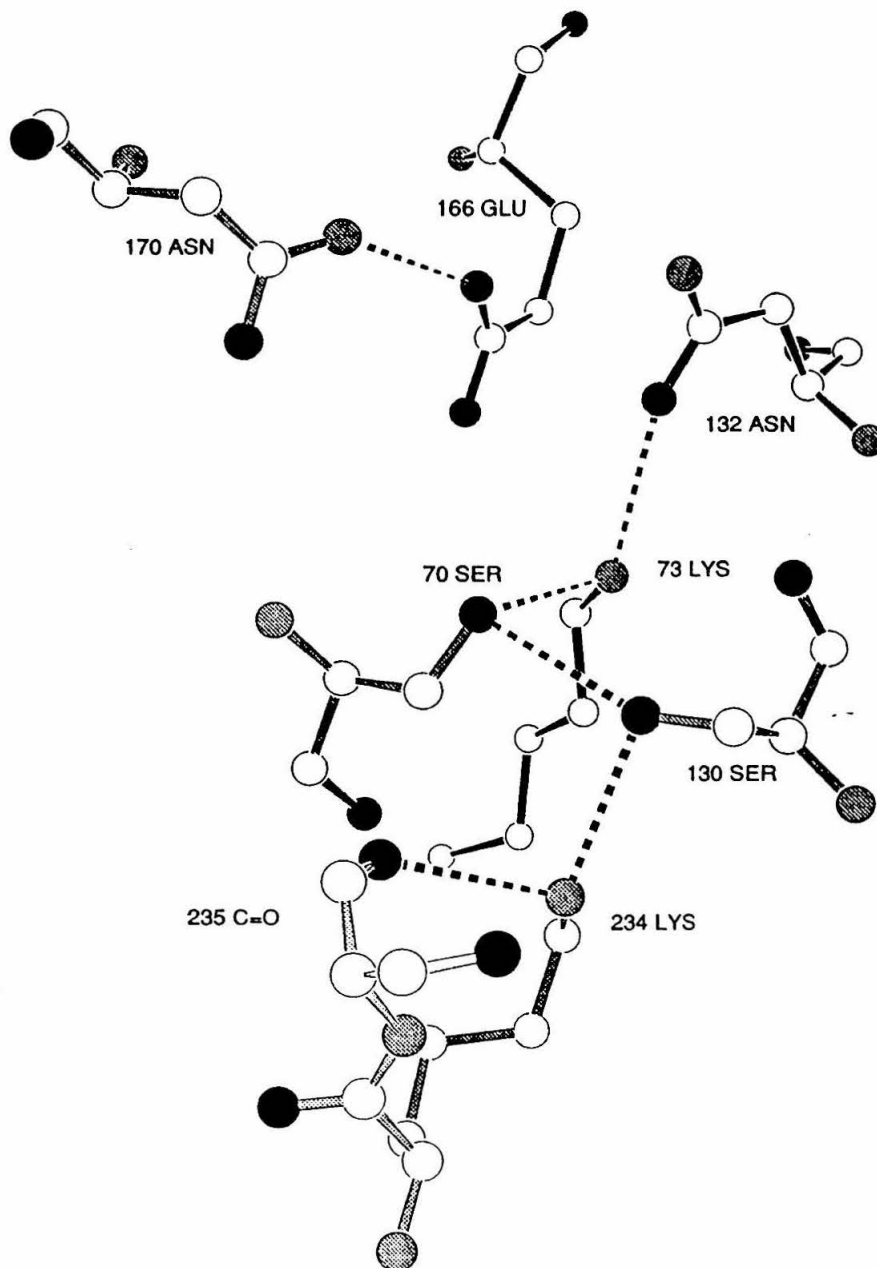


Figure 3. Arrangement of residues in the active site of RTEM-1  $\beta$ -lactamase.

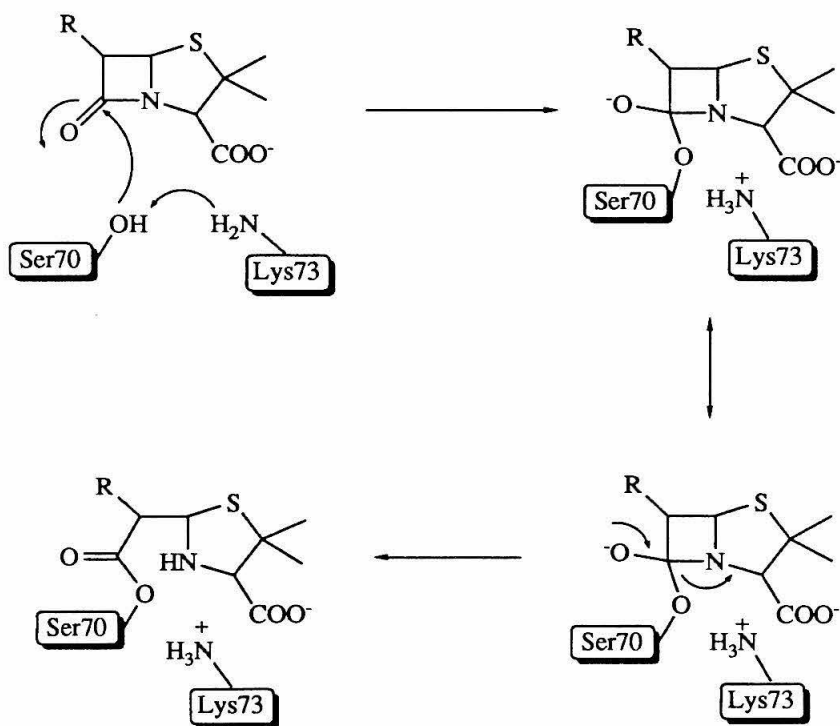


Figure 4. Formation of acyl-enzyme intermediate with Lys 73 functioning as a general base.

position 73, which effectively mimics the native lysine side chain, save the change of a single carbon to a sulfur atom (Figure 5). This result suggested an experiment where in the K73C mutant could be reacted with an amino ethylating reagent containing a stable isotope which would permit NMR studies in spite of  $\beta$ -lactamase size (Figure 6). Both  $^{15}\text{N}$  and  $^{13}\text{C}$  nuclei could be incorporated into a labeling molecule (Figures 7 and 8), and the  $\text{pK}_a$  of the resulting aminoethylcysteine could be determined by an NMR titration experiment.

The chemical shift of NMR active nuclei can shift when influenced by changes in charge and/or protonation on adjacent atoms. Specifically, a  $^{15}\text{N}$  atom's chemical shift changes by  $\sim 7$  ppm upon protonation of the neutral amine (Figure 9)(18). Similarly, a  $^{13}\text{C}$  nuclei  $\beta$  to an amine undergoes an  $\sim 6$  ppm shift upon protonation of the amine (Figure 10)(19). The  $\alpha$ -carbon shift is much less pronounced. These shifts theoretically could be followed by taking spectra at a variety of pH's, and a  $\text{pK}_a$  extracted from the data.

Indirect detection NMR methods can also be used to examine the ionization of residue 73. These so called Heteronuclear Multiple Nuclear Coherence (HMQC) experiments are advantageous in that the  $^1\text{H}$  nuclei is being detected, rather than  $^{13}\text{C}$  and  $^{15}\text{N}$ , which have much lower sensitivities than proton (20). The experiment also enables one to look only at protons which are bonded to  $^{13}\text{C}$  (or  $^{15}\text{N}$ ) heteronuclei (21). Thus the lion share of the proton signals from the enzyme are edited out, and only very specific protons are seen in the case of the above mentioned labeling experiments. Thus lower concentrations of protein can be used, avoiding potential solubility and related problems.

Using any of these experimental approaches, the  $\text{pK}_a$  of the native Lys 73 amine side chain could be inferred from the experimental  $\text{pK}_a$  of the aminoethylcysteine side chain, which is  $\sim 1$   $\text{pK}_a$  unit lower than lysine (22). The presence of a depressed  $\text{pK}_a$  ( $\sim 7$  or 8) in the aminoethylated enzyme would indicate that Lys 73 could indeed function as a general base, activating Ser 70.

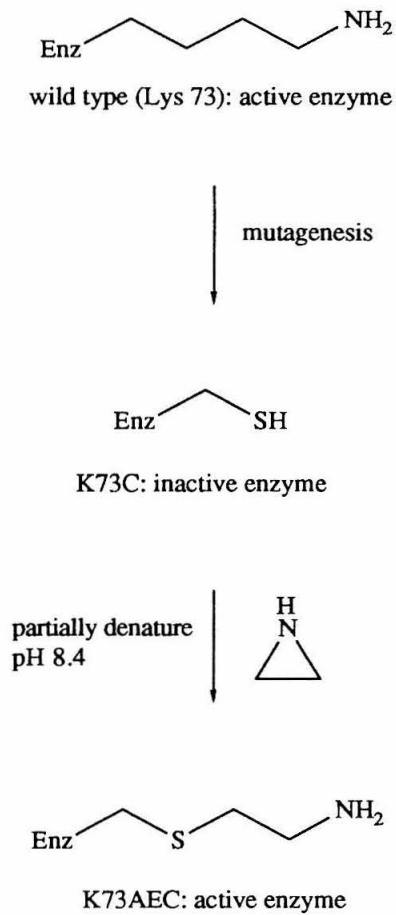


Figure 5. Reaction of inactive K73C mutant with ethyleneimine restores activity.

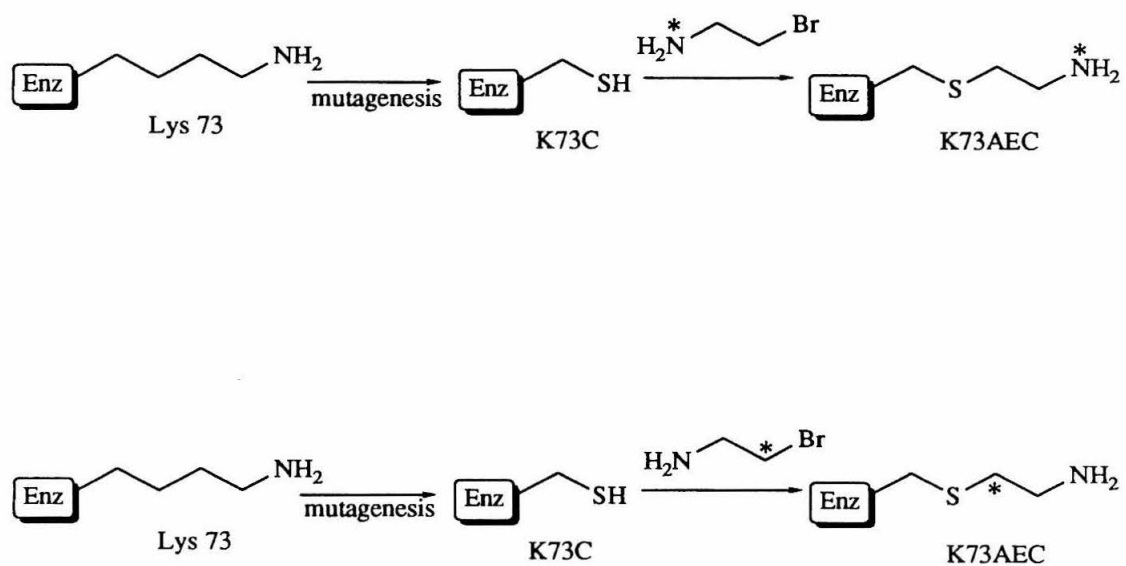


Figure 6. Scheme for introducing <sup>15</sup>N and <sup>13</sup>C at position 73 of RTEM-1 β-lactamase



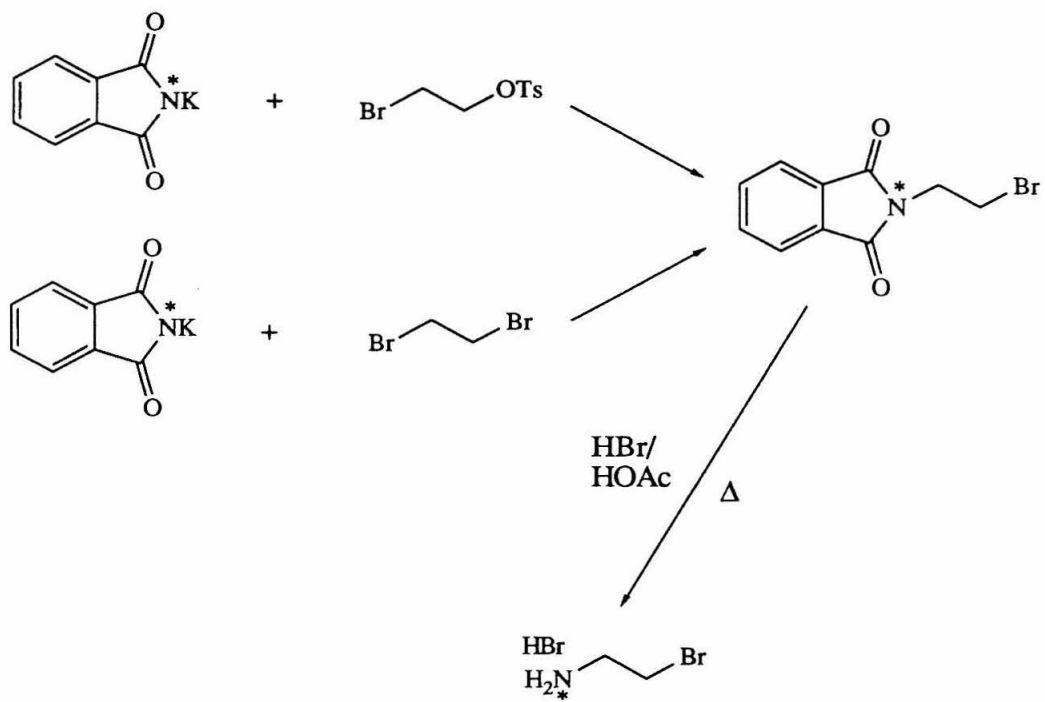


Figure 7. Synthesis of  $^{15}\text{N}$ -2-bromoethylamine (BEA).

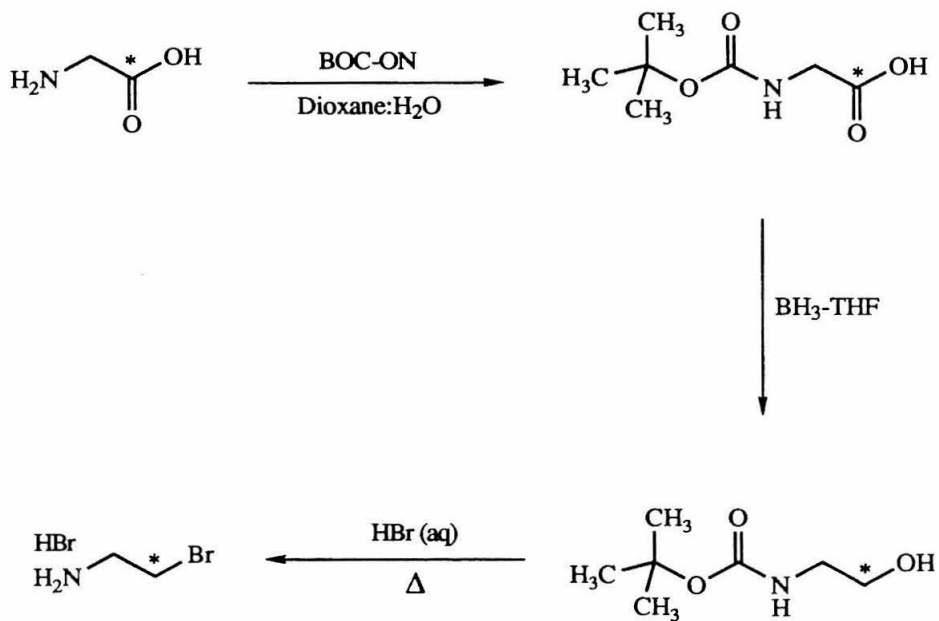


Figure 8. Scheme for synthesis of  $^{13}\text{C}$ -bromoethylamine hydrobromide

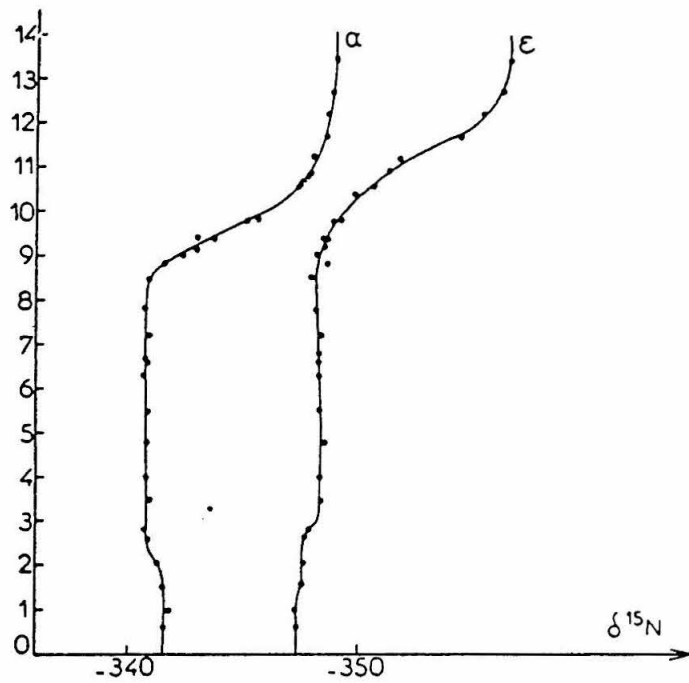
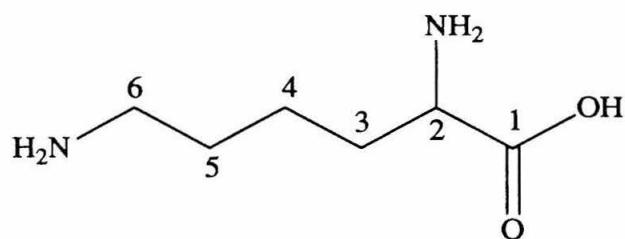


Figure 9. Plot of chemical shift vs. pH for  $^{15}\text{N}$  in lysine.



pH	<u>C-1</u>	<u>C-2</u>	<u>C-3</u>	<u>C-4</u>	<u>C-5</u>	<u>C-6</u>
0.5	173.2	54.0	30.5	22.6	27.6	40.5
6.0	175.8	55.9	31.2	22.6	27.7	40.5
13.9	184.8	57.3	35.7	23.6	33.0	41.8

Figure 10.  $^{13}\text{C}$  chemical shifts at different pH's for lysine.

## MATERIALS AND METHODS

*Enzymes and chemicals.*  $^{15}\text{N}$ -potassium phthalimide and (1)- $^{13}\text{C}$ -glycine were obtained from Cambridge Isotope Laboratories. Other reagents were from Aldrich Chemical Company. NMR spectra were taken on GE 300 Mhz, Bruker AMX-500, and Varian 600 Mhz spectrometers. Media was from Difco Laboratories. FPLC equipment and columns were from Pharmacia. Enzymes were purchased from Boehringer Mannheim Biochemicals, New England Biolabs, and Promega. Antibiotics were from Sigma. Radioactive compounds were supplied by Amersham. Isopropyl- $\beta$ -thiogalactoside (IPTG) was from International Biotechnologies Inc. (IBI). Molecular biology grade reagents agarose, acrylamide, phenol, chloroform, ammonium persulfate were from Bio Rad.

*Bacterial Strains.* *Escherichia coli* were used in all experiments. Plasmid DNA was grown in strain D1210 (23); the pJN expression vector was grown in strain D1210, which is lac  $i^Q$ . Culture media was L broth unless otherwise indicated. Cells were made competent for transformation of plasmid DNA using a process adapted from Hanahan (24).

### Synthesis of $^{15}\text{N}$ -bromoethylamine hydrobromide.

*2-bromoethyltosylate.* This procedure is adapted from Organic Syntheses (25). In a typical experiment, bromoethanol (Aldrich) and *p*-toluenesulfonylchloride (Aldrich) in a 2:1 molar ratio was combined in pyridine, and left at 4°C overnight. The formation of pyridine hydrochloride is evidenced by the presence of white crystals at the bottom of the flask. The entire mixture is added to cold  $\text{H}_2\text{O}$ , and the 2-bromoethyltosylate separates as an oil. The oil is taken up in diethyl ether, and the aqueous layer extracted with diethyl ether. The combined organic layers are washed with cold aqueous HCl, then dried over  $\text{MgSO}_4$ . Upon evaporation, a yellow oil is isolated.

*<sup>15</sup>N-2-bromoethylphthalimide.* Two different methods were employed for the synthesis of <sup>15</sup>N-2-bromoethylphthalimide. The first is a modification of the Gabriel synthesis (26) put forth by Brown and van Gulick (27). The Gabriel synthesis of primary amines uses potassium phthalimide and an alkyl halide, condensing to form an alkylphthalimide, which is hydrolyzed under acidic conditions to the primary amine acid salt. For the synthesis of <sup>15</sup>N-2-bromoethylphthalimide, <sup>15</sup>N-potassium phthalimide is added to excess 1,2-dibromoethane in dimethylformamide. This is heated to 90°C for 1 hour, and the solvent removed under reduced pressure. The residue is taken up in water, and extracted with CH<sub>2</sub>Cl<sub>2</sub>. The combined organic layers are dried over MgSO<sub>4</sub>, filtered, and the solvent removed under reduced pressure. The resulting residue is triturated in petroleum ether, and dried in vacuo. In an effort to increase the yield, 2-bromoethyltosylate was tried as an alkylating reagent, as the tosylate functionality is a much better leaving group than bromide. Equimolar amounts of <sup>15</sup>N-potassium phthalimide and 2-bromoethyltosylate were combined in dimethylformamide, and heated to 90° C for 1 hour. Water was added, followed by extraction with diethyl ether. The combined organic layers were dried over MgSO<sub>4</sub>, filtered, and solvent removed in vacuo, giving white crystals of <sup>15</sup>N-2-bromoethylphthalimide .

*<sup>15</sup>N-2-bromoethylamine hydrobromide.* <sup>15</sup>N-2-bromoethylphthalimide was added to HBr in acetic acid and water, and refluxed for 9 hours. The solution was chilled, and solidified phthalic acid was removed by filtration. The filtrate was evaporated in vacuo, and the product crystallized from acetone to give <sup>15</sup>N-2-bromoethylamine hydrobromide.

### **Synthesis of <sup>13</sup>C-bromoethylamine hydrobromide.**

*<sup>13</sup>C-BOC-glycine.* Synthesized according to the procedure set forth by Itoh *et al.* (28). <sup>13</sup>C-glycine, 2-(tert-butoxycarbonyloxyimine)-2-phenylacetonitrile (BOC-ON), and neat triethylamine were combined in 1:1 Dioxane:water and stirred at room temperature for

2 hours. Then water and ethyl acetate were added, and the organic layer discarded. The aqueous layer was washed with ethyl acetate. The aqueous layer was then acidified by the addition of 10% citric acid, and extracted with diethyl ether. The combined organic fractions were dried over  $\text{MgSO}_4$ , filtered, and the solvent removed in vacuo, giving  $^{13}\text{C}$ -BOC-glycine .

*$^{13}\text{C}$ -BOC-ethanolamine.* The reduction of  $^{13}\text{C}$ -BOC-glycine to  $^{13}\text{C}$ -BOC-ethanolamine was accomplished by the use of the borane reagent  $\text{BH}_3\text{-THF}$  (29).  $^{13}\text{C}$ -BOC-glycine was added to dry THF in a 3-necked round bottom flask. The resulting solution was chilled to  $0^\circ\text{C}$ , and 1M  $\text{BH}_3\text{-THF}$  was added over 20 minutes from a separatory funnel. The resulting mixture was removed from the ice bath, allowed to come to room temperature, then stirred for 5 hours. The mixture was again chilled to  $0^\circ\text{C}$ , and 1.5N NaOH was added over 20 minutes. The resulting mixture was allowed to come to room temperature, and stirred overnight. The solution was saturated with solid  $\text{K}_2\text{CO}_3$ , and extracted with diethyl ether. The combined organic fractions were dried over  $\text{MgSO}_4$ , filtered, and solvent removed in vacuo.

*$^{13}\text{C}$ -2-bromoethylamine hydrobromide.* Synthesis of  $^{13}\text{C}$ -2-bromoethylamine hydrobromide was based on the modifications of Wystrach of the original Organic Synthesis Prep (30, 31). Concentrated HBr (48% HBr) was added slowly to  $^{13}\text{C}$ -BOC-ethanolamine . The resulting mixture was heated until water began to distill at  $100^\circ\text{C}$ . The boiling point raised to  $122^\circ\text{C}$ , and aqueous HBr was collected. Heating was continued until no more HBr distilled. The pot temperature was never allowed to rise above  $140^\circ\text{C}$ . The residue was chilled to below  $100^\circ\text{C}$ , and acetone was added with stirring. The mixture was left at  $-20^\circ\text{C}$  for 3 hours, and resulting solid  $^{13}\text{C}$ -2-bromoethylamine hydrobromide was collected by filtration.

**K73C  $\beta$ -lactamase.**

*DNA.* Oligonucleotides were synthesized by the Caltech Microchemical Facility using phosphoramidite chemistry (32) on an Applied Biosystems automated DNA synthesizer 380A. Degenerate oligonucleotides were made equimolar in A, C, G, and T at positions 1 and 2 of the codon, and in C and G at position 3. These oligonucleotides were purified by preparative polyacrylamide gel electrophoresis.

Wild-type plasmid pBR322 and bacteriophage M13 mp18 replicative form (RF) DNA were purchased from Bethesda Research Laboratories. Mutant plasmids and RF phage were purified from *E. coli* by alkaline lysis method (33, 34). Single-stranded phage DNA was prepared from phage supernatant by precipitation with 20% polyethylene glycol-6000/2.5 M NaCl (35) followed by phenol/chloroform extraction and ethanol precipitation.

Restriction digest typically used 10-20  $\mu$ g plasmid DNA, 2-5 units of restriction enzyme, and 2  $\mu$ l 10X digest buffer in 20  $\mu$ l at 37°C for 1-2 hours. DNA restriction fragments were run in 1.2% low melt agarose gels, visualized with ethidium bromide, and isolated by established procedures (34).

*Mutagenesis.* Cassette mutagenesis is a technique wherein mutations can be introduced into a gene of interest using complementary synthetic oligonucleotides in conjunction with restriction endonucleases, followed by ligation. Providing convenient restriction sites are available in the gene, mutagenesis of one or more residues can be accomplished without the use of a single stranded vector or subcloning routines.

The site saturation of residue 73 was accomplished previously by Steve S. Carroll in our laboratories (18). Briefly, complementary synthetic oligonucleotides containing a degenerate codon at residue 73 and overhangs corresponding to *Ava* I and *Sca* I sites were kinased and annealed by standard procedures (34). Plasmid pBR-CR7 (39) was digested with *Sca* I and *Sal* I, and the 3286 bp fragment was isolated from a low melt agarose gel (34). Plasmid pBR322-XN1 (18) was digested with *Ava* I and *Sal* I, and the 1042 bp fragment isolated from a low melt agarose gel. These two fragments were mixed in



equimolar concentrations with a five-fold excess of the synthetic cassette insert, and ligated by standard procedures (34). 10  $\mu$ l of this ligation mixture were transfected directly into competent *E. coli* strain HB101 and cells were spread onto L plates containing 15mg/l tetracycline. The plasmid DNA was isolated by alkaline lysis, and subjected to restriction analysis and sequencing.

*DNA Sequencing.* Plasmid DNA was sequenced using a modification of the Sanger dideoxy method for denatured, double-stranded DNA (36). Plasmid DNA together with sequencing primer was boiled for 5 minutes, then snap frozen in dry ice/ethanol. Chain extension reactions were performed with a SEQUENASE™ kit from United States Biochemical (37). Radioactive labeling was accomplished with  $\alpha$ -<sup>35</sup>S-dATP. Labeled DNA was separated on 8% polyacrylamide sequencing gels, and resulting gels were dried *in vacuo*. Kodak AR x-ray film was then exposed in the presence of the sequencing gel for 12 hours.

*Protein Expression and Purification.* To facilitate expression, the mutant  $\beta$ -lactamases were subcloned into pJN, and expression vector which was developed in this lab (38). It contains the  $\beta$ -lactamase gene under control of the tac promoter (39), and well as a kanamycin gene for a selection marker. Synthesis of  $\beta$ -lactamase is induced by the addition of IPTG.

Twelve liter cultures of *E. coli* D1210 containing mutant plasmid were grown in TB broth (25 g Tryptone, 25 g yeast extract, 3 ml glycerol, 100 mls 1 M phosphate pH 8 per liter of broth) containing 50 mg/L kanamycin for 12-14 hours at 37°C. IPTG was added to a final concentration of 0.1 mM and growth continued for 2 hours at 37°C. Cells were centrifuged in 1 l bottles in a rotor for 30 minutes at 4,000 rpm.  $\beta$ -lactamase, which is located in the periplasm, was released by osmotic extrusion (40). The sample containing the periplasmic proteins made 25 mM TEA pH 7.3 by the addition of 1 M TEA pH 7.3, and added to ~ 150 mls of MonoQ fast Flow resin. This mixture was stirred at 4°C for 1 hour,

and applied to an empty gravity column. The resulting resin was washed further with ~ 200 mls of 25 mM TEA pH 7.3. The protein was eluted with 200 mM NaCl in 25 mM TEA pH 7.3 (~200 mls). This solution was dialyzed and concentrated to ~ 30 mls in 25 mM TEA pH 7.3 (Buffer A) by ultrafiltration (Amicon unit, YM 10 membrane, N<sub>2</sub> gas pressure). The resulting solution was then filtered through a Schleicher and Schuell 0.22 m Uniflow filter to remove any cellular debris.

Further purification was carried out using FPLC (fast protein liquid chromatography) first with a HR16/10 Fast Flow MonoQ™ column, followed by a HR10/10 MonoQ™, both by Pharmacia. Crude protein was loaded onto the fast flow column, and the column was washed in 100% A (25 mM triethanolamine (TEA), pH 7.65). Then crude β-lactamase was eluted with 20%B (25 mM TEA, 1M NaCl). This protein was loaded onto the HR 10/10 column in 25 mM TEA and eluted with a salt gradient. The gradient used was: t=0, 100% A, t=5, 100% A, t=35, 80%A, 20%B, t=45, 100% B. The flow rate was 1.0 ml/min. Elution was monitored by A<sub>280</sub>. Peak fractions were pooled and dialyzed versus 100 mM potassium phosphate, pH 7.0. Protein concentrations were estimated from OD<sub>280</sub> using an extinction coefficient of 29,400 M<sup>-1</sup>cm<sup>-1</sup>(2). Samples were run on 15% polyacrylamide gels (34) and stained with Coomassie blue to gauge purity.

*Aminoethylation of K73C β-lactamase.* Purified K73C β-lactamase was dialyzed into 500 mM sodium phosphate, pH 8.4 by ultrafiltration (Amicon unit, YM10 membrane). Two labeling conditions were employed. The first involved partial denaturation of the protein by addition of solid urea to a final concentration of 4.0 M urea. To this was added sufficient labeled 2-bromoethylamine hydrobromide to a final concentration of 100 mM. This solution was left at room temperature overnight. A five-fold excess of 500 mM phosphate pH 8.4/4.0 M urea was added to the solution, and this was dialyzed against 50 mM phosphate pH 7.0 (dialysis tubing MW cutoff 8000). Alternatively, the protein in pH 8.4 phosphate buffer was made 100 mM in 2-bromoethylamine hydrobromide by

addition of solid compound, and this solution left at 37°C overnight. This solution was diluted five-fold with 500 mM phosphate pH 8.4, and dialyzed against 50 mM phosphate pH 7.0 (dialysis tubing MW cutoff 8000).

*Kinetic Characterization of K73AEC  $\beta$ -lactamase.* Michaelis-Menten kinetic parameters ( $k_{cat}$ ,  $K_M$ , and  $k_{cat}/K_M$ ) for mutant  $\beta$ -lactamases were determined by Hanes plots using initial rates (41). Reactions were carried out at 30°C in 100 mM potassium phosphate pH 7.0. All reagent were maintained at 30°C prior to beginning the assay to avoid error from temperature flux. An HP 8420 spectrophotometer was used for the assays, with quartz cells of pathlength 1 cm at wavelength 232 nm.

*$^1H$  NMR Spectroscopy.* Proton spectra for small molecules was performed on a GE-300 QE plus NMR spectrometer. Typical parameters are:

Pulse Width	=	4.75 $\mu$ sec @ 43 degrees
Acquisition Time	=	2.72 seconds
Recycle Time	=	3.71 seconds
Line Broadening	=	0 Hz
Spin rate	=	23 rps
Observe Frequency	=	300.199850 MHz
Spectral Width	=	6024 Hz

*$^{15}N$  NMR Spectroscopy.*  $^{15}N$  spectra were taken on a Bruker AMX-500 NMR spectrometer. Typical parameters were:

Pulse Width	=	31 $\mu$ sec @ 30 degrees
Acquisition Time	=	500 msec
Recycle Time	=	2.5 seconds
Line Broadening	=	10 Hz
Spin Rate	=	20 rps
Observe Frequency	=	50.698 MHz
Spectral Width	=	10000 Hz
Decoupler	=	CPD
Decoupler Frequency	=	9500 Hz
Decoupler Power	=	7L

*<sup>13</sup>C NMR Spectroscopy.* <sup>13</sup>C spectra were taken on a GE 300 QE plus NMR spectrometer. Typical parameters are:

Pulse Width	=	3.47 μsec @ 30 degrees
Acquisition Time	=	819.20 msec
Recycle Time	=	2.81 seconds
Line Broadening	=	0 Hz
Spin Rate	=	23 rps
Observe Frequency	=	75.492893 MHz
Spectral Width	=	20000 Hz
Decoupler	=	Standard-16 Modulation
Decoupler Frequency	=	4.001 ppm
Decoupler Power	=	2880/3000

*HMQC NMR Experiment.* The HMQC sequence can be reduced to a heteronuclear spin-echo difference experiment as illustrated in Figure 11. The proton portion of this sequence consists of a simple spin-echo experiment with the phase of the receiver alternated from scan to scan. For protons attached to <sup>12</sup>C (X = <sup>13</sup>C), for which the <sup>1</sup>H pulses are the only relevant pulses, the signal remains in constant phase from scan to scan--alternation of the receiver causes these signals to cancel. On the first scan, the <sup>13</sup>C nuclei experience a 180° pulse (90°<sub>x</sub> + 90°<sub>x</sub>) simultaneously with the <sup>1</sup>H 180°. Because this occurs at a time equal to 1/2J<sub>XH</sub>, the signal that results from this scan refocuses on the +Y axis. On the second scan, the <sup>13</sup>C nuclei effectively experience no pulse at all (90°<sub>x</sub> + 90°<sub>-x</sub>) so the protons refocus on the -Y axis, but the receiver is now inverted so the net signal is positive. Thus, the protons attached to <sup>13</sup>C have produced a positive signal on both scans, so the signal from these protons time-averages at the same time that the signals from the <sup>12</sup>C-bound protons cancel out.

## RESULTS

### Synthesis of <sup>15</sup>N-2-bromoethylamine hydrobromide.

*2-bromoethyltosylate.* In a typical experiment, 80 mmol (10 g) of 2-bromoethanol (Aldrich) and 160 mmol *p*-toluenesulfonylchloride (Aldrich) was combined in 100 ml

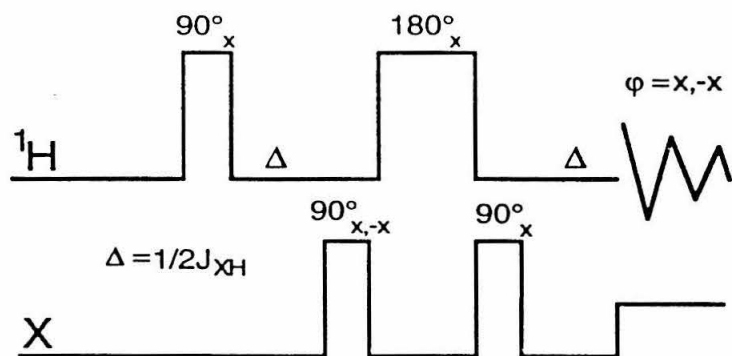


Figure 11. Pulse sequence for HMQC heteronuclear spin-echo difference experiment.

pyridine in a 250 ml Erlenmeyer flask, and left at 4°C overnight. The formation of pyridine hydrochloride is evidenced by the presence of white crystals at the bottom of the flask. The entire mixture is added to ~300 ml of cold water, and the 2-bromoethyltosylate separates as an oil. The oil is taken up in diethyl ether, and the aqueous layer extracted two times with diethyl ether. The combined organic layers are washed with cold aqueous HCl two times, then dried over MgSO<sub>4</sub>. Upon evaporation, a yellow oil is isolated, yield 21.3 g (90%).

*<sup>15</sup>N-2-bromoethylphthalimide.* Two different methods were employed for the synthesis of <sup>15</sup>N-2-bromoethylphthalimide. The Gabriel synthesis of primary amines uses potassium phthalimide and an alkyl halide, condensing to form an alkylphthalimide, which is hydrolyzed under acidic conditions to the primary amine acid salt. For the synthesis of <sup>15</sup>N-2-bromoethylphthalimide, 5.4 mmol <sup>15</sup>N-potassium phthalimide (1.0 g, Cambridge Isotope Laboratories) is added to 16.1 mmol 1,2-dibromoethane (3.0 g, Aldrich) in 5.2 ml dimethylformamide. This is heated to 90°C for 1 hour, and the solvent removed under reduced pressure. The residue is taken up in 6 mls water, and extracted three times with 6 mls CH<sub>2</sub>Cl<sub>2</sub>. The combined organic layers are dried over MgSO<sub>4</sub>, filtered, and the solvent removed under reduced pressure. The resulting residue is triturated in 6 mls petroleum ether, and dried in vacuo. Yield of <sup>15</sup>N-2-bromoethylphthalimide is 3.6 mmol (0.93g, 67%). In an effort to increase the yield, 2-bromoethyltosylate was tried as an alkylating reagent, as the tosylate functionality is a much better leaving group than bromide. 5 mmol <sup>15</sup>N-potassium phthalimide (0.93 g) and 5 mmol 2-bromoethyltosylate (1.40 g) were combined in 10 ml dimethylformamide, and heated to 90° C for 1 hour. 10 mls of water was added, followed by extraction with two times 20 ml diethyl ether. The combined organic layers were dried over MgSO<sub>4</sub>, filtered, and solvent removed in vacuo, giving white crystals of <sup>15</sup>N-2-bromoethylphthalimide (1.10 g, 4.3 mmol, 86% yield, <sup>1</sup>H NMR Figure 12)

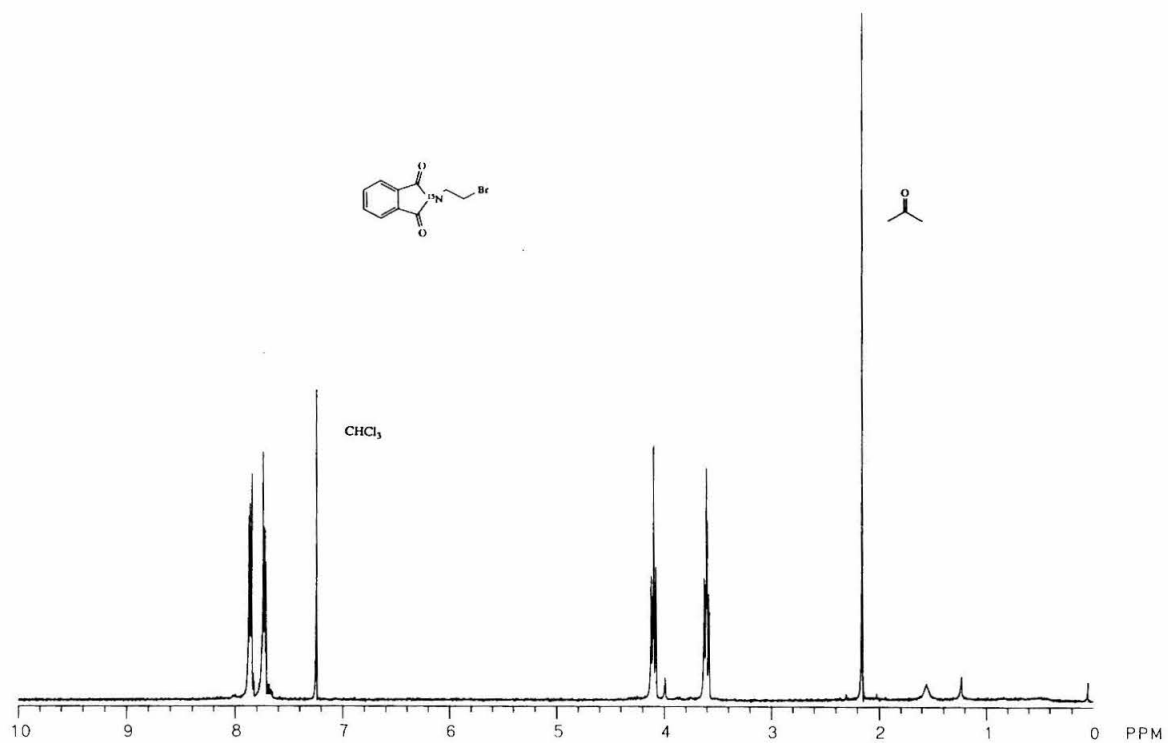


Figure 12.  $^1\text{H}$  NMR spectra of  $^{15}\text{N}$ -2-bromoethylphthalimide.

*<sup>15</sup>N-2-bromoethylamine hydrobromide.* <sup>15</sup>N-2-bromoethylphthalimide (2.5 g, 10 mmol) was added to 15 mls HBr in acetic acid and 5 ml water. This mixture was refluxed for 9 hours. The solution was chilled, and solidified phthalic acid was removed by filtration. The filtrate was evaporated in vacuo, and the product crystallized from acetone to give 0.93 g (45% yield) <sup>15</sup>N-2-bromoethylamine hydrobromide (<sup>1</sup>H NMR Figure 13)

Synthesis of <sup>13</sup>C-2-bromoethylamine hydrobromide.

*<sup>13</sup>C-BOC-glycine.* <sup>13</sup>C-glycine (0.75g, 10 mmol), 2-(tert-butoxycarbonyloxyimine)-2-phenylacetonitrile (BOC-ON, 2.7g, 11 mmol), and 2.8 mls neat triethylamine were combined in 12 mls of 1:1 dioxane:water and stirred at room temperature for 2 hours. Then 15 mls water and 20 mls ethyl acetate were added, and the organic layer discarded. The aqueous layer was washed with 20 mls ethyl acetate. The aqueous layer was then acidified by the addition of 10% citric acid, and extracted five times with 15 mls diethyl ether. The combined organic fractions were dried over MgSO<sub>4</sub>, filtered, and the solvent removed in vacuo, giving 1.53g <sup>13</sup>C-BOC-glycine (87%, <sup>1</sup>H NMR Figure 14, <sup>13</sup>C NMR Figure 15).

*<sup>13</sup>C-BOC-ethanolamine.* The reduction of <sup>13</sup>C-BOC-glycine to <sup>13</sup>C-BOC-ethanolamine was accomplished by the use of the borane reagent BH<sub>3</sub>-THF. 1.75g <sup>13</sup>C-BOC-glycine (10 mmol) was added to 3 mls dry THF in a 50 mls 3-necked round bottom flask. The resulting solution was chilled to 0°C, and 20 mls 1M BH<sub>3</sub>-THF (20 mmol) was added over 20 minutes from a separatory funnel. The resulting mixture was removed from the ice bath, allowed to come to room temperature, then stirred for 5 hours. The mixture was again chilled to 0°C, and 6 mls 1.5N NaOH was added over 20 minutes. The resulting mixture was allowed to come to room temperature, and stirred overnight. The solution was saturated with solid K<sub>2</sub>CO<sub>3</sub>, and extracted with 10 mls diethyl ether five times. The combined organic fractions were dried over MgSO<sub>4</sub>, filtered, and solvent removed.



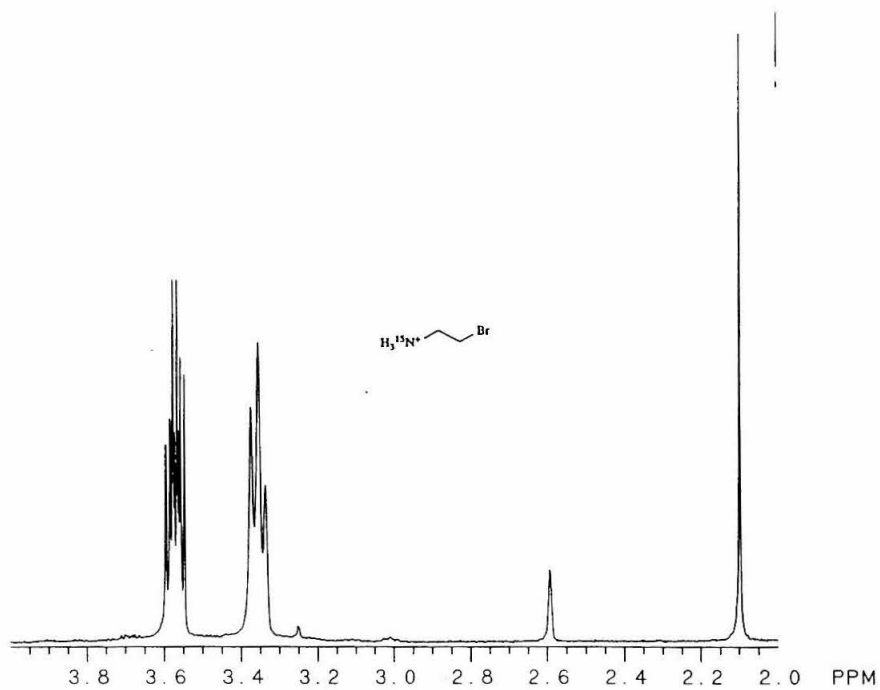


Figure 13.  $^1\text{H}$  NMR spectra of  $^{15}\text{N}$ -2-bromoethylamine hydrobromide.

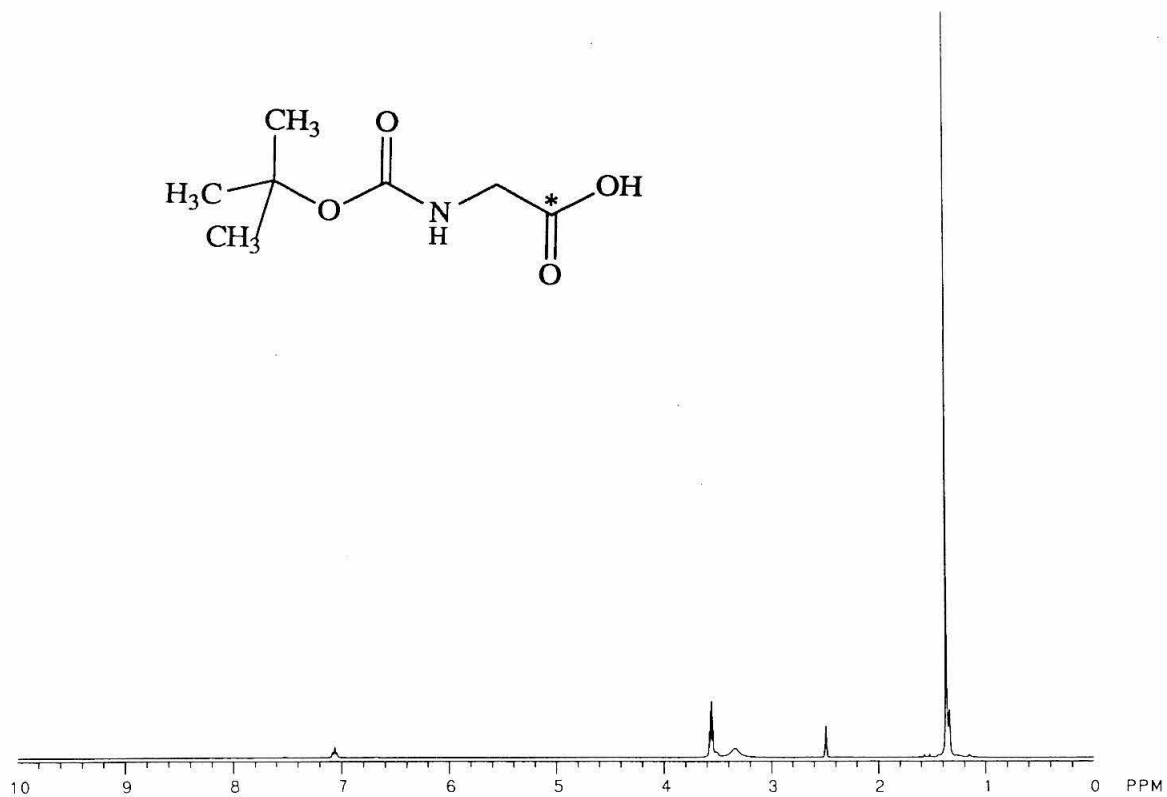


Figure 14.  $^1\text{H}$  NMR spectra of  $^{13}\text{C}$ -BOC-glycine. Solvent is  $\text{d}_6$ -DMSO.

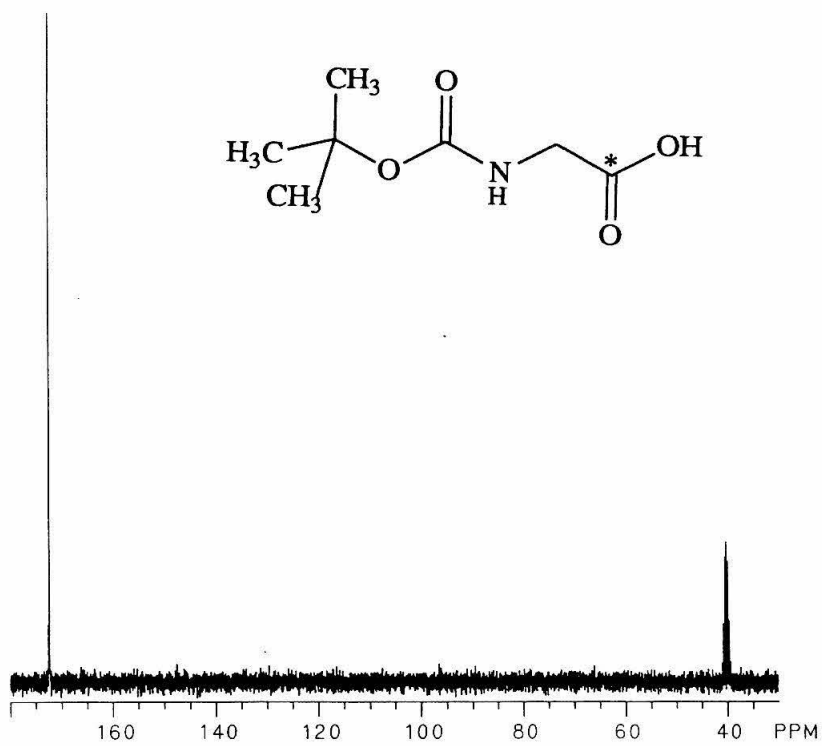


Figure 15.  $^{13}\text{C}$  NMR spectra of  $^{13}\text{C}$ -BOC-glycine. Solvent is  $\text{d}_6$ -DMSO.

Yield of  $^{13}\text{C}$ -BOC-ethanolamine was 1.29 g (78%,  $^1\text{H}$  NMR Figure 16,  $^{13}\text{C}$  NMR Figure 17).

*$^{13}\text{C}$ -2-bromoethylamine hydrobromide.* Synthesis of  $^{13}\text{C}$ -2-bromoethylamine hydrobromide was based on the modifications of X of the original Organic Synthesis Prep. 5.2 mls concentrated HBr (48% HBr, 36 mmol) was added slowly to 2.32 g  $^{13}\text{C}$ -BOC-ethanolamine (14.5 mmol). The resulting mixture was heated until water began to distill at  $100^\circ\text{C}$ . The boiling point increased to  $122^\circ\text{C}$ , and aqueous HBr was collected. Heating was continued until no more HBr distilled. The pot temperature was never allowed to rise above  $140^\circ\text{C}$ . The residue was chilled to below  $100^\circ\text{C}$ , and 3 mls acetone was added with stirring. The mixture was left at  $-20^\circ\text{C}$  for 3 hours, and resulting solid  $^{13}\text{C}$ -2-bromoethylamine hydrobromide was collected by filtration (1.10g, 37% yield,  $^1\text{H}$  NMR Figure 18,  $^{13}\text{C}$  NMR Figure 19)

*Expression and Purification of K73C mutant.* Twelve liters of media with proper antibiotic were grown to saturation at  $37^\circ\text{C}$ . IPTG was added (24 mg/l) and incubation continued for 1 hour. After dialysis into Buffer A and concentration by Amicon,  $\beta$ -lactamase was purified on a Mono Q column by FPLC (Figure 20). Fractions containing  $\beta$ -lactamase were identified by PAGE (Figure 21).

*Aminoethylation of K73C mutant.* Early attempts to label the K73C mutant were plagued by renaturation difficulties. Test labeling reaction with a small amount of enzyme was successful, but upon scale up to amounts necessary for NMR experiments, protein precipitated upon refolding and dialysis into the pH 7.0 buffer. Initial conditions were worked out by Steve S. Carroll in our labs (18), but these conditions proved unsatisfactory for larger amounts of protein. So modifications of his original protocol were made, switching from Tris as a buffer, to phosphate. Also, dilution of the labeling solutions prior to dialysis was found to be helpful. Up to 30 mg of protein was labeled in 4 mls of labeling solution, split between 4.0 M urea conditions and  $37^\circ\text{C}$  conditions. Upon dilution and

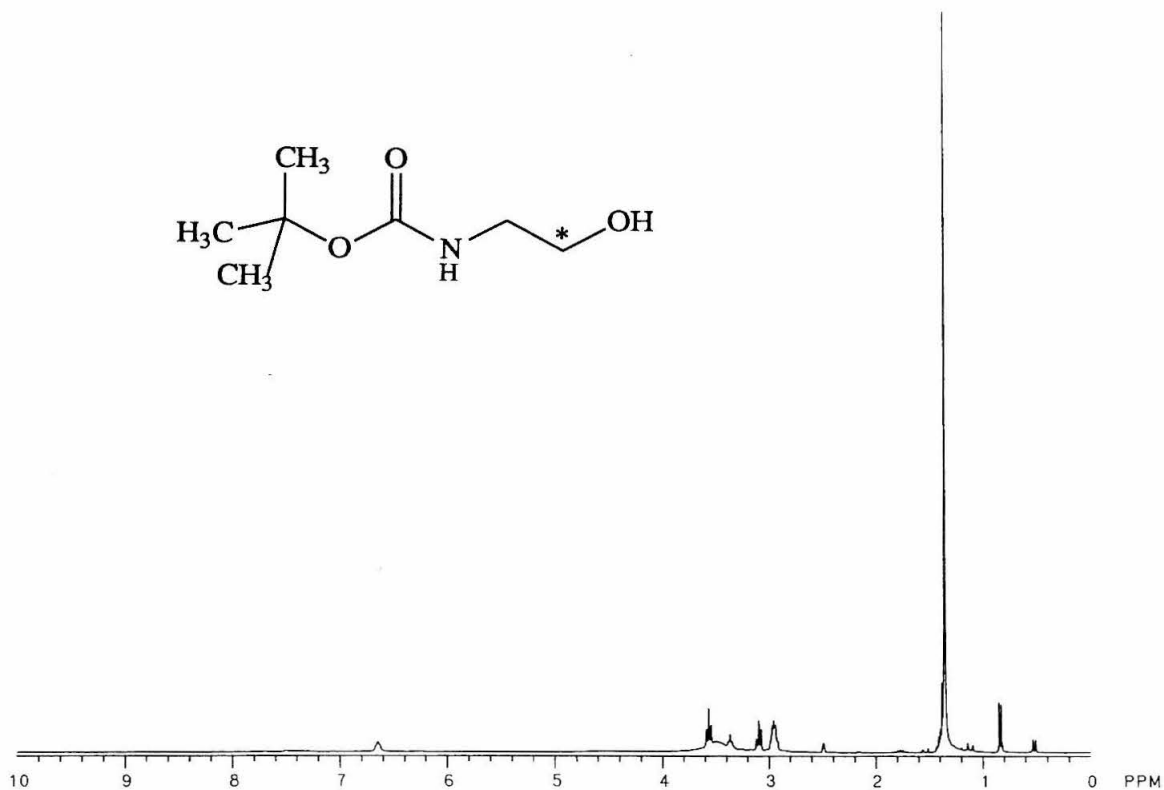


Figure 16.  $^1\text{H}$  NMR spectra of  $^{13}\text{C}$ -BOC-ethanolamine. Solvent is  $\text{d}_6$ -DMSO.

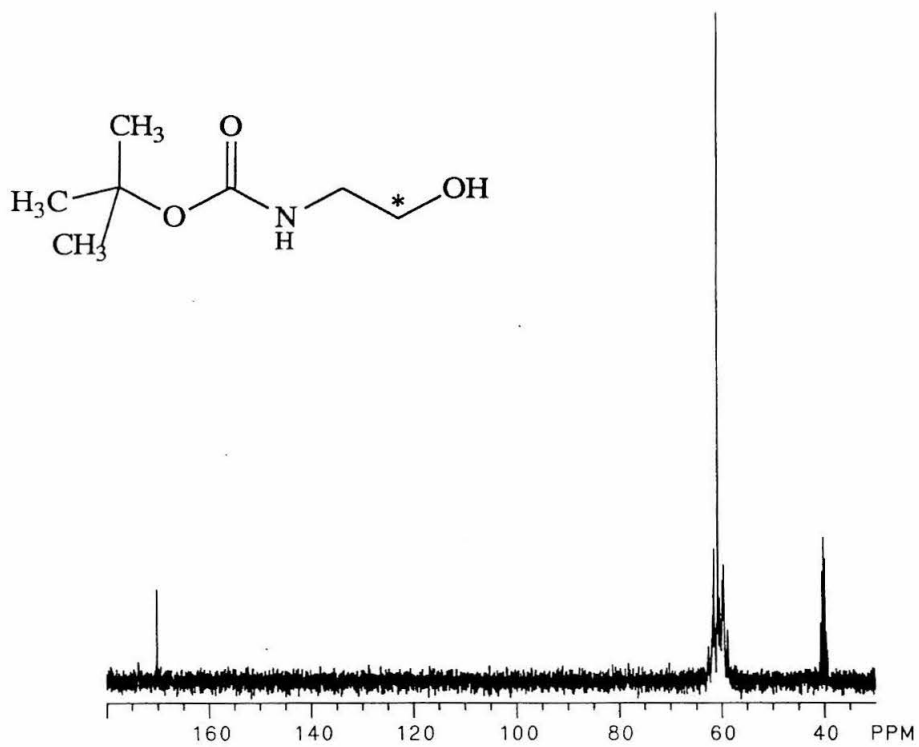


Figure 17.  $^{13}\text{C}$  NMR spectra of  $^{13}\text{C}$ -BOC-ethanolamine. Solvent is  $\text{d}_6$ -DMSO.

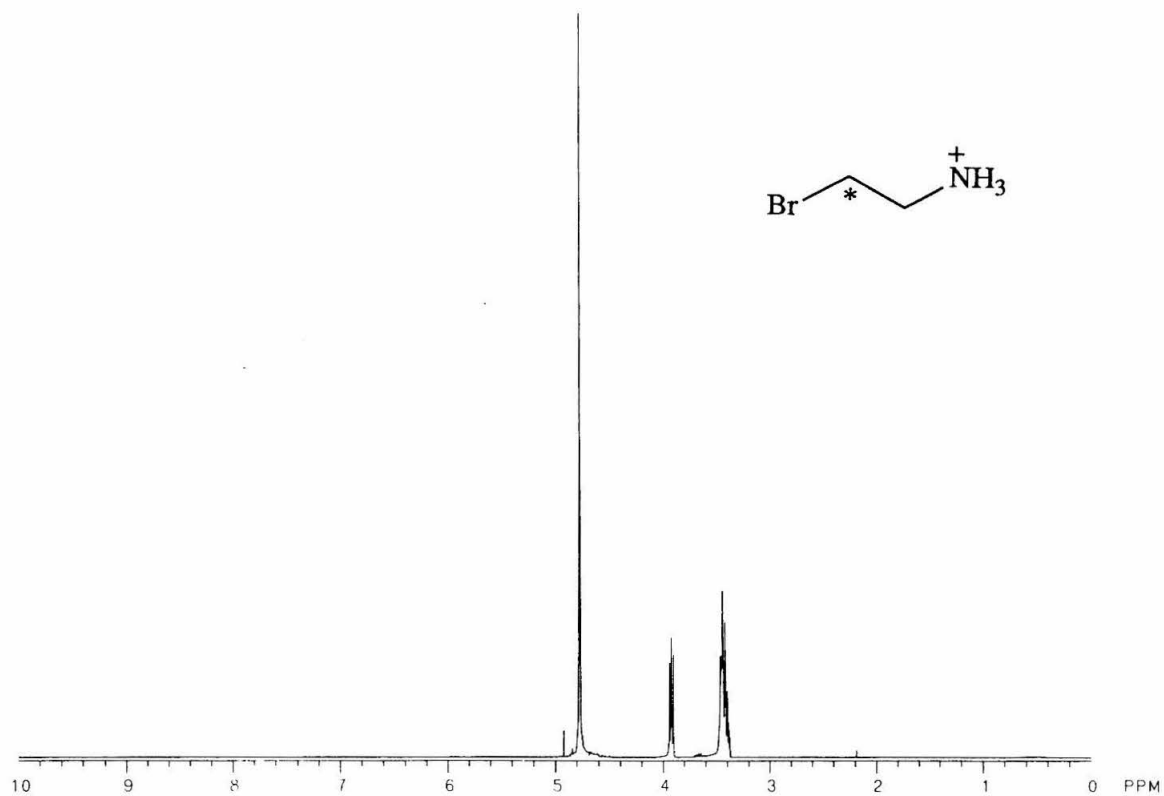


Figure 18.  $^1\text{H}$  NMR spectra of  $^{13}\text{C}$ -2-bromoethyamine hydrobromide. Solvent is  $\text{D}_2\text{O}$ .

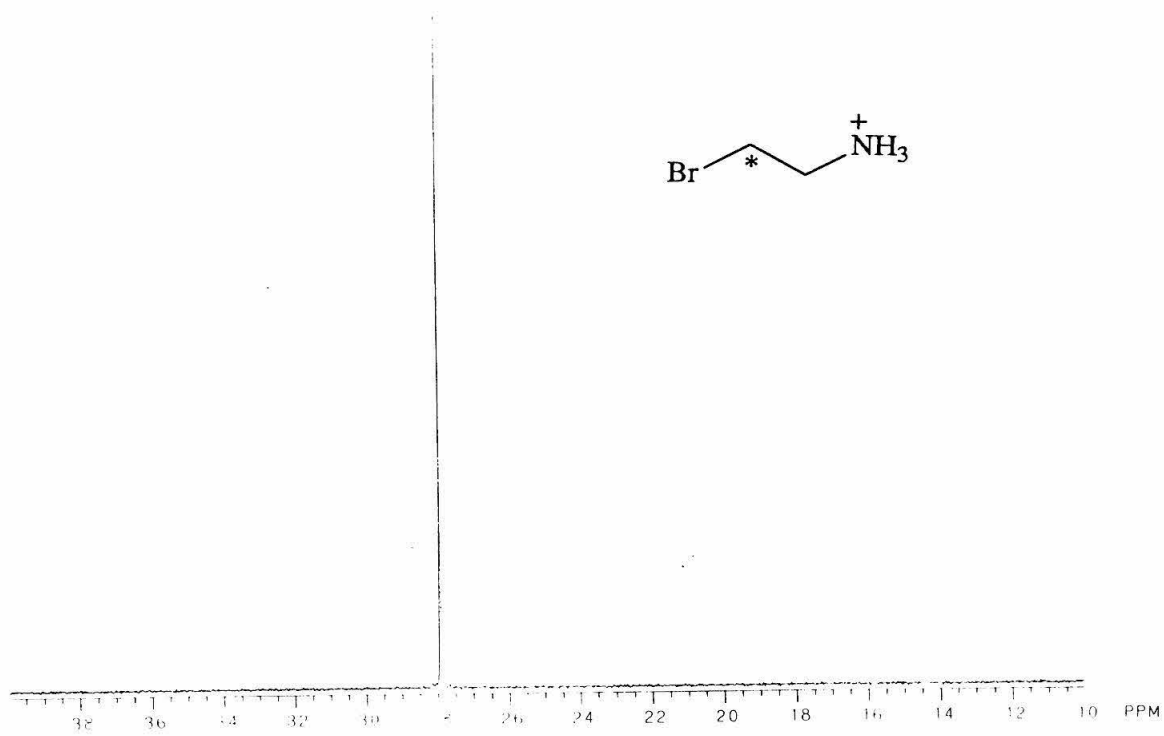


Figure 19.  $^{13}\text{C}$  NMR spectra of  $^{13}\text{C}$ -2-bromoethylamine hydrobromide. Solvent is  $\text{D}_2\text{O}$ .



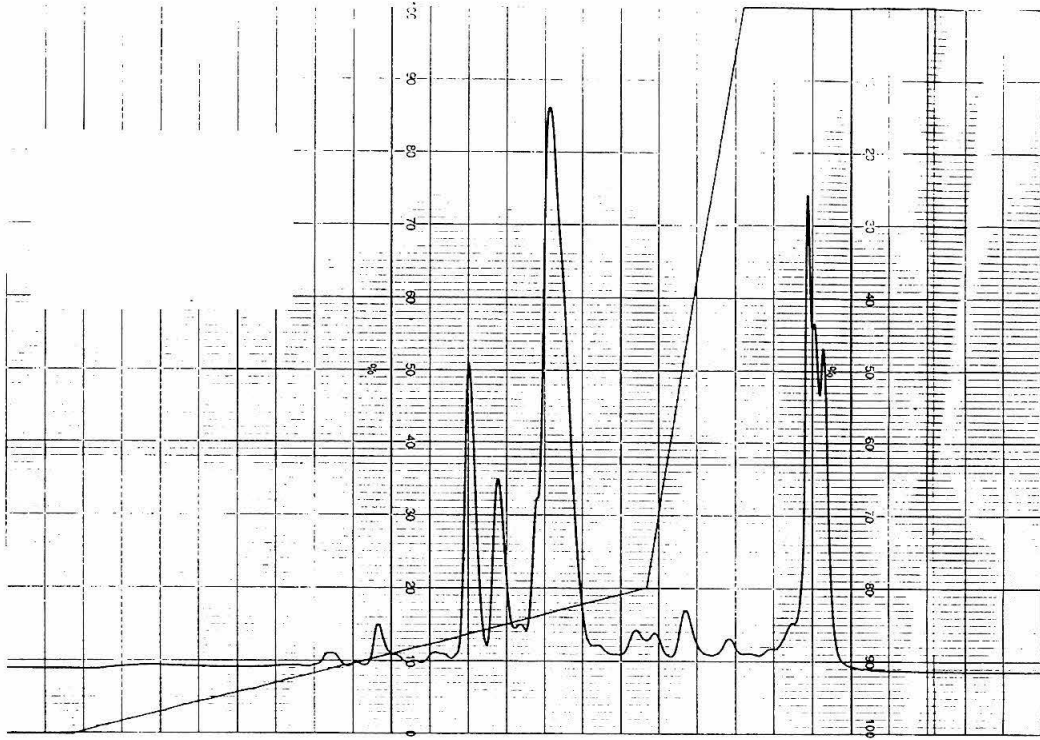


Figure 20. FPLC trace for purification of K73C mutant.  $\beta$ -lactamase is in peak @ 15% B.

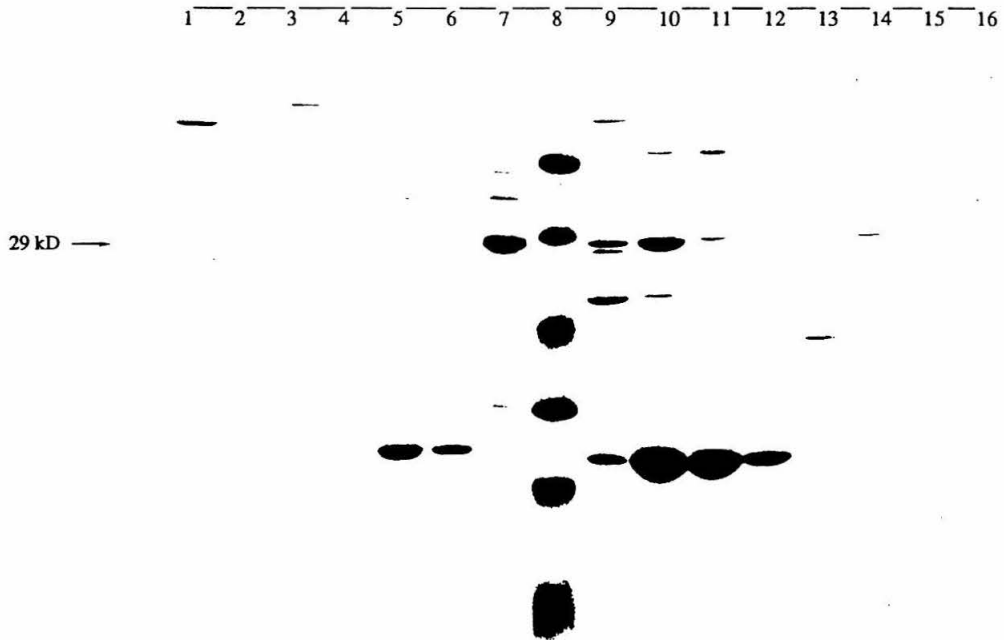


Figure 21. PAGE of FPLC fractions for K73C mutant.  $\beta$ -lactamase is in fraction 7.

dialysis eventually into 50 mM phosphate, enzyme was isolated, with activity analyzed by kinetic studies, and purity assayed by PAGE. Enzyme was found to be homogeneous before and after labeling (data not shown).

*Activity of K73AEC mutant.* The activity of the labeled mutant was checked by kinetic analysis under standard conditions. The highest level of activity was found to be ~50% that of wild-type, and activity before and after labeling was assayed (Figure 22).

*<sup>15</sup>N-Titration of K73AEC.* Labeled protein was added to a 10 ml NMR tube in ~50% D<sub>2</sub>O, 25 mM phosphate pH 7.0 at a concentration of ~20 mg/ml. At this concentration, protein slowly precipitated out of solution, indicating that this is the upper limit of β-lactamase solubility. Repeated attempts to see an <sup>15</sup>N signal were unsuccessful. A variety of pulse delay times were tried to allow for long relaxation times, but experiments involving upwards of 20,000 scans still revealed no <sup>15</sup>N signal (Figure 23).

*<sup>13</sup>C-Titration of K73AEC.* A <sup>13</sup>C spectra of aminoethylcysteine (Aldrich) was taken to ascertain where the <sup>13</sup>C nuclei of the carbons α- and β- to the amine would be. It was determined that these two carbons had a chemical shift of 37 ppm and 27 ppm (Figure 24). Labeled protein was added to a 5 ml NMR tube in ~50% D<sub>2</sub>O, 25 mM phosphate pH 7.0 at a concentration of ~10 mg/ml. A small amount of d<sub>6</sub>-DMSO was used as a <sup>13</sup>C reference. The initial experiment with a delay time of 1 second and 18,000 scans revealed no <sup>13</sup>C peak other than the DMSO reference. Another experiment was run on the same sample with an increased delay time of 2 seconds. This gave what appeared to be a small single peak at 30 ppm, but was determined to be an artifact. The protein concentration was increased to 20 mg/ml, but still no <sup>13</sup>C signal for the protein was seen (Figure 25).

*HMQC NMR Experiment.* To determine the correct parameters for the spin-echo experiment, <sup>13</sup>C-2-bromoethylamine hydrobromide was used in model experiments. Figure 26 shows the results of these experiments. The bottom spectra is a <sup>1</sup>H spectra for <sup>13</sup>C-2-bromoethylamine hydrobromide. The middle spectra is the <sup>13</sup>C edited <sup>1</sup>H spectra, and the

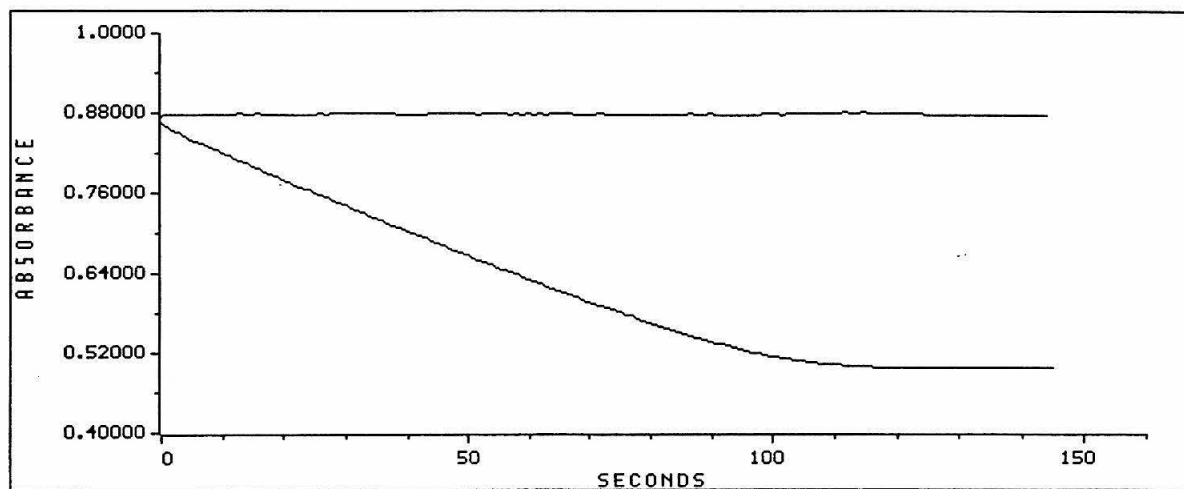


Figure 22. Plot of absorbance vs. time for hydrolysis of benzyl penicillin catalyzed by K73C before and after labeling with  $^{13}\text{C}$ -2-bromoethylamine hydrobromide.

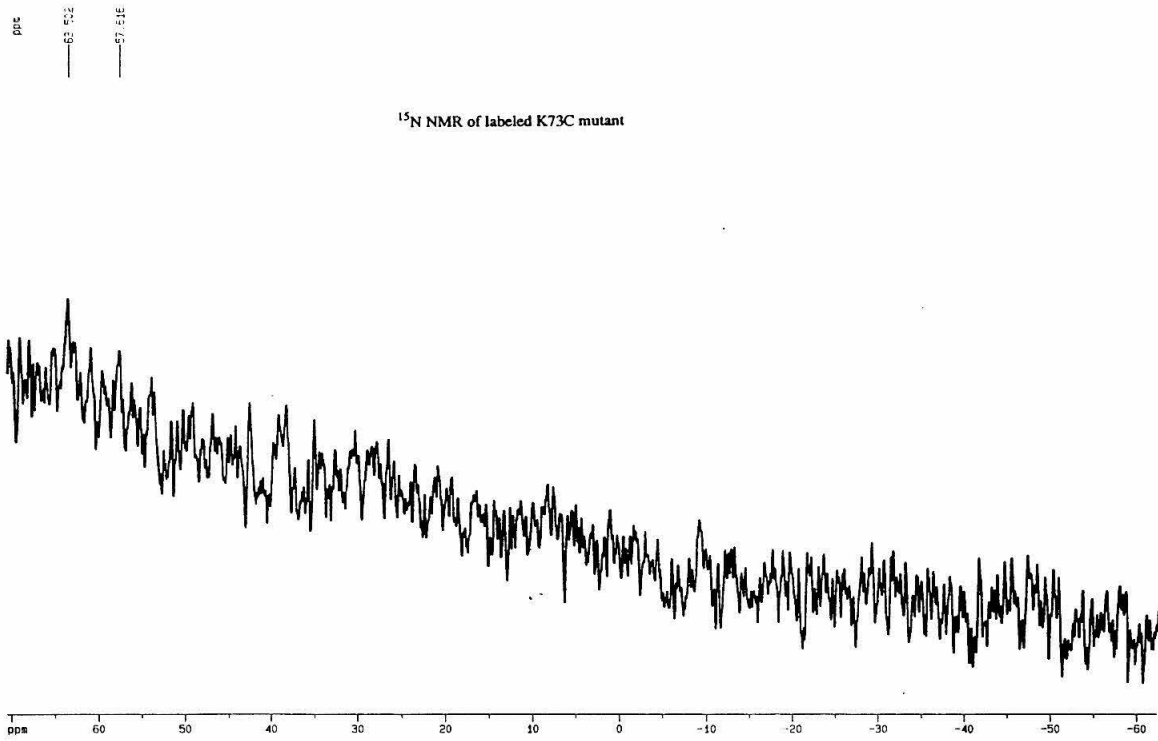


Figure 23.  $^{15}\text{N}$  NMR spectra of K73AEC  $\beta$ -lactamase.

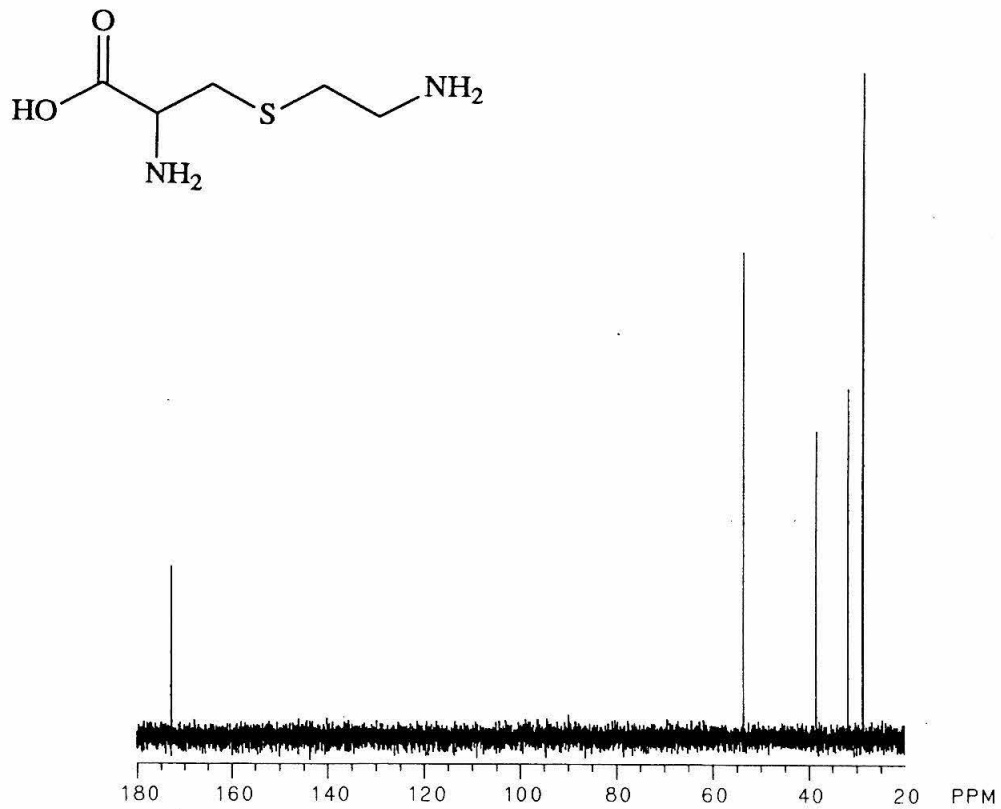


Figure 24.  $^{13}\text{C}$  NMR spectra of aminoethylcysteine.

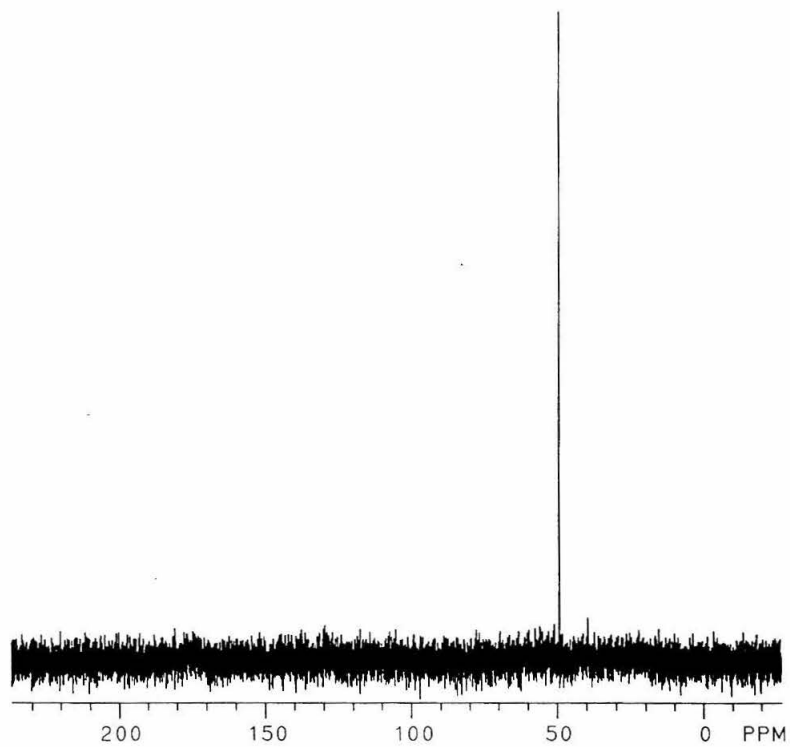


Figure 25.  $^{13}\text{C}$  NMR spectra of  $^{13}\text{C}$ -K73AEC  $\beta$ -lactamase.

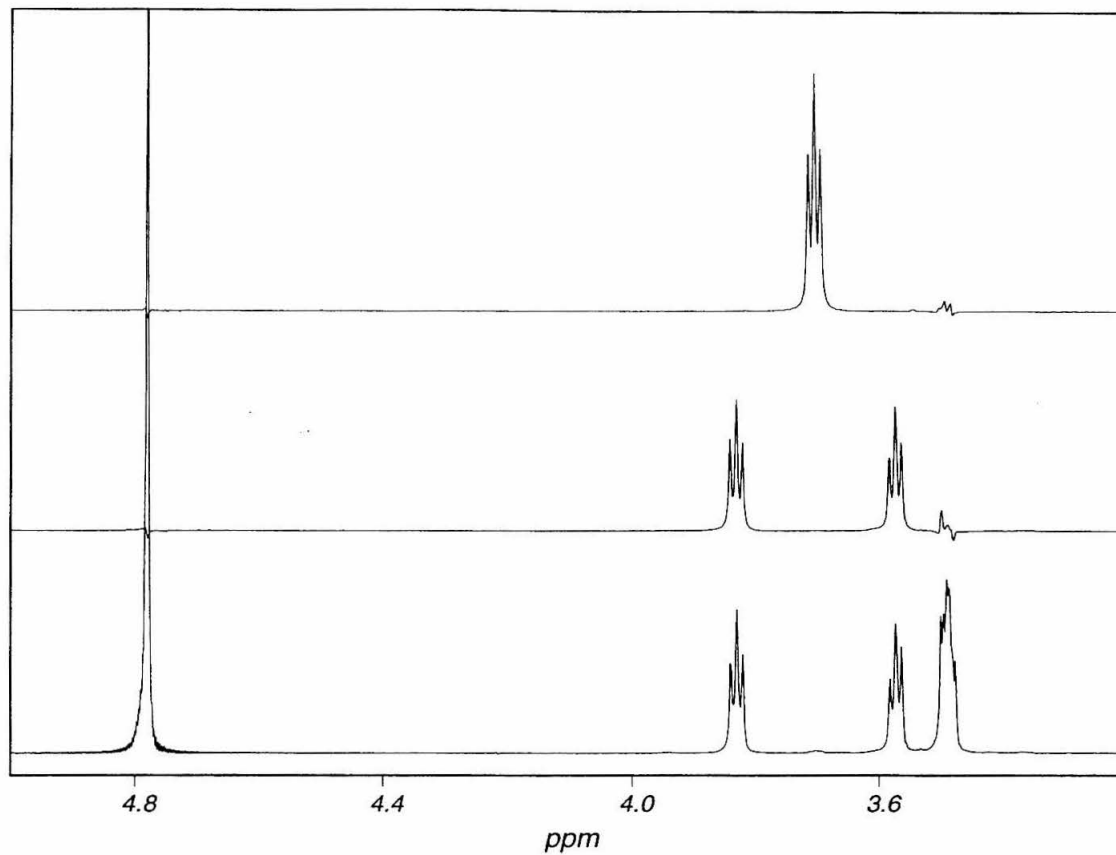


Figure 26. HMQC experiment for  $^{13}\text{C}$ -2-bromoethylamine hydrobromide. Bottom,  $^1\text{H}$  spectra of  $^{13}\text{C}$ -BEA. Middle,  $^{13}\text{C}$ -edited spectra. Top,  $^{13}\text{C}$ -edited/ $^{13}\text{C}$ - $^1\text{H}$  decoupled spectra.



top is the  $^{13}\text{C}$  edited  $^1\text{H}$  spectra decoupled. Next, the  $^{13}\text{C}$  labeled  $\beta$ -lactamase was run, with the unedited protein  $^1\text{H}$  spectra shown in Figure 27. This sample was then subjected to spin-echo experiments giving a  $^{13}\text{C}$  edited spectra (Figure 28). The spectra showed a large number of peaks. This suggested a couple of possibilities; the sample had impurity proteins which were labeled under the labeling conditions,  $\beta$ -lactamase was not labeled at only one site, and/or the experimental parameters were not correct for editing. To assay the latter two possibilities, wild-type  $\beta$ -lactamase was subjected to labeling with  $^{13}\text{C}$ -2-bromoethylamine hydrobromide under both standard conditions (4 M urea, and  $37^\circ\text{C}$ ). The results of this control experiment are shown in Figure 29. The NMR parameters appear to be correct, as the editing is successful; only one other peak is seen, either from another residue or *n*-terminus being modified, or perhaps an artifact from incomplete dialysis. The  $^{13}\text{C}$  labeled K73C  $\beta$ -lactamase was rechromatographed by FPLC, and indeed impurities were seen.

This rechromatographed sample was subjected to the HMQC experiment, with the results shown in figures 30 and 31. Figure 30 shows the unedited spectra (bottom), and the  $^{13}\text{C}$ -edited spectra (top). A clean broad singlet is seen in the  $^{13}\text{C}$ -edited spectra at  $\sim 2.7$  ppm (referenced to water @ 4.8 ppm), which is not apparent in the  $^1\text{H}$  spectra. When referencing these spectra to the labeled wild type control, it seems that this peak is not an artifact, and could be the peak of interest (Figure 31). Unfortunately, the sample had degraded over time and repeated purification's, and the pH behavior of this peak could not be assayed (the spectra were obtained over 60 hours of acquisition time). Efforts are underway to analyze new samples.

## DISCUSSION

The first requirement for all of these NMR experiments is a large amount of protein. The pJN expression vector gives  $\sim 1$  mg/L of growth. Therefore, rather large protein preps

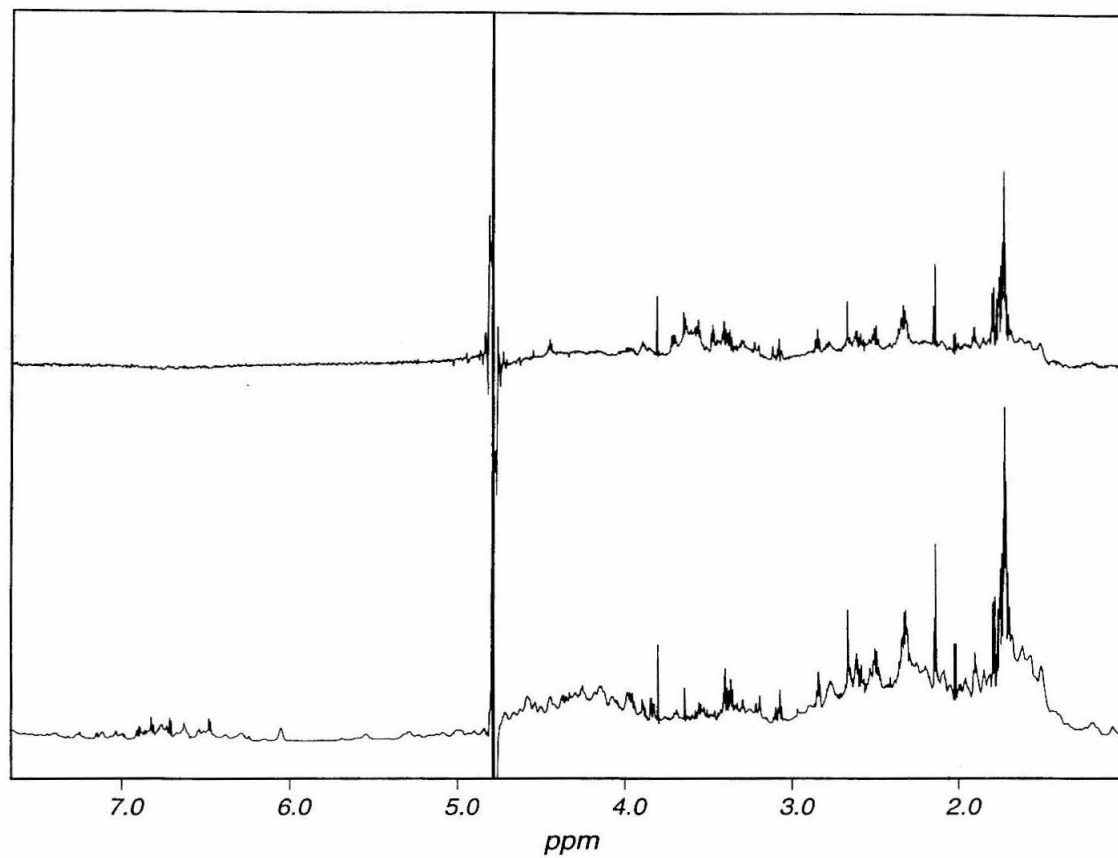


Figure 27.  $^1\text{H}$  spectra of  $^{13}\text{C}$ -K73AEC  $\beta$ -lactamase. Bottom,  $^1\text{H}$  spectra. Top,  $^{13}\text{C}$ -edited.

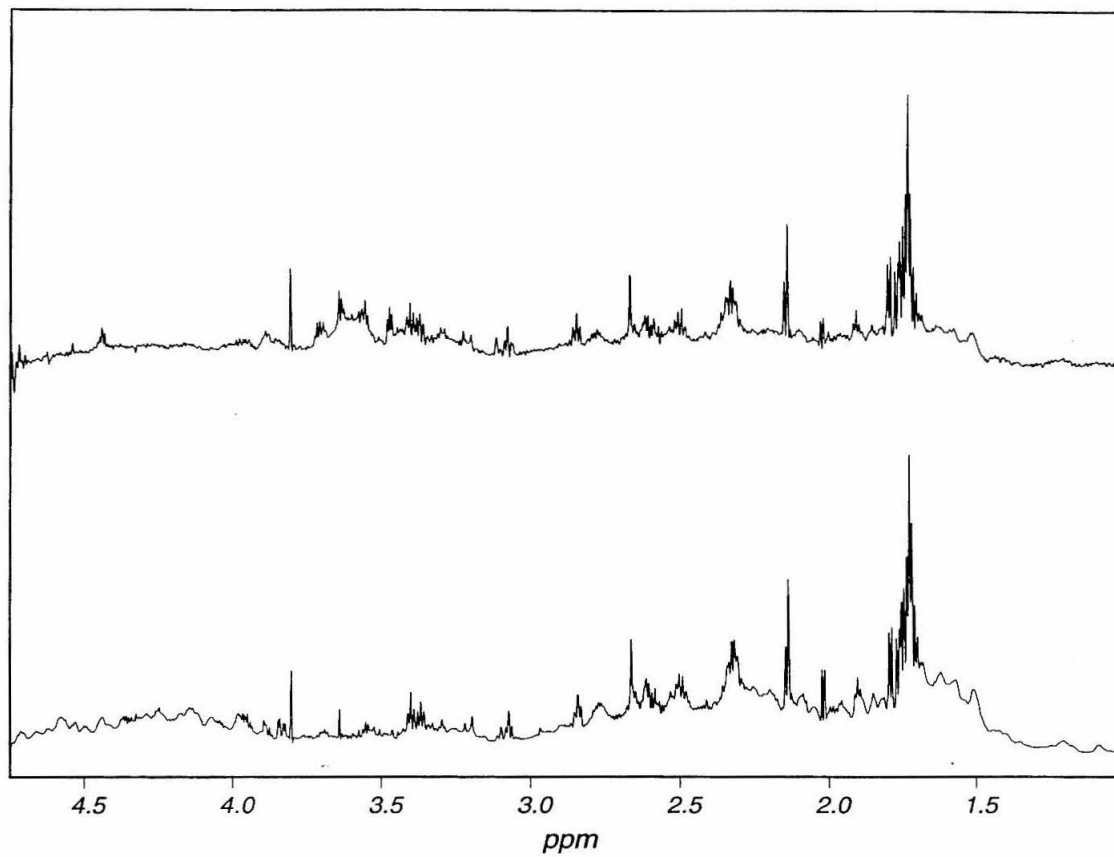


Figure 28. HMQC experiment on  $^{13}\text{C}$ -K73AEC  $\beta$ -lactamase. Bottom,  $^1\text{H}$  spectra. Top,  $^{13}\text{C}$ -edited spectra.

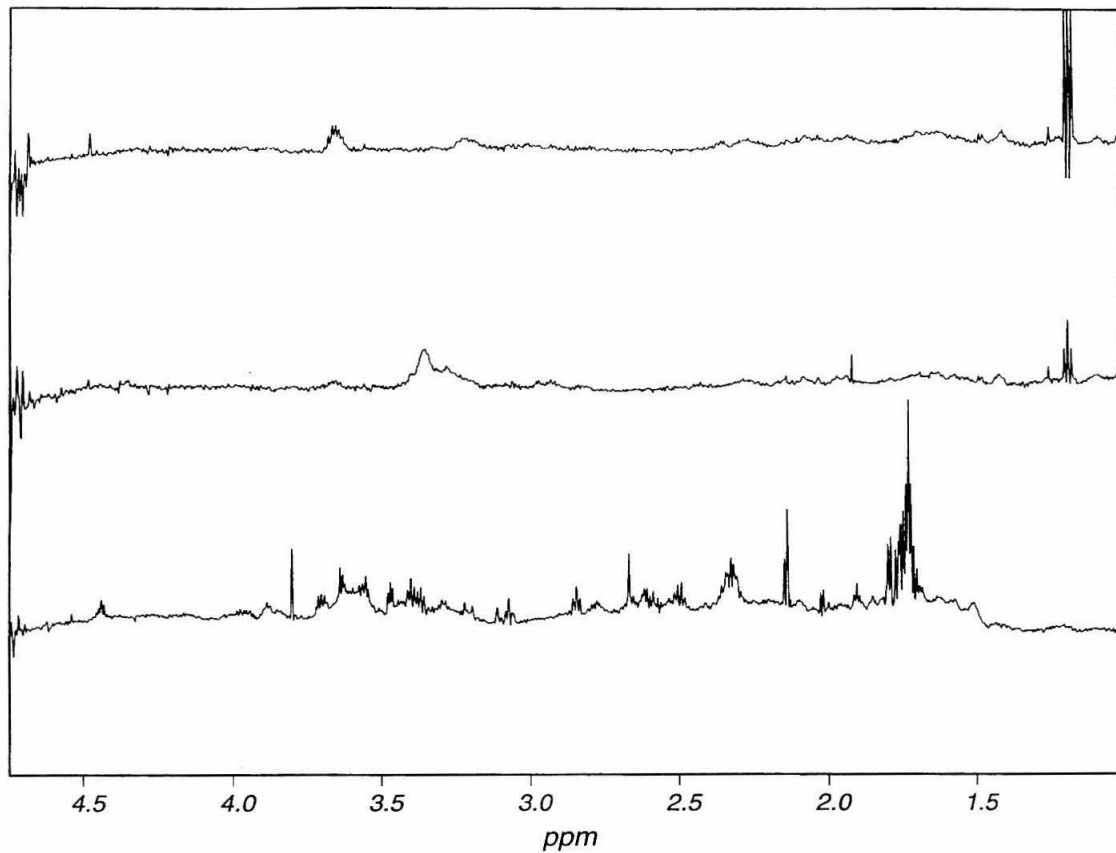


Figure 29. HMQC control experiment on  $^{13}\text{C}$ -wild type  $\beta$ -lactamase. Bottom,  $^{13}\text{C}$ -edited spectra of 13C-K73AEC. Middle,  $^{13}\text{C}$ -edited spectra of wild type  $\beta$ -lactamase labeled @  $37^\circ$ . Top,  $^{13}\text{C}$ -edited spectra of wild type  $\beta$ -lactamase labeled under urea conditions.

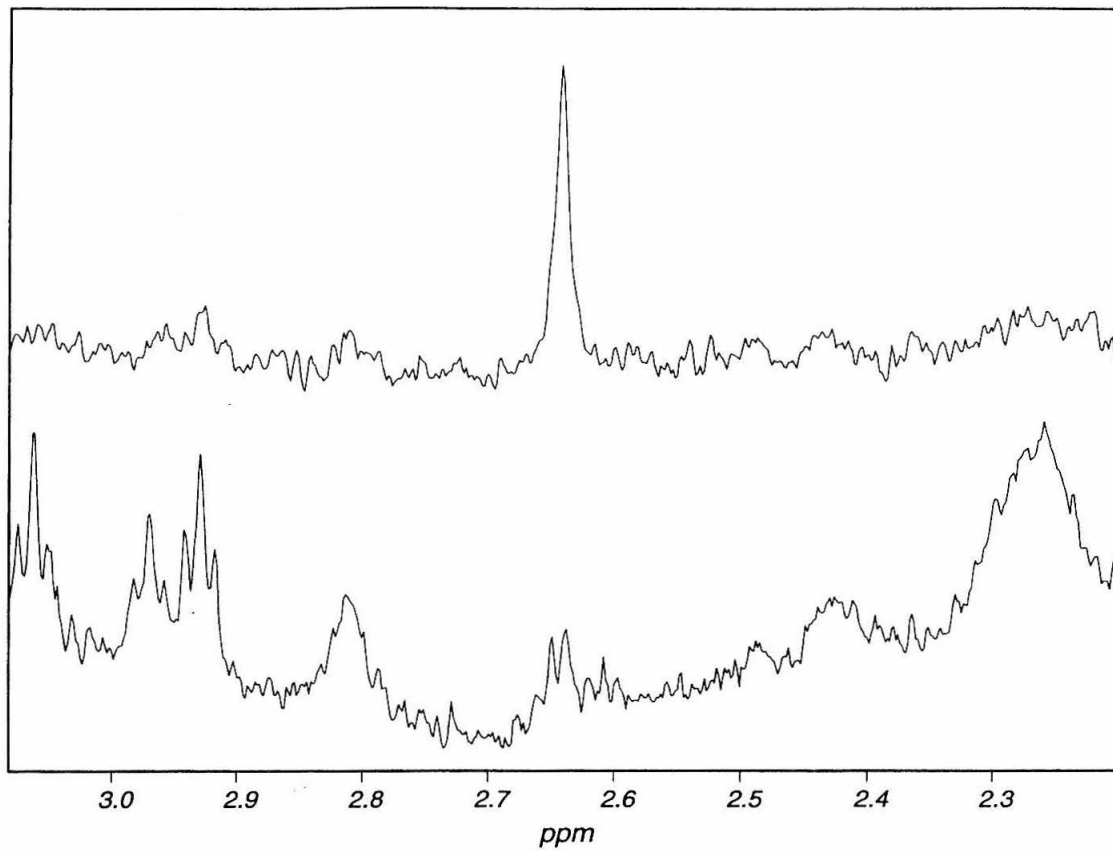


Figure 30. HMQC experiment on repurified  $^{13}\text{C}$ -K73AEC  $\beta$ -lactamase. Bottom,  $^1\text{H}$  spectra. Top,  $^{13}\text{C}$ -edited spectra.

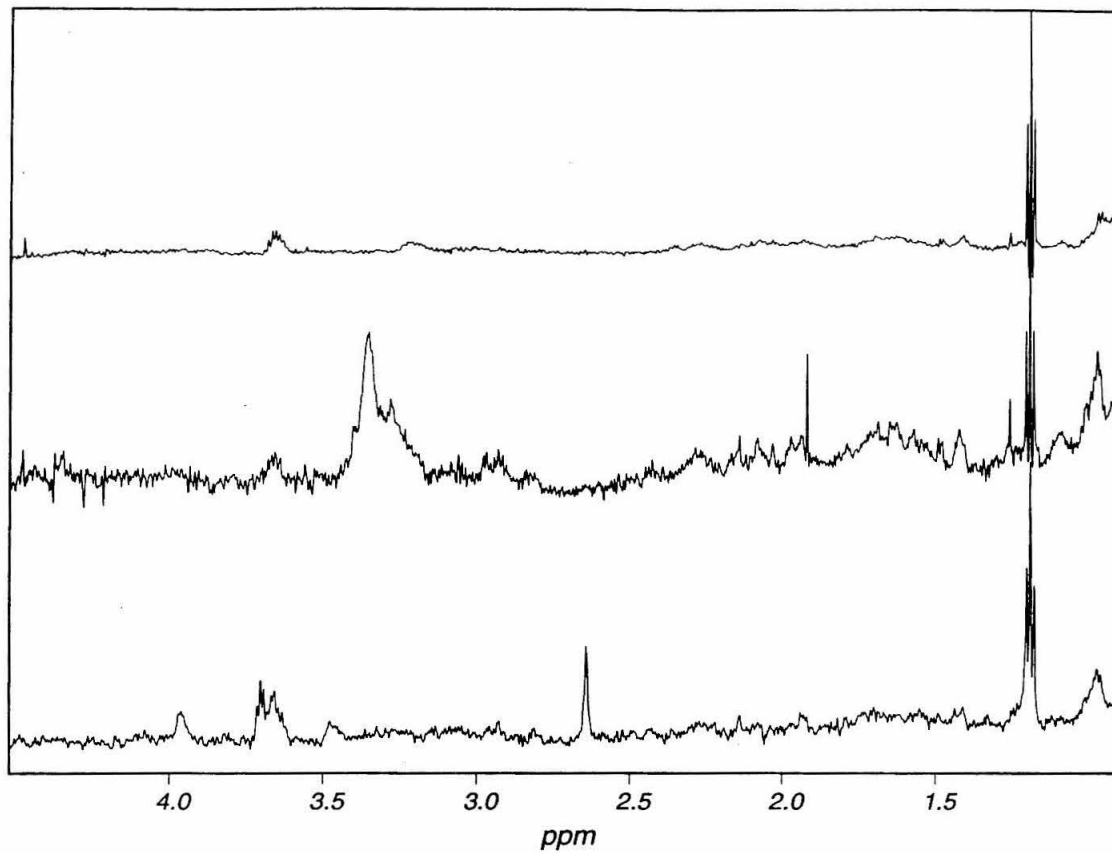


Figure 31. HMQC experiment on  $^{13}\text{C}$ -K73AEC  $\beta$ -lactamase. Bottom,  $^{13}\text{C}$ -edited spectra of repurified  $^{13}\text{C}$ -K73AEC. Middle,  $^{13}\text{C}$ -edited spectra of wild type control using urea. Top,  $^{13}\text{C}$ -edited spectra of wild type control @  $37^\circ$ .

are required to give the tens of milligrams of  $\beta$ -lactamase required. Large-scale fermentations could be used, but the osmotic extrusion procedure does not work well when scaled up. All of these factors would indicate the requirement of a more efficient expression system.

Other members of our group have had success with the T7 expression system from Novagen. C. Slutter in our group has achieved yields of up to 40 mg/L of culture using this system (42). This system would appear to be ideal for the large amounts of protein required for these NMR experiments, so insertion of the K73C  $\beta$ -lactamase gene into the pET system was attempted. Briefly, PCR was used to create proper restriction sites flanking the K73C mutant gene, with the PCR product digested and ligated into the pET vector. Unfortunately, repeated attempts at protein expression resulted in the build up of large amounts of the preprotein in the cytoplasm, with almost no processing and secretion into the periplasm. One possible problem is that the expression system is so good, it overpowers the cellular processing system. Another potential problem lies in the mutation K73C. Other groups have reported seeing similar expression problems with Ser to Cys mutated proteins in T7 systems (43). Agglomeration of protein in the cytoplasm might be facilitated by the extra Cys residue, resulting in the facile formation of inclusion bodies, which cannot be processed. Whatever the problem, the T7 system was abandoned in favor of sequential 12L protein preps. This brute force approach, while labor intensive and inelegant, did give mature K73C  $\beta$ -lactamase.

The  $^{15}\text{N}$  experiment was hindered in part by the inherent low sensitivity of  $^{15}\text{N}$  NMR. It was determined that  $\sim 70$  mgs of protein would be required to see a signal, but unfortunately the upper limit of solubility of RTEM-1  $\beta$ -lactamase is 20 mg/ml. These two factors conspired to doom the  $\text{p}K_{\text{a}}$  determination by direct observation of the  $^{15}\text{N}$  chemical shift change with pH. Repeated attempts to see a signal, using both 5 mm and 10 mm probes and accumulation times of up to 24 hours failed to give any  $^{15}\text{N}$  signal.

It was hoped that the greater sensitivity of  $^{13}\text{C}$  NMR would overcome the solubility problems, and that the  $^{13}\text{C}$  signal could be seen directly in labeled protein. However, a different problem arose. The labeled bromoethylamine hydrobromide was synthesized so as to put the  $^{13}\text{C}$ -carbon in the position  $\beta$ - to the amine, as this carbon undergoes much greater change in chemical shift. Unfortunately, the proposed mechanism of labeling causes the  $^{13}\text{C}$  label to be scramble (Figure 32). Since the actual labeling species is hypothesized to be ethyleneimine, there is actually a 50:50 distribution of  $^{13}\text{C}$  label in the C-1 and C-2 positions. Therefore, the concentration of label at a given position is cut in half, effectively lowering the labeled protein concentration to  $<10$  mg/ml. This amount of labeled protein was unfortunately not enough to see in a direct observation  $^{13}\text{C}$  experiment.

The only possibility of determining the  $\text{p}K_{\text{a}}$  by NMR was in an HMQC indirect observation experiment. The initial experiments involving the  $^{13}\text{C}$ -2-bromoethylamine hydrobromide model compound were encouraging, with excellent editing and resolution seen. However studies on the labeled enzyme were not so clean and clear cut. The presence of a great number of peaks in the labeled K73AEC  $\beta$ -lactamase indicated fundamental problems with either the sample or the experiment. A control experiment was devised to assay not only the NMR parameters, but also the possibility of other residues in the protein being modified, thus giving more than one peak. Since two different labeling conditions were used in the creation of the  $^{13}\text{C}$ -K73AEC, these conditions were duplicated in the wild-type control experiment; (1) 500 mM phosphate, pH 8.4, 100 mM  $^{13}\text{C}$ -2-bromoethylamine hydrobromide, and  $37^{\circ}$ ; (2) 500 mM phosphate, pH 8.4, 100 mM  $^{13}\text{C}$ -2-bromoethylamine hydrobromide, 4 M urea. Interestingly, these two conditions yielded protein that showed only one non-artifact peak, but the chemical shifts of the peaks were different by  $\sim 0.3$  ppm. The identity of the labeled species, and the reason for the differences in chemical shifts is not known.



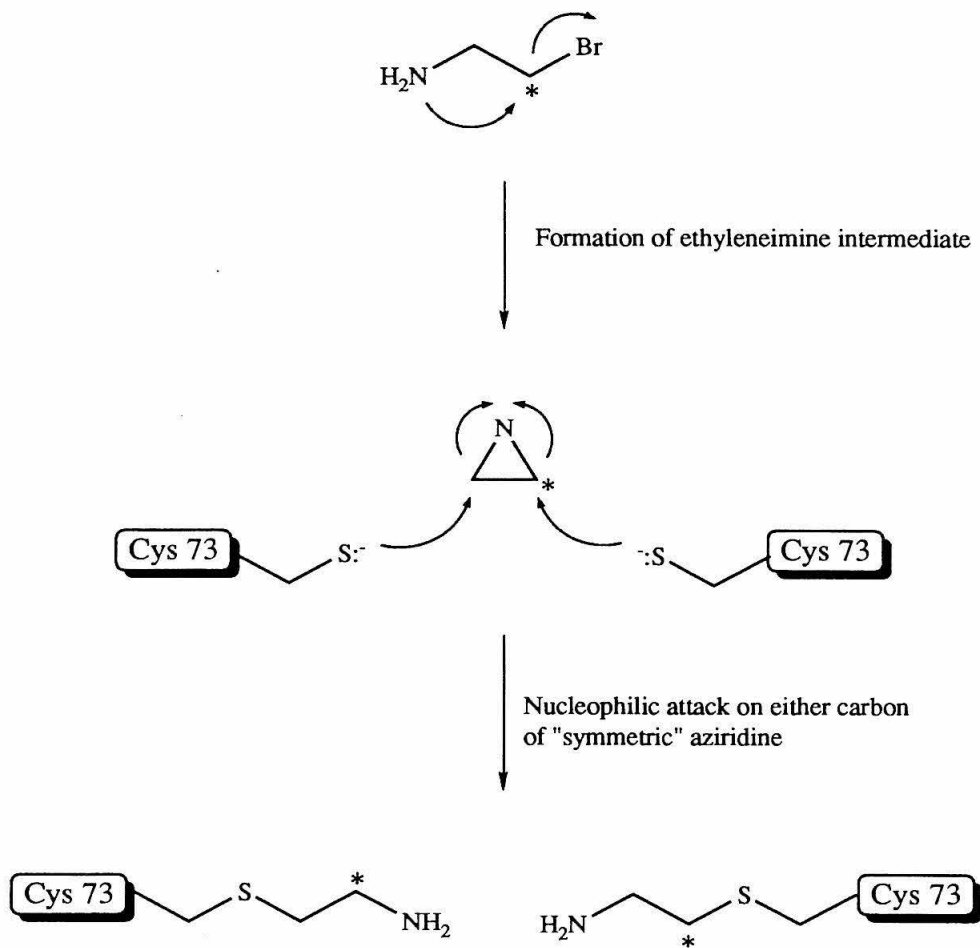


Figure 32. Mechanism of  $^{13}\text{C}$  label scrambling during  $\beta$ -lactamase modification.

The results of only one peak being seen in the control experiments were encouraging, indicating that the plethora of peaks seen in the K73AEC sample were due to impurities that were labeled. The sample was subjected to FPLC purification, and five peaks were seen, with the peak containing the  $\beta$ -lactamase being the largest (data not shown). This rechromatographed sample was subjected to another HMQC experiment with identical parameters to the other, with the exception of acquisition time, which was much greater for the rechromatographed sample. It was very encouraging that one peak rose out of the aliphatic region in the  $^{13}\text{C}$ -edited spectra. The chemical shift of this broad singlet is  $\sim 2.7$  ppm (referenced to water). Calculated chemical shifts for the protons in the aminoethyl cysteine residue range from  $\sim 2.8$  to 3.45 ppm depending on protonation state of the amine. Thus the observed peak could be from the aminoethyl cysteine; the chemical shift is in the correct range, and the peak is rather broad, which would be expected for a proton signal from a large molecule. It is interesting that only one peak is seen. This could be evidence that the actual labeling mechanism follows a  $\text{S}_{\text{N}}2$  pathway rather than the achiral intermediate shown in Figure 32. Unfortunately, the sample had degraded to a point that excessive acquisition times were required to see a signal. Therefore, the pH behavior of this observed peak could not be assayed. Calculations indicate that both the  $\alpha$ - and  $\beta$ -protons (relative to the amine) should shift  $\sim 0.3$  ppm upon protonation of the amine (Figure 33). This chemical shift change is well within the observable range under the experimental conditions.

A new sample was generated as above ( $\sim 15$  mg K73AEC  $\beta$ -lactamase), and was labeled under the urea conditions. HMQC NMR analysis did not show any strong peaks, but many weak peaks indicative of signals from background  $^{13}\text{C}$  molecules in the protein. The protein was labeled under the  $37^\circ\text{C}$  conditions, with the resulting spectra shown in Figure 34. Two peaks of interest are seen, one at  $\sim 3.2$  ppm (triplet), and one at  $\sim 2.3$  ppm. Calculations for the chemical shift for protons in an aminoethylcysteine indicate that the

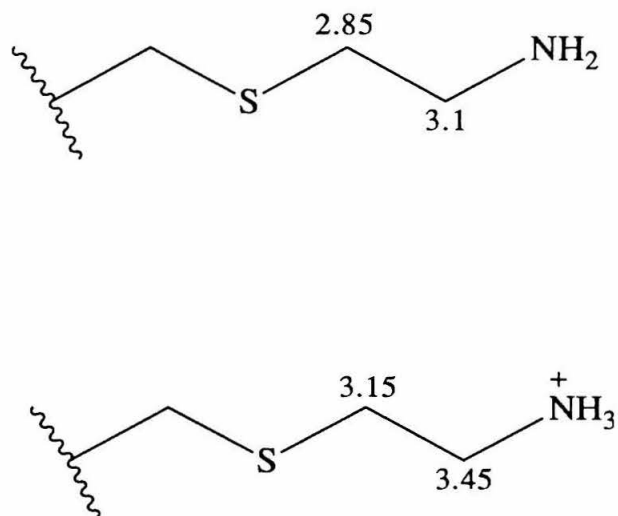


Figure 33. Calculated chemical shift values for aminethylcysteine in K73AEC  $\beta$ -lactamase.

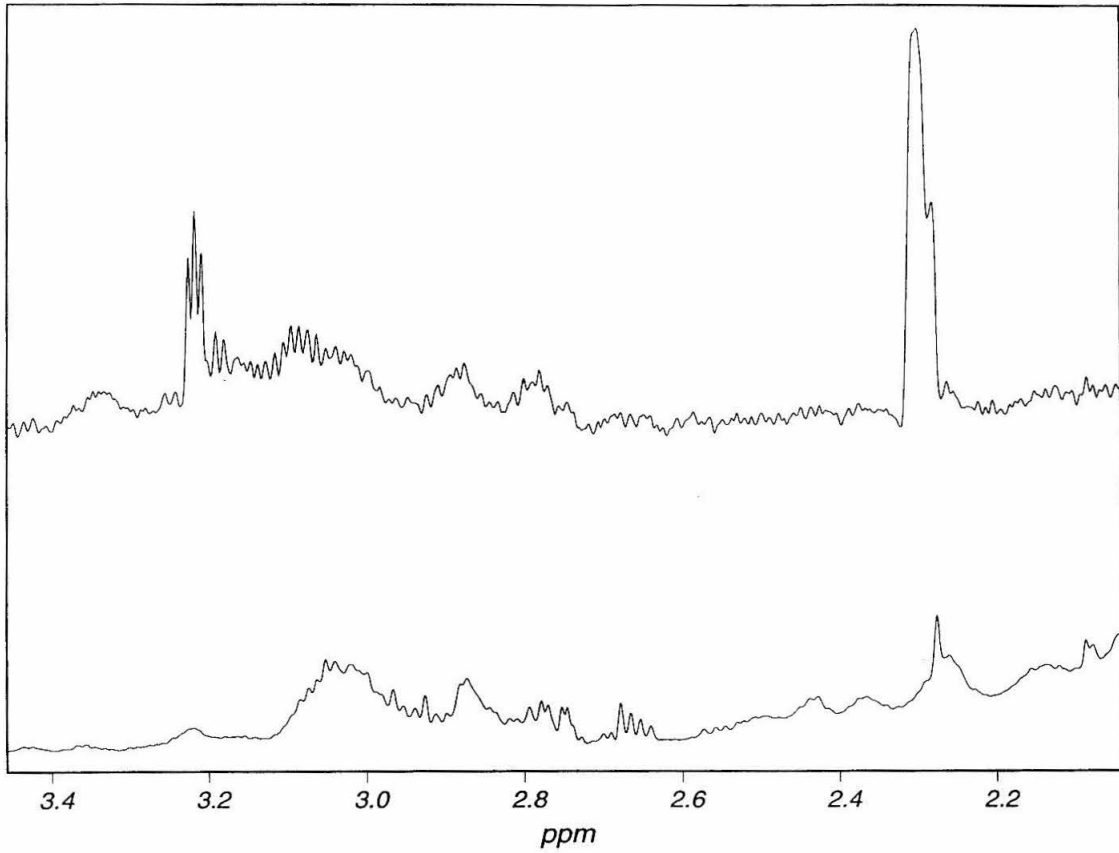


Figure 34. Spectra from HMQC NMR experiment on  $^{13}\text{C}$ -K73AEC  $\beta$ -lactamase.

peak at 3.2 ppm is from the protons  $\beta$ - to the amine, which is where the  $^{13}\text{C}$  label would be expected. Also since this spectra is not proton decoupled, a triplet would be expected. The identity of the other peak is unknown and deserves further investigation.

With the observation of a peak at the assumed correct chemical shift, the NMR titration experiment was undertaken. NMR spectra were generated at five different pH's; 6.6, 7.7, 8.5, 9.8, 12.5 (Figures 35-37). The sample was in  $\text{D}_2\text{O}$ , with 25 mM potassium phosphate buffer. pH was adjusted with  $\text{D}_3\text{PO}_4$  and KOD solutions in  $\text{D}_2\text{O}$ . The two observed peaks did move, with the peak at 3.2 shifting  $\sim 0.4$  ppm, as predicted by calculations. The other peak showed a much greater sensitivity to pH, with chemical shift varying by  $\sim 1$  ppm. The  $\text{p}K_a$  of the ionizable group adjacent to the observed protons can be estimated by plotting the chemical shift change. The amine functionality assumed to be  $\beta$ - to the protons observed in the 3.2 ppm peak (in the aminoethylcysteine residue at position 73) has a  $\text{p}K_a$  of  $\sim 10.5$  (Figure 38). This is what would be expected for a typical lysyl amine. Thus, it would appear that the amine at position 73 cannot function as a general base. However it must be pointed out that this NMR measurement is made on the free enzyme; there is no substrate available. It has been suggested that  $\beta$ -lactamase undergoes a significant conformational change upon binding of substrate (14). It could be envisioned that this altered protein conformation could induce a lowered  $\text{p}K_a$  for Lys 73, thus deprotonating the amine, making it available to act as a general base in the acylation step of the reaction. This hypothesis could be tested by using a double mutant which gives the chemical modification abilities at position 73 (K73C), along with acylation deficiency (S70A). This mutant should bind substrate, but not be acylated. Thus, the  $\text{p}K_a$  of the K73AEC derivative could be assayed as free enzyme, and also in the presence of bound substrate. This would indicate whether the conformational changes influence the chemical behavior of the active site residues.

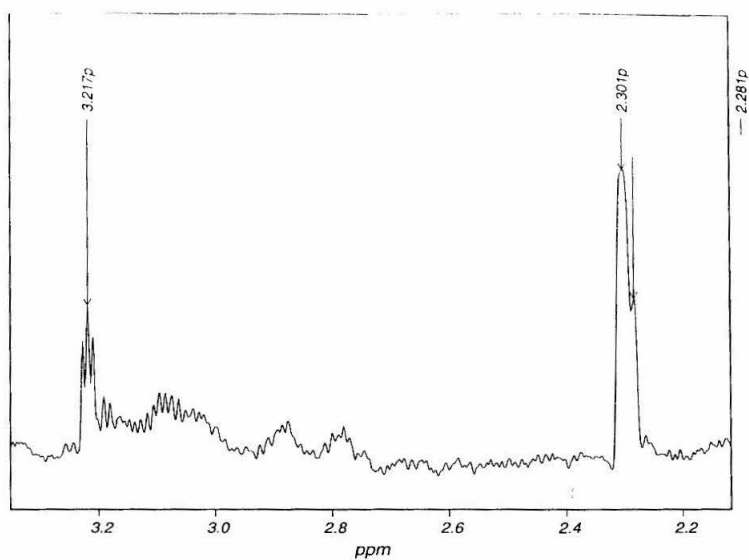
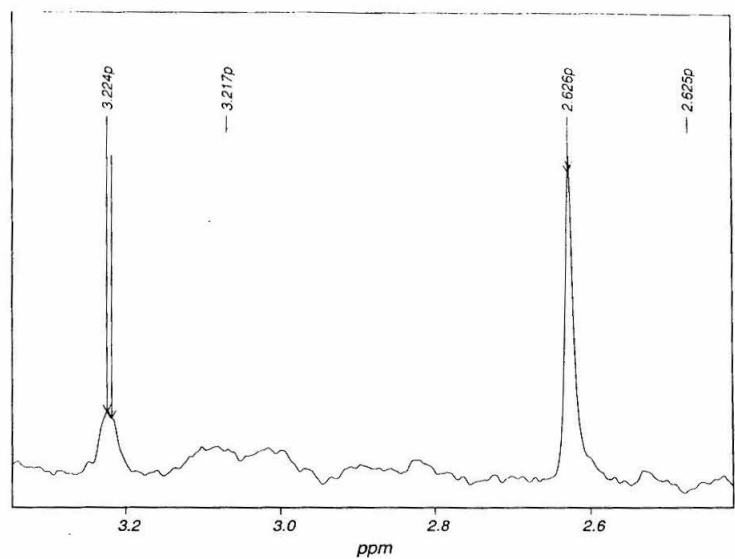


Figure 35. Spectra from HMQC NMR titration experiments for pH's 6.6 (top) and 7.7 (bottom).

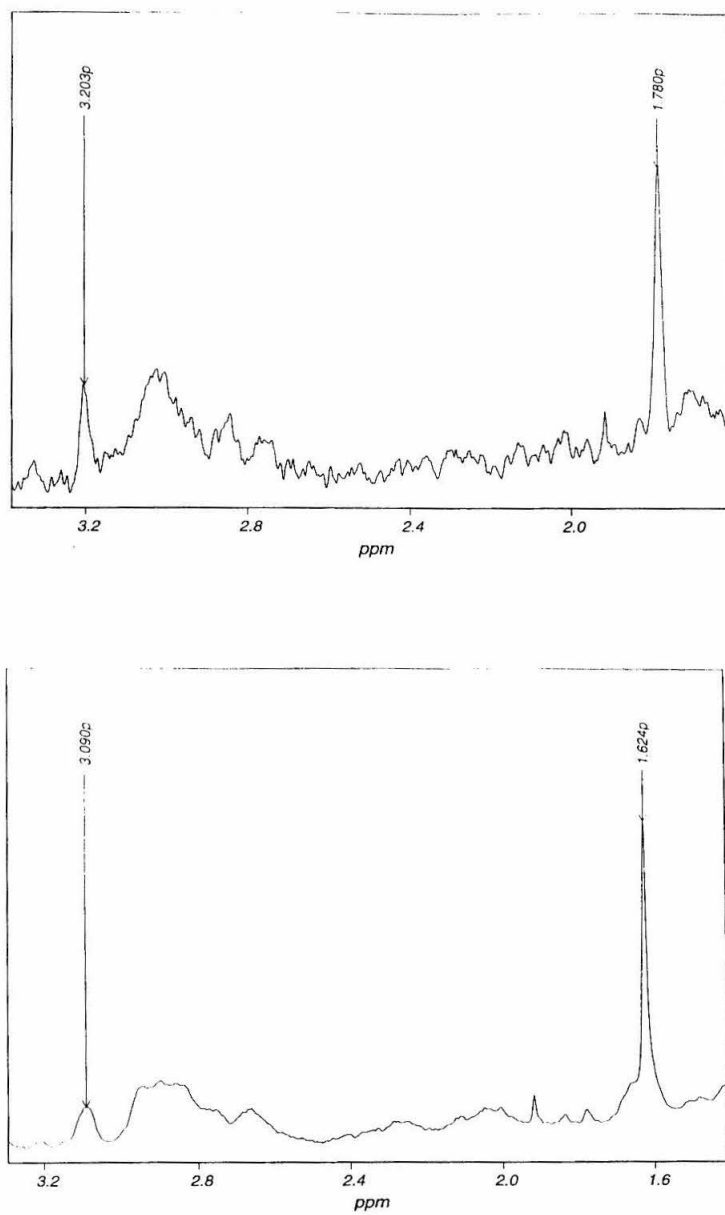


Figure 36. Spectra from HMQC NMR titration experiments for pH's 8.5 (top) and 9.8 (bottom).

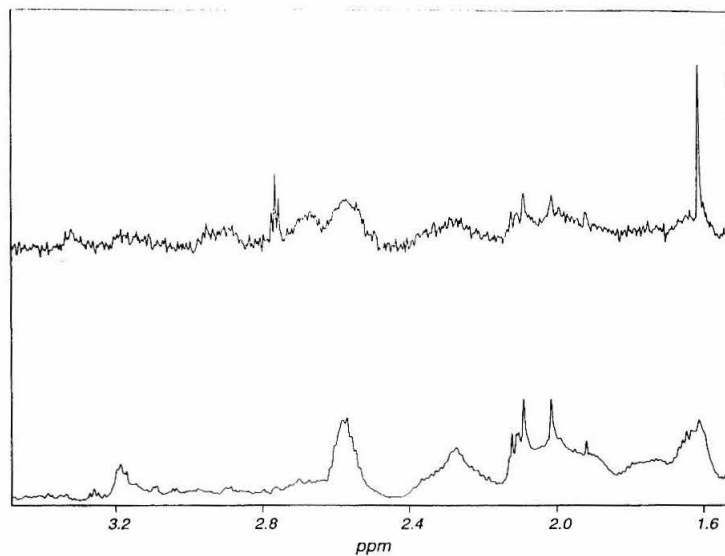


Figure 37. Spectra from HMQC NMR titration experiments for pH 12.5.



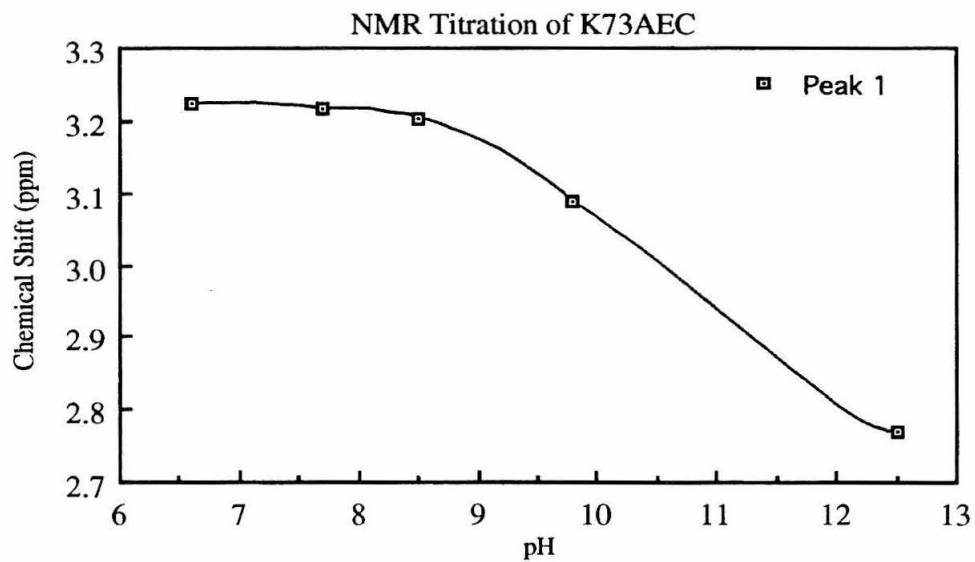


Figure 38. Plot of chemical shift vs. pH for first peak seen in HMQC NMR titration experiments.

The other peak seen also undergoes a chemical shift change with alteration of pH. The  $pK_a$  of the group being ionized which influences the protons being seen is  $\sim 8$  (Figure 39). The presence of this peak is puzzling. Its chemical shift does not jibe with known or calculated chemical shifts for any expected derivatization products. Also, the magnitude of the chemical shift change is very large ( $\sim 1$  ppm). It is perhaps possible that the two signals (3.2 ppm and 2.6 ppm) seen are from identical protons, but that the enzyme is has adopted two distinct conformations which create markedly different environments for the protons observed. It is known that the K73AEC enzyme only has  $\sim 50\%$  of the activity of wild-type. It is not known whether this is due to incorrect positioning of the modified enzyme catalytic groups, or folding problems encountered upon renaturation following labeling. If this peak is in fact from correctly labeled and folded enzyme, then the observed  $pK_a$  would support the hypothesis that Lys 73 functions as a general base, as the  $pK_a$  is depressed. Efforts are underway to investigate the identity of labeled residue(s) in the protein by tryptic digest and sequence analysis. Also, further studies using  $^{15}\text{N}$  chemical editing experiments are planned, which should unequivocally identify the  $pK_a$  of the amine functionality at position 73.

In spite of the myriad experimental problems encountered, this approach of using site-directed mutagenesis in conjunction with chemical modification and NMR to determine  $pK_a$  could be applicable to other system, not only for the determination of acidity constants, but also for use in 2D and 3D NMR experiments for structure determination and or substrate binding studies. The subtle nature of the -S- for -CH<sub>2</sub>- substitution [bond length 1.54Å (C-C) vs. 1.82Å (C-S); bond angles 109° (C-C-C) vs. 105° (C-S-C)] results in only a minor repositioning of the  $\epsilon$ -NH<sub>2</sub> group (44). One especially attractive application would be in the field of rational drug design, with active site labeled protein being used to analyzed the solution substrate binding of a large variety of small molecule drug analogs. Thus a relatively large number of drug candidates could be examined for binding geometry

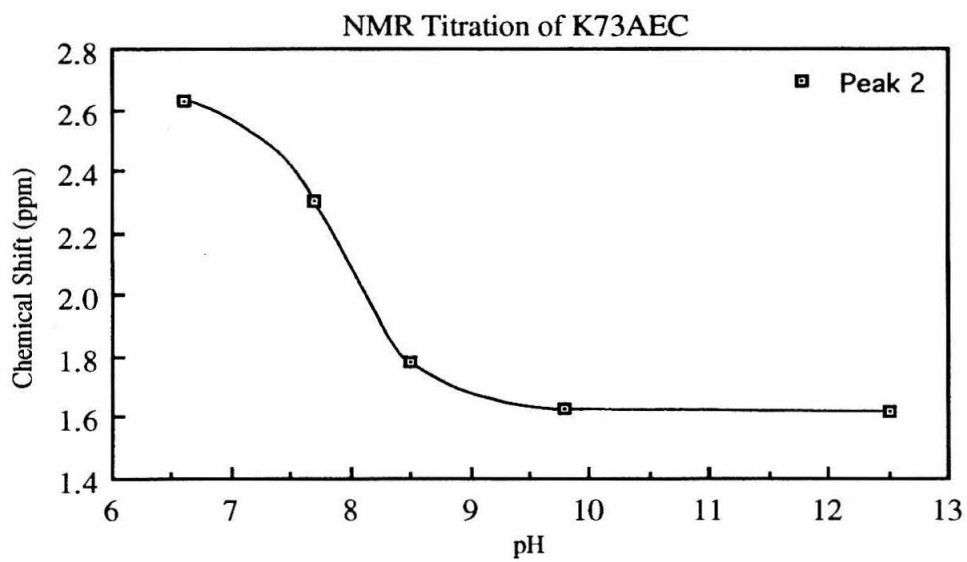


Figure 39. Plot of chemical shift vs. pH for second peak seen in HMQC NMR titration experiments.

and efficiency by NMR without the requirement of crystallization. All of these applications would nonetheless contribute to the ever broadening body of knowledge of protein structure/function relationships.

**REFERENCES**

1. Ambler, R. (1980) *Phil. Trans. R. Soc. Lond.* **289**, 321.
2. Sutcliffe, J.G. (1978) *Proc. Natl. Acad. Sci. U.S.A.* **75**, 3737.
3. Ambler, R.P. (1975) *Biochem J.* **151**, 197.
4. Neugebauer, K., Sprengel, R. and Schaller, H. (1981) *Nucleic Acids Res.* **9**, 2577.
5. Madgwick, P.J. and Waley, S.G. (1987) *Biochem J.* **248**, 657.
6. Huletsky, A., Couture, F., and Levesque, R.C. (1990) *Antimicrob. Agents Chemother.* **34**, 1725.
7. Bicknell, R. and Waley, I.G. (1985) *Biochemistry* **24**, 6876.
8. Knot-Hunziker, V., Petursson, S., Waley, S.G., Jarrin, B., and Grundstrom, T. (1982) *Biochem. J.* **207**, 315.
9. Datta, N., and Kontomichalou, P. (1965) *Nature (London)* **208**, 239.
10. Koshland, D., and Botstein, D. (1980) *Cell* **20**, 749.
11. Palva, I., Sarvas, M., Lechtovaara, P., Sibalow, M., and Kaariainen, L. (1982) *Proc. Natl. Acad. Sci. U.S.A.* **79**, 5582.
12. Roggenkamp, R., Kustermann-Kuhn, B., and Hellenberg, C.D. (1981) *Proc. Natl. Acad. Sci. U.S.A.* **78**, 4466.
13. Hertzberg, O. and Moulton, J. (1987) *Science* **236**, 694.
14. Strynadka, N.C.J., Adachi, H., Jensen, S.E., Johns, K., Sielecki, A., Betzel, C., Sutoh, K., James, M.N.G. (1992) *Nature (London)* **359**, 700.
15. Schmidt, D.E. Jr., and Westheimer, F.H. (1971) *Biochemistry* **10**, 1249.
16. Richmond, T.A., Long, D.M., Emerling, M.R., Carroll, S.S., Cho, W., Healy, W.J., and Richards, J.H., in preparation.
17. Carroll, S.S. (1986) Ph.D. Thesis, California Institute of Technology.
18. Naulet, J. (1983) *Org. Mag. Res.* **21**, 564.

19. Sarneski, J.E., Surprenant, H.L., Molen, F.K., and Reilley, C.N. (1975) *Anal. Chem.* **47**, 2116.
20. Aue, W.P., Bartholdi, E. and Ernst, R.R. (1976) *J. Chem. Phys.* **64**, 2229.
21. Anonymous, (1992) "Guide to NMR Experiments," Varian Instruments.
22. Hermann, P., and Lemke, K. (1968) *Hoppe-Seyler's Z. Physiol. Chem.* **349**, 390.
23. Boyer, H. and Roullard-Dussoix, D. (1969) *J. Mol. Biol.* **41**, 459.
24. Hanahan, D. (1983) *J. Mol. Biol.* **166**, 557.
25. Marvel, C.S. and Sekera, V.C. (1955) *Org. Syn., Coll. Vol. 3*, 366.
26. Gabriel, S. (1887) *Ber. Dtsch. Chem. Ges.* **29**, 2224.
27. Brown, R.F. and van Gulick, N.M. (1955) *J. Amer. Chem. Soc.* **77**, 1089.
28. Itoh, M., Hagiwara, D., and Kamiya, T. (1977) *Bull. Chem. Soc. Japan* **50**, 718.
29. Yoon, N.M., Pak, C.S., Brown, H.C., Krishnamurthy, S., and Stocky, T.P. (1973) *J. Org. Chem.* **38**, 2786.
30. Org Syn BEA.HBr
31. Wystrach, V.P., Kaiser, D.W., and Schaefer, F.C. (1955) *J. Amer. Chem. Soc.* **77**, 5915.
32. Beaucage, S.L. and Carruthers, M.H. (1981) *Tet. Lett.* **22**, 1859.
33. Ish-Horowitz, D., Burke, J. (1981) *Nucl. Acids Res.* **9**, 2989.
35. Nakmaye, K., Eckstein, F. (1986) *Nucl. Acids Res.* **14**, 9679.
34. Maniatis, T., Fritsch, E., Sambrook, J. (1982) "Molecular Cloning, A laboratory Manual". Cold Spring Harbor, N.Y., Cold Spring Harbor Laboratory.
36. Sanger, F. Nicklen, S., Coulson, A. (1977) *Proc. Natl. Acad. Sci. U.S.A.* **74**, 5463.
37. U.S. Biochemicals (1988) "Sequenase Manual," Cleveland, OH, U.S. Biochemical.
38. Neitzel, J. (1987) Ph.D. Thesis, California Institute of Technology.
39. De Boer, H.A., Comstock, L.J., and Vasser, M. (1983) *Proc. Natl. Acad. Sci. U.S.A.* **80**, 21.

40. Fisher, J., Belasco, J. Khosla, S., Knowles, J. (1980) *Biochemistry* **19**, 2895.
41. Hanes, J. (1932) *Biochem. J.* **26**, 1406.
42. Slutter, C.E., personal communication.
43. Wells, J.A., personal communication.
44. Weast, R.C., Ed. (1975) "Handbook of Chemistry and Physics," 56th ed., p F214, CRC Press, Cleveland OH.